Fibrogenesis in progressive renal disease

Baelde, J.J.

Fibrogenesis in progressive renal disease

The cover and lay-out of this thesis were designed in cooperation with Klaas van der Ham
Cover: anatomy of the kidney, drawn by Wilbert Baelde and coloured by Rianne Baelde.

Fibrogenesis in progressive renal disease / J.J. Baelde
Thesis, University of Leiden, Leiden, The Netherlands
ISBN-10: 90-9019994-2
ISBN-13: 97-8909019994-8

Printed by Febodruk BV, Enschede, The Netherlands

Fibrogenesis in progressive renal disease

PROEFSCHRIFT

ter verkrijging van
de graad van Doctor aan de Universiteit Leiden,
op gezag van de Rector Magnificus Dr. D.D. Breimer,
hoogleraar in de faculteit der Wiskunde en
Natuurwetenschappen en die der Geneeskunde,
volgens besluit van het College voor Promoties
te verdedigen op maandag 12 december 2005
klokke 16.15 uur

door

Jacobus Johannes Baelde

geboren te Bodegraven

in 1966

Promotiecommissie

Promotor:	Prof. Dr. J.A. Bruijn
Co-promotores:	Dr. E. de Heer
	Dr. M. Eikmans
Referent:	Prof. Dr. F.J. van der Woude
	Universiteit Heidelberg, Mannheim
Lid:	Prof. Dr. P.C.W. Hogendoorn

The studies described in this thesis were performed at the Department of Pathology (Head: Prof. G.J. Fleuren), Leiden University Medical Center, Leiden, The Netherlands.

The printing of this thesis was financially supported by the Matty Brand Stichting and the Leids Universiteits Fonds

Contents

Chapter 1

General Introduction

General introduction

Glomerulosclerosis results from an excess accumulation of extracellular matrix (ECM) molecules leading to glomerular scarring. Accumulation of ECM leads to progression of renal disease, a process called fibrogenesis. This progression is characterized clinically by loss of renal function. Glomerulosclerosis can be caused by several factors, which have been summarized in Table 1.

The aim of the work described in this thesis was to investigate the underlying molecular mechanisms of the development of glomerulosclerosis. Quantification of gene expression provides insight into the molecules and mechanisms involved in fibrogenesis. Animals developing glomerulosclerosis are being investigated as models for glomerulosclerosis in patients.

The introductory section for this thesis is structured as follows. After discussing the anatomy and function of the normal kidney, the role of the ECM in normal kidneys and during progression to glomerulosclerosis will be elaborated on. The increase of ECM observed in progression to glomerulosclerosis results from an altered balance between ECM production and degradation. In addition to quantitative changes, qualitative changes in the ECM production may also play a role in its accumulation. These processes are regulated by growth factors and cytokines. After giving an overview of animal models for glomerulonephritis, an introduction on diabetic nephropathy (DN) is provided. DN is a major complication of both type 1 and type 2 diabetes and is the most common cause of end-stage renal disease (ESRD) (1); thus, this introduction includes several factors involved in the progression of DN and a review of the most commonly used animal models for DN. To bring the molecular interactions into focus, an overview of the current knowledge of the role that growth factors, such as transforming growth factor-beta (TGF-β), connective tissue growth factor (CTGF), and vascular endothelial growth

Table 1. Causes of glomerulosclerosis

- Immune-mediated glomerulonephritis
- Metabolic disease
- Infection
- Drug induced nephrotoxicity
- Hemodynamic abnormalities
- Genetic
- Aging
- Idiopathic

factor (VEGF), play in the progression of DN is given. This overview is followed by a summary of mRNA detection methods and discussion of their effectiveness. The introductory section concludes with a description of the goals of the studies described in this thesis.

Anatomy and function of the kidney

The kidneys are organs that are specialized in maintenance of water and electrolyte balance. The human kidneys are located in the retroperitoneum and weigh 130–150 g each. The organs are encased in a capsule, which is surrounded by retroperitoneal fat. The hilum of the kidney opens onto the renal vessels, lymphatics, and ureter. The anatomic unit of the kidney is the

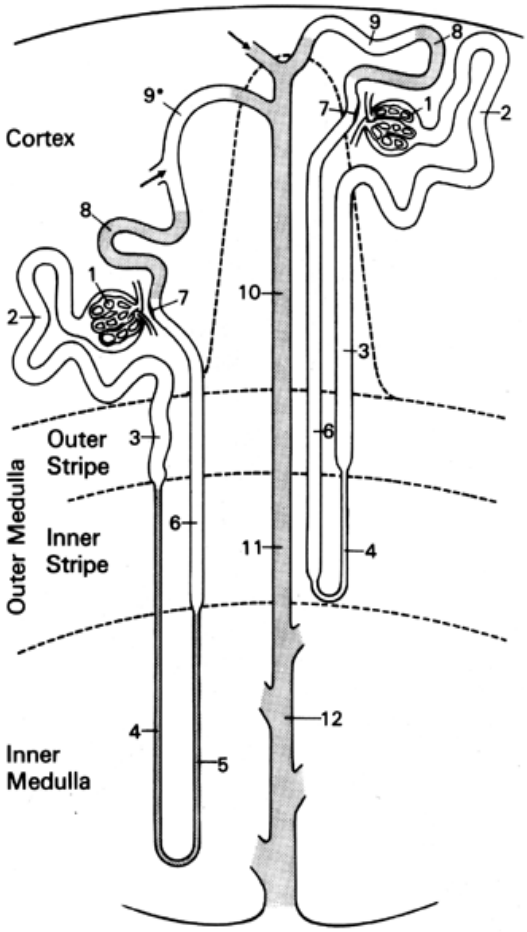

Figure 1. Schematic drawing of the nephron. Glomerulus (1). Proximal tubule (2-3). Descending thin limb (4). Ascending thin limb (5). Distal tubule (6). Macula densa (7). Distal tubule (8). Collecting duct (9-12).

nephron, which is composed of the glomerulus, proximal tubule, loop of Henle, distal tubule, and collecting duct (Fig. 1). Each kidney contains approximately 1.8 million nephrons (2).

Filtration of the blood plasma takes place in the glomerulus of the kidney. The glomerulus is composed of an afferent and efferent arteriole, the mesangium consisting of mesangial cells and ECM, and intervening capillaries lined by endothelial cells that cover the glomerular basement membrane (GBM). The outer surface of the capillaries, which is covered by glomerular epithelial cells (podocytes) (Fig. 2), is continuous with the epithelium of Bowman's space and the proximal tubule. Filtration of blood plasma takes place in the glomerular capillaries and is driven by the hydrostatic pressure of the blood flow. Filtration takes place at three different levels. First, it occurs at the level of the fenestrated endothelial cells, which are permeable to water and small solutes. The fenestrae themselves are too large to effectively filter macromolecules, but the endothelial cells are covered by a layer of negatively charged glycosylated macromolecules known as the glycocalyx (3). Haraldsson et al. (4) found that this negatively charged glycocalyx may play a role in glomerular size and charge selectivity.

The second layer is the GBM, which is a gel-like material consisting of 90% water (5). The structural integrity of the GBM is derived from a network of different ECM molecules, including

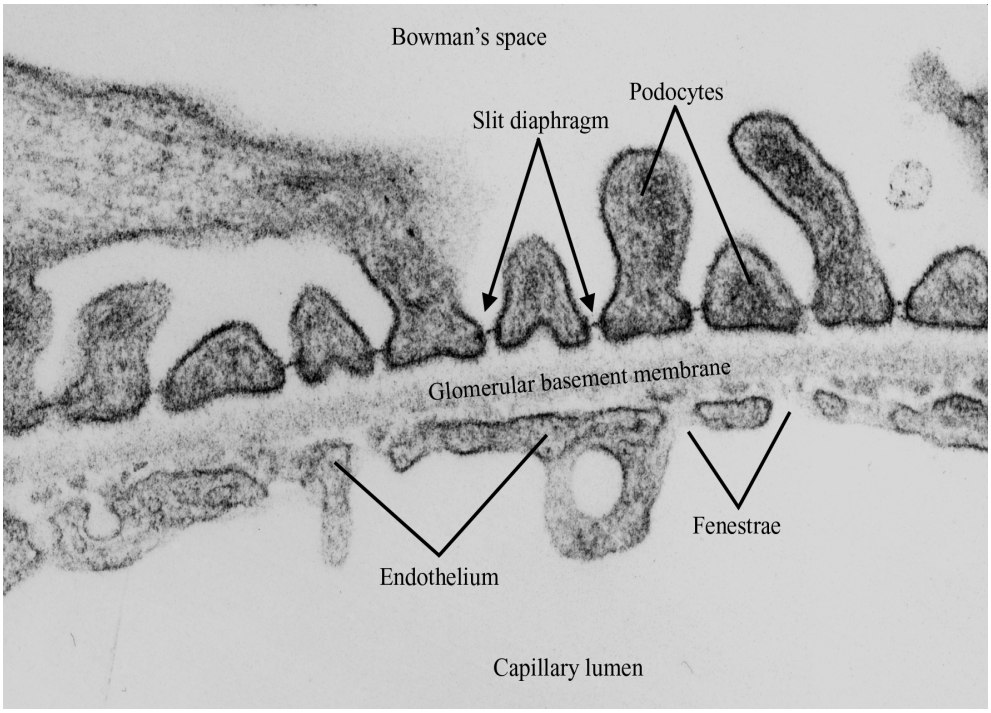

Figure 2. Schematic drawing of the filtration barrier.

type IV collagen, laminin, fibronectin, entactin, and heparan sulphate proteoglycans (6). The composition of the GBM and its molecular size and charge play an important role in permeability. The third barrier is the slit pore, located between the foot processes of the podocytes. The foot process is a contractile structure composed of many different molecules, including nephrin, CD2-associated protein, podocin, P-cadherin, densin, filtrin, actin, myosin, a-actinin, vinculin, and talin. These molecules are connected to each other or to the GBM at focal contacts such as the $\alpha_3\beta_1$-integrin complex (7). Podocytes also contribute to the specific size and charge characteristics of the glomerular filtration barrier, and damage to these cells leads to a retraction of their foot processes and proteinuria (8,9).

Extracellular matrix

In addition to their presence in the GBM, ECM molecules can be found in the mesangial area. Apart from its direct function in filtration, the GBM and the mesangial matrix serve as an anchoring place for glomerular cells through cell/matrix interacting sites such as integrins. The major components of the ECM in the glomerulus are collagens and laminins. Of all collagens, type IV is the primary one found here. It is encoded by six genetically distinct alpha-chains (alpha 1 through alpha 6) (10). Altered expression of collagen type IV alpha chains and laminin chains has been described in animal models for membranous nephropathy and lupus nephritis (11,12).

Progression of renal diseases as a result of disturbed ECM homeostasis

Most glomerulopathies are characterized by a decreased glomerular filtration rate (GFR) and proteinuria. Progression of renal diseases is morphologically characterized by the accumulation of ECM molecules in the glomerulus, the tubulointerstitial area, or both. Excessive accumulation of basement membrane, mesangial matrix, and interstitial matrix molecules are hallmarks of progression to glomerulosclerosis and interstitial fibrosis. A normal homeostasis of the ECM

Table 2. Causes of ECM accumulation

- Increased translation of ECM protein
- Increased transcription of ECM protein
- Reduced degradation of ECM protein
- Establishment of ECM binding sites on cells
- Establishment of novel binding (cellular/matrix) sites in ECM molecules via alternative splicing

is maintained by a continuous balance between the production and degradation of matrix molecules. Accumulation of ECM molecules in glomerulosclerotic and interstitial fibrotic lesions can be the result of increased local transcription or translation of ECM-encoding genes or RNA, trapping of ECM molecules from the circulation, or a diminished degradation of ECM proteins by matrix metalloproteases (MMPs) (Table 2). The MMPs belong to a large family of ECM-degrading enzymes, which include the interstitial collagenases (MMP-1, MMP-2, MMP-8, and MMP-13), stromelysins, gelatinases (MMP-2 and MMP-9), and elastases (13). Changes in MMP expression or activity may result into altered ECM turnover, which may lead to glomerulosclerosis. Cytokines such as TGF-β (14) and platelet-derived growth factor (PDGF) (15) can influence expression of ECM molecules and MMPs, thereby disturbing the balance between ECM synthesis and degradation. These cytokines can also lead to an altered composition of ECM molecules

Alternative splicing of ECM molecules in renal disease

Alternative splicing of ECM molecules can account for an alteration of the ECM composition by influencing the degradability of the matrix or by introducing matrix–matrix and matrix–cell interactions (Table 2). Splicing of mRNA takes place after DNA transcription. The encoding regions of most genes are split into segments (exons) separated by noncoding intervening sequences (introns). After transcription of DNA, the pre-mRNA molecules of most genes undergo further processing. This processing involves removal of the intron segments and rejoining of the remaining exon segments. The splicing of mRNA is mediated through a complex called the spliceosome, which consists of five types of small nuclear RNAs (snRNAs) and many other proteins (16) that assemble at splice sites. Each of the snRNA molecules is attached to specific proteins to form the spliceosome. The specificity of the splicing reaction is established by RNA-RNA base-pairing between the RNA transcript and snRNA molecules. In addition to physiologic RNA splicing, alternative splicing of RNA can occur. This process introduces splicing out or retention of exon sequences in addition to the intron sequences. With this mechanism, different cell types or environmental conditions can induce several types of mRNA molecules from a single gene.

Alternative splicing can be detected with reverse transcriptase polymerase chain reaction (RT-PCR) in combination with specific primers flanking the site where the splicing takes place. Separation on an agarose gel can discriminate between normally and alternatively spliced mRNA. Fibronectin is an example of alternative splicing of an ECM molecule. This glycoprotein plays a role in cell–matrix and matrix–matrix interactions and is found in the normal kidney. Its expression increases during glomerulosclerosis and interstitial fibrosis (17). Fibronectin is composed of a number of repeats of three different types and has several binding domains,

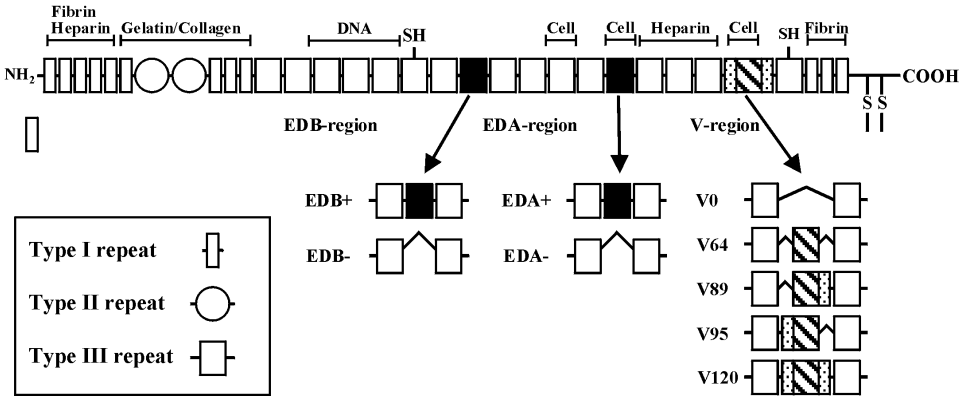

Figure 3. General structure of the fibronectin polypeptide. The fibronectin molecule consists of different repeats (types I, II, and III), several binding sites (fibrin, heparin, DNA, and cell), and three different sites that can be alternatively spliced (EDA, EDB, and V).

including collagen-, heparin-, and integrin-binding sites. Alternative splicing of certain domains within the fibronectin molecule can take place at three different regions, the EDA, EDB, or V regions. This alternative splicing can result in the retention of additional binding domains (Fig. 3) that play a role in biological processes, including maintenance of normal cell morphology, cell migration, cell differentiation, and cell remodeling (18). It has been shown that fibronectin proteins, including the EDA and V regions, are increased in the mesangium of nephritic rats. Coinciding with the up-regulation of the EDA and V120 isoforms, there was an increase in mesangial cell proliferation and in the number of infiltrating cells positive for a4ß1-integrin (a ligand for fibronectin) (19). Upon ischemic injury in rat kidneys, the expression of EDA-positive fibronectin increases dramatically in the renal interstitium and continues to be produced at high levels 6 weeks later. The V-region-containing fibronectin also increases in the interstitial space (20).

Animal models for glomerulosclerosis

Animal models of renal disease can be used as a tool to investigate the development and progression of human renal diseases. In this section, the animal models employed in the studies presented in this thesis will be discussed. First of all, anti-Thy-1 nephritis in rats, which is induced by a single injection of antibodies directed against the Thy-1 epitope on the glomerular mesangial cells, results in complement-dependent mesangial cell lysis, apoptosis, mesangial proliferation, and ECM deposition (21). Depending on the rat strain used, anti-Thy-1 glomerulonephritis either spontaneously resolves within several weeks or progresses to

glomerulosclerosis (22). Chronic serum sickness is a model for human membranous glomerulonephritis and can be induced by injection of human IgG in rats pre-immunized with human IgG (23). Immune complex glomerulonephritis is observed within a few weeks, accompanied by proliferation of mesangial cells and influx of macrophages. At the electron microscopic level, subepithelial and mesangial electron-dense deposits can be observed within the glomerulus (24). After 10 to 20 weeks, the rats develop mesangial matrix expansion followed by glomerulosclerosis and interstitial fibrosis.

In the mouse, chronic graft-versus-host (GVH) disease is used as a model for human membranous glomerulonephritis. Injection of parental-derived donor lymphocytes into F1-hybrids results in polyclonal B-cell activation (25). An array of autoantibodies is produced that can bind directly to the glomerular capillary wall. Immunofluorescence microscopy shows granular localization of immunoglobulins along the GBM in the mesangial area. The mice show global glomerulosclerosis 10 to 12 weeks after the induction of the disease (26).

Anti-glomerular basement membrane nephritis (anti-GBM) can be induced in mice through injection of rabbit anti-GBM antibodies. The antibody can be prepared by immunization of rabbits with mouse GBM (27). Animals develop glomerulonephritis and glomerulosclerosis within 14 days after injection.

Diabetic nephropathy

In several studies described in this thesis, we have focused our research on the development of glomerulosclerosis in patients with DN. DN is the most common cause of ESRD (1). After retinopathy, it is the most prevalent complication in patients with type 2 diabetes (28). Type 2 diabetes accounts for approximately 90% of all cases of diabetes. It is caused by a decreased response of liver and muscles to insulin or a disorganized insulin secretion by β-cells in the pancreas. As a result of these changes, patients experience high blood glucose levels. Diabetes mellitus can also lead to chronic vascular complications, which are the most important causes of morbidity and mortality. These consist of microvascular complications (microangiopathy) leading to retinopathy, neuropathy, and nephropathy, or macrovascular complications (macroangiopathy) leading to cardiovascular diseases. These vasculopathies are likely to result from endothelial cell dysfunction and damage caused by metabolic and hemodynamic factors (29).

DN is morphologically characterized by expansion of the mesangial matrix, thickening of the glomerular and tubular basement membranes, and glomerular hypertrophy (30). These features precede the development of glomerulosclerosis and interstitial fibrosis and the onset of the progression to ESRD. Nodular glomerulosclerosis, a characteristic pathological feature

first described by Kimmelstiel and Wilson (Kimmelstiel-Wilson lesion) (31), refers to the appearance of eosinophilic nodules at the periphery of the glomerulus. The nodules are the result of an expansion of the mesangium in combination with progressive occlusion of the glomerular capillaries (32). Red blood cell fragments in such lesions in combination with the presence of activated plasminogen activator inhibitor 1 indicate microvascular injury and mesangiolysis in DN (33).

Although many factors whose expression is associated with the progression of DN have been identified, the precise pathogenesis of this disease is still unknown. Several mechanisms by which diabetes can cause ESRD have been proposed (34-36). The most important postulated risk factors for DN are systemic hypertension, hyperglycemia, cigarette smoking, hyperlipidemia, duration of diabetes mellitus, dietary protein intake, and genetic predisposition (37,38). The following paragraphs provide an overview of several factors involved in the progression of DN.

Metabolic factors in the progression of DN

An increased blood glucose level is a major risk factor for the onset and progression of DN. Hyperglycemia mediates its effect in several ways. First of all, activation of the protein kinase C (PKC)-MAP kinase pathway plays a prime role in the development and progression of early tissue damage in DN (39,40). PKC has been implicated as a cause of altered renal blood flow (41) and of induction of several growth factors and ECM production in the diabetic kidney (42-47).

Progression of DN may be accelerated by the formation of metabolic derivatives such as oxidants and glycation products. Formation of reactive oxygen species due to metabolic changes in diabetes can contribute to the development of DN via oxidative stress and increased oxygen consumption (48).

Accelerated non-enzymatic glycation in diabetes, resulting from high glucose levels, is also linked to the pathogenesis of DN (49-52). This glycation, called the Amadori reaction, is a reaction between sugar molecules and polypeptides that irreversibly generates advanced glycation end products (AGEs) (53). AGEs can stimulate ECM production through activation of growth factors (54-58). There is also evidence that AGEs induce transition of tubular epithelial cells to myofibroblasts, which are major producers of ECM (59). Because of the slow turnover of ECM molecules, these proteins are highly susceptible to modification by AGEs, which possibly leads to decreased susceptibility of ECM proteins to degradation by MMPs (60). AGEs exert their effects on cells by interacting with specific cellular receptors, e.g., the receptor for advanced glycation endproducts (RAGE). This AGE-RAGE interaction can lead to cellular oxidative stress, resulting in several cellular responses, including activation of transcription factors.

Hemodynamic factors in the progression of diabetic nephropathy

Activation of the renin-angiotensin system (RAS) is one of the major mechanisms for changes in renal hemodynamics contributing to the progression of DN. Apart from the circulating RAS that regulates blood pressure, fluid-, and electrolyte balance, the kidney has an independently regulated local RAS (61). In the tubular cells and glomeruli, renin and angiotensinogen are expressed (62,63). High glucose activates the intrarenal RAS in cultured mesangial cells, resulting in decreased matrix degradation and increased matrix accumulation via induction of TGF-ß1 secretion (64). Streptozotocin (STZ)-induced diabetes in rats is accompanied by an increase of renin mRNA in the proximal tubules and by downregulation of cortical angiotensin receptors in the renal cortex (65).

The endothelin system is another mechanism in the kidney that regulates renal hemodynamics (66). Endothelin-1 (ET-1) is one of the most potent vasoconstrictors and acts as a paracrine and autocrine factor (67). ET-1 is present in the kidney, where it is secreted by mesangial (68), endothelial (69), and tubular epithelial cells (70). ET-1 production increases under high glucose conditions via TGF-ß stimulation (33,71,72) and by shear-stress as a result of glomerular hyperfiltration (73). ET-1 can stimulate cell proliferation and increase the expression of PDGF (74). Studies on the expression of ET-1 in diabetic animal models show conflicting results. Some studies show increased urine ET-1 levels in diabetic animals (75), while others found that renal ET-1 mRNA expression and protein were significantly reduced in diabetic kidneys (76). In hypertensive patients with type 2 diabetes, plasma ET-1 concentrations were increased compared to control subjects. This increase could be reduced by enalapril or nicardipine treatment (77).

Genetic predisposition to DN

Although blood glucose levels are often poorly controlled in diabetes mellitus, 60–70% of patients with type 2 diabetes mellitus never develop DN. Several studies show a higher incidence of DN in some families or ethnic populations (78-80). The prevalence of DN in diabetic patients with siblings with DN is about 50% higher than that in diabetic patients whose have siblings do not have DN (81). This observation suggests that a genetic predisposition underlies the progression of DN. Indeed, several single nucleotide polymorphisms (SNPs) associated with DN have been described. Two DN-related polymorphisms in the endothelial nitric oxide synthase gene have been identified (82). Others have found DN-related SNPs in the PKC-β1 gene (83), in the solute carrier family 12 member 3 gene (84), and in glutamine/fructose-6-phosphate amidotransferase-2 (85). Vardarli et al. found a strong linkage of chromosome 18q (LOD score of 6.1) with the occurrence of DN in Turkish families with type 2 diabetes mellitus (86). This

locus was confirmed by a genome-wide, gene-based SNP search for DN-related susceptibility genes in African-Americans (87).

Animal models for diabetic nephropathy

Several animal models for DN have been described in the literature. Mice and rats can be made diabetic by a single injection of STZ, providing a model for human insulin-dependent diabetes mellitus. There are several genetic knockout and transgenic mouse models for diabetes. These include the hypoinsulinemic non-obese diabetic (NOD) mouse, the Kkay mouse, the New Zealand obese mouse, the hyperinsulinemic ob/ob mouse, and the different strains of obese hyperinsulinemic db/db mice [summarized by Allen et al. (88)]. Each of model displays some morphological changes in the kidney that resemble those seen in diabetic patients. The db/db mouse model has been the most extensively investigated model for human DN. Db/db mice display substantial glomerular pathology, including mesangial matrix expansion and modest albuminuria. Diabetes can also be induced in PVG.RT1 rats. These relatively T-cell deficient rats develop diabetes after adult thymectomy and sublethal irradiation (89). More recently, OVE26 mice have been described as a transgenic model of severe, early-onset type 1 diabetes (90). These mice develop diabetes within the first weeks of life and survive well over one year without insulin treatment. The OVE26 mice show most of the characteristics of human DN, including glomerular hypertrophy and mesangial matrix expansion, followed by diffuse and nodular sclerosis, and tubulointerstitial fibrosis. The GFR of these mice increases significantly between 2 and 3 months of age and then decreases between 5 and 9 months.

Growth factors in renal diseases

TGF-β

Growth factors play a role in the progression of renal diseases. They mediate ECM homeostasis by increasing ECM production and diminishing degradation of ECM proteins. Growth factors can indirectly influence progression of renal disease via their proliferative and chemoattractive effects on cells that are involved in ECM homeostasis. TGF-β is one of the first and most extensively investigated growth factors in the progression of renal diseases. It is a 25-kD protein that is secreted in a latent form and requires cleaving before it can become active. The release of the latency-associated protein from the mature TGF-β protein by enzymes such as trombospondin and plasmin (91,92) is necessary for activation (93). TGF-β can directly induce ECM production in mesangial cells (94-97). TGF-β can also promote matrix accumulation via downregulation of MMPs or upregulation of tissue inhibitors of metalloproteinases (TIMPs) (98-100). TGF-β can also contribute to matrix expansion via induction of expression of receptors

for (circulating) matrix molecules. Kagami et al. have shown that TGF-ß can induce mRNA expression of α1β1 integrin in mesangial cells, resulting in a significant increase in adhesion of fibronectin, collagen I, and laminin to these cells (101).

In experimental animal models, Border et al. identified an important role for TGF-β in anti-Thy-1 nephritis (102). Administration of the natural TGF-β inhibitor decorin or antibodies against TGF-β to glomerulonephritic rats suppressed glomerular matrix production and prevented matrix accumulation (103,104). These findings have stimulated investigation of TGF-β in experimental renal diseases and human renal diseases. For example, TGF-β has been widely investigated in animal models for DN (58,105) and in anti-GBM nephritis (106,107). On the other hand, in mice suffering from chronic GVH disease, there was no evidence for a role of TGF-β in the development of glomerulosclerosis (108), indicating that TGF-β is not always necessary for the development of glomerulosclerosis.

Although there is considerable evidence for the role of TGF-β in the development of glomerulosclerosis in animal models, the evidence for its role in the development of glomerulosclerosis in patients is less convincing. Iwano et al., using quantitative RT-PCR, found higher expression of TGF-β1 mRNA in glomeruli of patients with DN (109). An increase of TGF-β expression has also been described in other renal diseases (110,111), including IgA nephropathy (112,113) and membranous nephropathy (114). On the other hand, in a study of patients with lupus nephritis and glomerulosclerosis, there was no increase of TGF-β mRNA in glomeruli (108). In biopsies from transplanted kidneys with acute rejection, higher levels of TGF-β were found compared to control tissue (115-118). Eikmans et al. showed that relatively high levels of TGF-β during acute rejection are associated with good prognosis (119). They hypothesized that TGF-β has beneficial effects during acute rejection through its anti-inflammatory actions or as an inducer of tissue repair. Until now, the precise role for TGF-β in progression of human renal disease has not yet been entirely clarified.

VEGF

VEGF, a highly conserved homodimeric glycoprotein with a relative molecular mass of 45 kD, is the only mitogen that specifically acts on endothelial cells. In addition to its potent mitogenic actions, VEGF also plays a prominent role in developmental angiogenesis (120). It can bind to Flk1, the major cell surface receptor for VEGF, which is exclusively expressed in endothelial cells (121). Hypoxia and hypoglycemia are major stimulators of VEGF expression (122). Hypoxia-induced transcription of VEGF mRNA is mediated, at least in part, by the binding of hypoxia-inducible factor 1 alpha (HIF-1α) to the VEGF promoter (123). More recently, hypoxia-induced c-Src thyrosine kinase activation was found to be another mechanism involved in VEGF induction (124). Other factors, including AGEs, PDGF, angiotensin II, nitric oxide,

prostaglandins, estrogen, and thyroid-stimulating hormone can also up regulate VEGF expression *in vitro* (125-130).

In the normal kidney, VEGF is present in podocytes and tubular epithelial cells, while it is absent in glomerular endothelial and mesangial cells (131). The specific mechanism by which VEGF may influence glomerular filtration is unknown. It has been suggested that VEGF is important for the maintenance of glomerular endothelial cells and that lowering local or circulating VEGF levels results in abnormal remodeling of the glomerular capillaries (132,133). Treatment of STZ-induced diabetic rats with monoclonal anti-VEGF antibodies decreases hyperfiltration, albuminuria, and glomerular hypertrophy (134). In the same model, VEGF was reduced in the glomeruli one week after induction (135). This reduction can be restored by treatment of the rats with insulin. Decreased VEGF expression was recently documented in the remnant kidney model, and treatment of these animals with VEGF reduces renal fibrosis (136). Administration of VEGF to rats after induction of anti-Thy-1 nephritis leads to enhanced endothelial cell proliferation and glomerular capillary repair (137). Proliferating endothelial cells were found in the mesangiolytic lesions and aneurysms. Thereafter, a new glomerular capillary network developed. In rats with anti-Thy-1 nephritis, a positive association was seen between impairment of vascular regeneration and the development of glomerulosclerosis (137-139). Studies in mice showed that both glomerular-selective depletion or overexpression of VEGF-A leads to glomerular abnormalities (140).

In glomeruli of patients suffering from DN, a decrease of VEGF mRNA has been described (132,133,141). At the same time, no correlation was found between renal function and circulating VEGF levels (142), indicating that local VEGF production seems to be more important for endothelial cell maintenance than circulating VEGF. In idiopathic membranous glomerulonephritis and in minimal change disease, expression of VEGF mRNA was considerably reduced compared to controls (143,144). In cell culture experiments on VEGF, opposing results have been obtained. Deposition of glycosylated IgA proteins result in reduced VEGF synthesis by mesangial cells (145), while high glucose can directly increase VEGF expression in mesangial cells via the PKC pathway (45,146). In the retinal pigment epithelial cell line, it has been shown that glycosylated albumin stimulates VEGF expression through an ERK-dependent pathway (147). In podocytes, high glucose induces activator protein-1–dependent transcriptional activity and expression of VEGF. AGE-induced activation of monocytes/macrophages resulted in augmented induction of VEGF and other angiogenic and inflammatory factors in these cells (148).

CTGF

CTGF is encoded by a 2.4-kb mRNA molecule. Northern blot analysis has shown that CTGF is

expressed in a wide variety of human tissues (149). It is a major chemotactic and mitogenic factor for connective tissue cells (150) and is associated with both systemic and localized fibrotic diseases and ECM synthesis (151-154). CTGF gene expression is increased in human fibroblasts upon stimulation with TGF-β but not with PDGF, epidermal growth factor, or basic fibroblast growth factor (bFGF) (155). Induction of CTGF expression in epithelial cells can occur directly via HIF-1α, independently of TGF-β (156). In addition to the fibrotic properties of CTGF, it is a potent angiogenic factor (157,158). It can regulate progression in invasive tumor angiogenesis by inducing expression of MMPs and by decreasing expression of TIMPs by vascular endothelial cells (159). The precise molecular mechanisms of CTGF's action as a growth factor are not completely known. Although much research has focused on unraveling its signaling pathway, a specific receptor has not yet been found.

In normal kidneys, CTGF mRNA is expressed mainly by visceral epithelial cells and to a lesser extent in parietal epithelial cells and interstitial fibroblasts (160). The role of CTGF in the normal kidney is still unclear, but we hypothesize that glomerular CTGF, in combination with other angiogenic factors such as VEGF, contributes to the normal maintenance of glomerular endothelial cells.

CTGF expression is increased in glomeruli and tubulointerstitial lesions from patients with glomerulonephritis, including IgA nephropathy, crescentic glomerulonephritis, lupus nephritis, and membranoproliferative glomerulonephritis. CTGF is involved in cellular proliferation and matrix accumulation (160-162).

Suppression subtractive hybridization techniques showed that CTGF is highly expressed in mesangial cells under high glucose conditions (163,164). This finding in mesangial cells was confirmed by others (165,166). Angiotensin II can induce CTGF in proximal tubular cells *in vitro* (71).

An increase in CTGF mRNA has been found in glomeruli of microalbuminuric and overt albuminuric patients compared to healthy and normo-albuminuric patients (167). In this study, it was proposed that CTGF mRNA, in combination with other glomerular mRNA markers chosen because of their pathogenetic relevance, may complement albuminuria and histology in predicting progression of DN. In diabetic NOD mice, a correlation was found between CTGF mRNA levels and the duration of diabetes. The most prominent mesangial CTGF immunostaining was seen in older animals (164). Other animal models for DN also showed an increase in CTGF mRNA and protein expression (165,168). Treatment of these animals with aminoguanidine or aspirin attenuated mesangial expansion suppressed CTGF induction and inhibited upregulation of TGF-β1 and fibronectin expression (169,170).

mRNA detection methods

To study the development of glomerulosclerosis, measurements of mRNA levels can be used as tools to investigate the molecular mechanisms behind this process. The genomic DNA itself does not direct protein synthesis, but uses mRNA as an intermediary molecule. The nucleotide sequence of the appropriate portion of the DNA molecule in a chromosome is first transcribed into mRNA. These mRNA molecules are used as templates for protein synthesis, a process called translation (Fig. 4). Proteins can be further modified posttranslationally. Quantification of gene expression levels in cells is important for investigating the gene patterns responsible for cell behavior during disease progression and response or resistance to treatment. Gene expression levels can also be used as a diagnostic tool (171) or as a predictor for disease outcome (119). Different techniques are available to measure gene expression levels.

Northern blot

One of the most conventional techniques for assessment of mRNA expression is Northern blot analysis. Negatively charged RNA is loaded into an agarose gel, and a negative current is applied to repel to molecules toward the positively charged electrical current at the opposite end of the gel. Because smaller RNA molecules move faster through the gel, RNA molecules are separated by size. The separated RNA molecules are transferred to a nylon filter, which is then

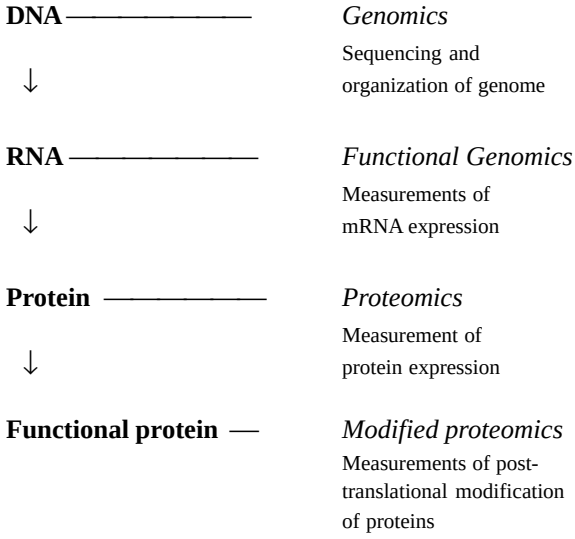

Figure 4. Transcription and translation: Genetic information is transcribed from DNA into mRNA and then translated from mRNA to protein. Proteins can be further modified posttranslationally to alter their function.

hybridized with a labeled, single-stranded DNA fragment encoding the gene of interest. The visualized DNA probe on the membrane is a measure for the expression level of the gene. With this labor-intensive technique, one can only quantify one gene at a time (Fig. 5). The sensitivity of Northern blotting is relatively low.

RNase protection assay

Another technique to quantify mRNA levels is the ribonuclease (RNase) protection assay (RPA). The principle of this method is based on protection against nucleases though specific binding of labeled antisense RNA probes. Subsequent treatment with RNase results in progressive cleavage of the overhanging mRNA sequence until the antisense RNA is hybridized only with the mRNA sequence of interest. Size-fractionation by denaturing gel electrophoresis can identify the sizes of different RNA probes. The amount of protected, labeled antisense probe corresponds with the relative gene transcription level of the mRNA sample. With this method, 5 to 20 genes can be quantified in one run.

RNA in situ *hybridization*

Hybridization of a gene-specific probe to tissue on the slide in combination with immunohistochemistry with cell-specific markers can give a detailed expression pattern showing which cells are expressing the particular mRNA transcript in the tissue. With the RNA *in situ* hybridization procedure, a labeled probe is hybridized to mRNA molecules present in frozen or paraffin sections. Optimal results are obtained with the use of an antisense riboprobe, which is generated by *in vitro* transcription of a cDNA cloned in a suitable vector. The labeled probe binds only to places in the tissue where the complementary mRNA is present.

Real-time PCR

PCR is based on the logarithmic amplification of specific DNA sequences. The first step in the analysis of mRNA is generation of cDNA copies from the mRNA molecules using reverse transcriptase in combination with Oligo-dT or random hexamer primers (172). The cDNA molecules can be used as templates for further amplification. One of the major problems with conventional PCR technique is the lack of correlation between the amount of cDNA input and the eventual amount of PCR product. This problem can be overcome by the use of quantitative real-time PCR (173). The principle of this method is continuous monitoring of the amplification with the use of a fluorescent probe that gives a signal when it binds to generated DNA. The real-time PCR machine can detect the fluorescent dye. This method makes quantitative comparisons of amplifications during the linear range possible. This method shows a high correlation with generated fluorescence and the amount of input cDNA and makes it possible

to quantify mRNA levels in samples containing 1 to 10 pg RNA.

Microarray analysis

Traditional efforts to understand disease pathogenesis have relied on a gene-by-gene analysis strategy, thereby limiting our abilities to devise novel therapeutic approaches. With the use of DNA microarray techniques (also known as DNA-chip technology), it is possible to generate mRNA expression profiles of thousands of genes within one sample. Two basic types of DNA microarrays are currently available: oligonucleotide arrays (174) and cDNA arrays (175). In the case of oligonucleotide arrays, 25-nucleotide–long fragments of known DNA sequences are synthesized *in situ* on the surface of the chip by using a series of light-directed coupling reactions similar to photolithography. By using this method, as many as 400,000 distinct sequences representing over 18,000 genes can be synthesized on a single 1.3-×-1.3-cm microarray chip. In the case of cDNA microarrays, cDNA fragments are placed onto the surface of a glass slide using a robotic spotting device. Both approaches involve hybridization of fluorescent labeled cRNA or cDNA material isolated from the tissue of interest (e.g., from renal biopsies or isolated glomeruli) to the microarray. The surface of the microarray slides is then scanned with a laser scanning device, which measures the fluorescence intensity at each position on the microarray. The fluorescence intensity of each spot on the array is proportional to the level of expression of the gene represented by that spot. This analysis results in an enormous amount of information, which needs careful indexing, storage, and organization. Computers are required for storage, distribution, and analysis of the data. The principal data banks holding such gene expression profiles are GenBank at the U.S. National Institutes of Health in Bethesda, Maryland, and the EMBL Sequence Data Base at the European Molecular Biology Laboratory in Heidelberg. These databases continuously exchange newly reported data and make them available via the Internet to biologists throughout the world. Computer programs are available to cluster genes in relation to each other or in relation to the disease. These techniques can be used to unravel the complexities of kidney diseases.

	Sensitivity	Input	No of genes	Quantitative	Tissue localization
Northern blot	+	10 µg	1	++	-
RPA	++	1-5 µg	5-20	++	-
Real time PCR	+++	1-10 pg	1	++	-
Microarray	+	1-20µg	$1\text{-}2*10^4$	+	-
RISH	+	1 slide	1	$\pm$	+++

Figure 5. Characteristics of different mRNA detection methods

Aims of this thesis

The central aim of the studies described in this thesis was to investigate the molecular mechanisms underlying the development of glomerulosclerosis in human renal diseases. To achieve this, measurements of mRNA steady-state levels can be used to obtain insights into the molecular processes occurring in the kidney. To study mRNA expression in the development of sclerosis in the glomerulus, it is important to isolate high-quality RNA from purified glomeruli. The aim of the first study was to assess the feasibility of isolating glomeruli from mouse kidneys and extracting their RNA (**Chapter 2**). Previous studies have shown that the ECM molecule fibronectin is abundantly present in glomerulosclerotic lesions. Fibronectin can be alternatively spliced at the EDA, EDB, and V regions, thereby generating different fibronectin isoforms. The aim of our second study was to investigate which fibronectin isoforms are present in biopsies from patients with kidney diseases leading to glomerulosclerosis (**Chapter 3**). To study the regulation of alternative splicing of fibronectin, we also investigated splicing at the mRNA level. For this, we used different animal models to test the presence of alternatively spliced EDA and EDB regions and correlated this with the presence of TFG-β. Cell culture experiments with rat mesangial cells were performed to study the effect of the cytokines TGF-β and IL-4 on the splicing of fibronectin mRNA *in vitro*. Finally, we measured mRNA levels of TGF-ß and fibronectin and the splicing pattern for fibronectin mRNA in human renal biopsies from patients developing glomerulosclerosis. These data were compared with data obtained from the animal models and cell culture experiments (**Chapter 4**).

In addition to assessing local fibronectin production, we also investigated trapping of plasma fibronectin from the circulation during the development of glomerulosclerosis. Earlier studies have shown that plasma fibronectin from the circulation can accumulate in glomerulosclerotic lesions. The aim of this study was to obtain more insight into the binding sites that play a role in the accumulation of fibronectin in pre-sclerotic glomeruli (**Chapter 5**). We also investigated the role of the heparin-binding domain on the binding of fibronectin in glomerulosclerotic lesions.

In **Chapter 6,** our goal was to identify genes and molecular pathways that are involved in the progression of DN. With the evolution of microarray techniques, it is possible to measure thousands of genes within one sample. We have used this powerful technique to measure gene expression levels in glomeruli from patients suffering from DN.

From the microarray studies, we found that several genes involved in angiogenesis were differentially expressed in patients with DN. We confirmed these data in biopsies from a larger patient group suffering from DN. The data were correlated with clinical and histological data of the patients to examine the role of angiogenic factors in different stages of the disease (**Chapter 7**).

References

1. Andersen AR, Christiansen JS, Andersen JK, Kreiner S, Deckert T: Diabetic nephropathy in Type 1 (insulin-dependent) diabetes: an epidemiological study. *Diabetologia* 25:496-501, 1983
2. Tryggvason K, Kouvalainen K: Number of nephrons in normal human kidneys and kidneys of patients with the congenital nephrotic syndrome. A study using a sieving method for counting of glomeruli. *Nephron* 15:62-68, 1975
3. Rostgaard J, Qvortrup K: Electron microscopic demonstrations of filamentous molecular sieve plugs in capillary fenestrae. *Microvasc Res* 53:1-13, 1997
4. Haraldsson B, Sorensson J: Why do we not all have proteinuria? An update of our current understanding of the glomerular barrier. *News Physiol Sci* 19:7-10.:7-10, 2004
5. Comper WD, Lee AS, Tay M, Adal Y: Anionic charge concentration of rat kidney glomeruli and glomerular basement membrane. *Biochem J* 289:647-652, 1993
6. Laurie GW, Leblond CP, Inoue S, Martin GR, Chung A: Fine structure of the glomerular basement membrane and immunolocalization of five basement membrane components to the lamina densa (basal lamina) and its extensions in both glomeruli and tubules of the rat kidney. *Am J Anat* 169:463-481, 1984
7. Ahola H, Heikkila E, Astrom E, Inagaki M, Izawa I, Pavenstadt H, Kerjaschki D, Holthofer H: A novel protein, densin, expressed by glomerular podocytes. *J Am Soc Nephrol* 14:1731-1737, 2003
8. Pavenstadt H: Roles of the podocyte in glomerular function. *Am J Physiol Renal Physiol* 278:F173-F179, 2000
9. Kestila M, Lenkkeri U, Mannikko M, Lamerdin J, McCready P, Putaala H, Ruotsalainen V, Morita T, Nissinen M, Herva R, Kashtan CE, Peltonen L, Holmberg C, Olsen A, Tryggvason K: Positionally cloned gene for a novel glomerular protein—nephrin—is mutated in congenital nephrotic syndrome. *Mol Cell* 1:575-582, 1998
10. Miner JH: Renal basement membrane components. *Kidney Int* 56:2016-2024, 1999
11. Van Vliet AI, Van Alderwegen IE, Baelde HJ, De Heer E, Killen PD, Kalluri RK, Bruijn JA, Bergijk EC: Differential expression of collagen type IV alpha-chains in the tubulointerstitial compartment in experimental chronic serum sickness nephritis. *J Pathol* 189:279-287, 1999
12. Kootstra CJ, Bergijk EC, Veninga A, Prins FA, De Heer E, Abrahamson DR, Bruijn JA: Qualitative alterations in laminin expression in experimental lupus nephritis. *Am J Pathol* 147:476-488, 1995
13. Stetler-Stevenson WG: Dynamics of matrix turnover during pathologic remodeling of the extracellular matrix. *Am J Pathol* 148:1345-1350, 1996
14. Border WA: Transforming growth factor-beta and the pathogenesis of glomerular diseases. *Curr Opin Nephrol Hypertens* 3:54-58, 1994
15. Floege J, Johnson RJ: Multiple roles for platelet-derived growth factor in renal disease. *Miner Electrolyte Metab* 21:271-282, 1995
16. Staley JP, Guthrie C: Mechanical devices of the spliceosome: motors, clocks, springs, and things. *Cell* 92:315-326, 1998
17. Vleming LJ, Baelde JJ, Westendorp RG, Daha MR, van Es LA, Bruijn JA: The glomerular deposition of PAS positive material correlates with renal function in human kidney diseases. *Clin Nephrol* 47:158-167, 1997
18. Ruoslahti E: Fibronectin and its receptors. *Annu Rev Biochem* 57:375-413, 1988
19. Alonso J, Mampaso F, Martin A, Palacios I, Egido J: Changes in the pattern of fibronectin mRNA alternative splicing in acute experimental mesangioproliferative nephritis. *Lab Invest* 79:185-194, 1999
20. Zuk A, Bonventre JV, Matlin KS: Expression of fibronectin splice variants in the postischemic rat kidney. *Am J Physiol Renal Physiol* 280:F1037-F1053, 2001
21. Bagchus WM, Hoedemaeker PJ, Rozing J, Bakker WW: Glomerulonephritis induced by monoclonal anti-Thy 1.1 antibodies. A sequential histological and ultrastructural study in the rat. *Lab Invest* 55:680-687, 1986
22. Aben JA, Hoogervorst DA, Paul LC, Borrias MC, Noble NA, Border WA, Bruijn JA, De Heer E: Genes expressed by the kidney, but not by bone marrow-derived cells, underlie the genetic predisposition to progressive glomerulosclerosis after mesangial injury. *J Am Soc Nephrol* 14:2264-2270, 2003
23. Bergijk EC, Baelde HJ, De Heer E, Killen PD, Bruijn JA: Role of the extracellular matrix in the development of glomerulosclerosis in experimental chronic serum sickness. *Exp Nephrol* 3:338-347, 1995
24. Furness PN, Turner DR: Chronic serum sickness glomerulonephritis: removal of glomerular antigen and electron-dense deposits is largely dependent on plasma complement. *Clin Exp Immunol* 74:126-130, 1988
25. Bruijn JA, Elven van EH, Hogendoorn PCW, Corver WE, Hoedemaker PJ: Murine chronic graft-versus-host disease as a model for lupus nephritis. Animal model of human disease. *Am J Pathol*

130(3):639-641, 1988
26. Bergijk EC, Munaut C, Baelde JJ, Prins F, Foidart JM, Hoedemaeker PJ, Bruijn JA: A histologic study of the extracellular matrix during the development of glomerulosclerosis in murine chronic graft-versus-host disease. *Am J Pathol* 140:1147-1156, 1992
27. Schrijver G, Bogman MJ, Assmann KJ, de Waal RM, Robben HC, van Gasteren H, Koene RA: Anti-GBM nephritis in the mouse: role of granulocytes in the heterologous phase. *Kidney Int* 38:86-95, 1990
28. John L, Kirubakaran MG, Shastry JC: Diabetic nephropathy: a clinical study of 498 patients. *J Diabet Complications* 1:87-90, 1987
29. Stehouwer CDA, Lambert J, Donker AJM, van Hinsbergh VWM: Endothelial dysfunction and pathogenesis of diabetic angiopathy. *Cardiovasc Res* 34:55-68, 1997
30. Ziyadeh FN: The extracellular matrix in diabetic nephropathy. *Am J Kidney Dis* 22:736-744, 1993
31. Kimmelstiel P, Wilson C: Intercapillary lesions in glomeruli of kidney. *Am J Pathol* 12:83, 1936
32. Grcevska L, Polenakovic M, Petrusevska G: Diabetic glomerulosclerosis without overt diabetes mellitus. *Nephron* 90:106-108, 2002
33. Paueksakon P, Revelo MP, Ma LJ, Marcantoni C, Fogo AB: Microangiopathic injury and augmented PAI-1 in human diabetic nephropathy. *Kidney Int* 61:2142-2148, 2002
34. Wolf G: Growth factors and the development of diabetic nephropathy. *Curr Diab Rep* 3:485-490, 2003
35. Stitt AW, Jenkins AJ, Cooper ME: Advanced glycation end products and diabetic complications. *Expert Opin Investig Drugs* 11:1205-1223, 2002
36. Lehmann R, Schleicher ED: Molecular mechanism of diabetic nephropathy. *Clin Chim Acta* 297:135-144, 2000
37. Shumway JT, Gambert SR: Diabetic nephropathy-pathophysiology and management. *Int Urol Nephrol* 34:257-264, 2002
38. Caramori ML, Mauer M: Diabetes and nephropathy. *Curr Opin Nephrol Hypertens* 12:273-282, 2003
39. Whiteside CI, Dlugosz JA: Mesangial cell protein kinase C isozyme activation in the diabetic milieu. *Am J Physiol Renal Physiol* 282:F975-F980, 2002
40. Toyoda M, Suzuki D, Honma M, Uehara G, Sakai T, Umezono T, Sakai H: High expression of PKC-MAPK pathway mRNAs correlates with glomerular lesions in human diabetic nephropathy. *Kidney Int* 66:1107-1114, 2004
41. Kirton CA, Loutzenhiser R: Alterations in basal protein kinase C activity modulate renal afferent arteriolar myogenic reactivity. *Am J Physiol* 275:H467-H475, 1998
42. Datta K, Li J, Karumanchi SA, Wang E, Rondeau E, Mukhopadhyay D: Regulation of vascular permeability factor/vascular endothelial growth factor (VPF/VEGF-A) expression in podocytes. *Kidney Int* 66:1471-1478, 2004
43. Ikehara K, Tada H, Kuboki K, Inokuchi T: Role of protein kinase C-angiotensin II pathway for extracellular matrix production in cultured human mesangial cells exposed to high glucose levels. *Diabetes Res Clin Pract* 59:25-30, 2003
44. Lin S, Sahai A, Chugh SS, Pan X, Wallner EI, Danesh FR, Lomasney JW, Kanwar YS: High glucose stimulates synthesis of fibronectin via a novel protein kinase C, Rap1b, and B-Raf signaling pathway. *J Biol Chem* 277:41725-41735, 2002
45. Hoshi S, Nomoto K, Kuromitsu J, Tomari S, Nagata M: High glucose induced VEGF expression via PKC and ERK in glomerular podocytes. *Biochem Biophys Res Commun* 290:177-184, 2002
46. Takeda M, Babazono T, Nitta K, Iwamoto Y: High glucose stimulates hyaluronan production by renal interstitial fibroblasts through the protein kinase C and transforming growth factor-beta cascade. *Metabolism* 50:789-794, 2001
47. Park SH, Choi HJ, Lee JH, Woo CH, Kim JH, Han HJ: High glucose inhibits renal proximal tubule cell proliferation and involves PKC, oxidative stress, and TGF-beta 1. *Kidney Int* 59:1695-1705, 2001
48. Palm F, Cederberg J, Hansell P, Liss P, Carlsson PO: Reactive oxygen species cause diabetes-induced decrease in renal oxygen tension. *Diabetologia* 46:1153-1160, 2003
49. Cohen MP, Ziyadeh FN: Role of Amadori-modified nonenzymatically glycated serum proteins in the pathogenesis of diabetic nephropathy. *J Am Soc Nephrol* 7:183-190, 1996
50. Makino H, Shikata K, Kushiro M, Hironaka K, Yamasaki Y, Sugimoto H, Ota Z, Araki N, Horiuchi S: Roles of advanced glycation end-products in the progression of diabetic nephropathy. *Nephrol Dial Transplant* 11:76-80, 1996
51. Bucala R, Vlassara H: Advanced glycosylation end products in diabetic renal and vascular disease. *Am J Kidney Dis* 26:875-888, 1995

52. Cohen MP, Hud E, Wu VY: Amelioration of diabetic nephropathy by treatment with monoclonal antibodies against glycated albumin. *Kidney Int* 45:1673-1679, 1994
53. Sharma SD, Pandey BN, Mishra KP, Sivakami S: Amadori product and age formation during nonenzymatic glycosylation of bovine serum albumin in vitro. *J Biochem Mol Biol Biophys* 6:233-242, 2002
54. Abe H, Matsubara T, Iehara N, Nagai K, Takahashi T, Arai H, Kita T, Doi T: Type IV collagen is transcriptionally regulated by Smad1 under advanced glycation end product (AGE) stimulation. *J Biol Chem* 279:14201-14206, 2004
55. Yamagishi S, Inagaki Y, Okamoto T, Amano S, Koga K, Takeuchi M, Makita Z: Advanced glycation end product-induced apoptosis and overexpression of vascular endothelial growth factor and monocyte chemoattractant protein-1 in human-cultured mesangial cells. *J Biol Chem* 277:20309-20315, 2002
56. Kelly DJ, Gilbert RE, Cox AJ, Soulis T, Jerums G, Cooper ME: Aminoguanidine ameliorates overexpression of prosclerotic growth factors and collagen deposition in experimental diabetic nephropathy. *J Am Soc Nephrol* 12:2098-2107, 2001
57. Kim YS, Kim BC, Song CY, Hong HK, Moon KC, Lee HS: Advanced glycosylation end products stimulate collagen mRNA synthesis in mesangial cells mediated by protein kinase C and transforming growth factor-beta. *J Lab Clin Med* 138:59-68, 2001
58. Tsuchida K, Makita Z, Yamagishi S, Atsumi T, Miyoshi H, Obara S, Ishida M, Ishikawa S, Yasumura K, Koike T: Suppression of transforming growth factor beta and vascular endothelial growth factor in diabetic nephropathy in rats by a novel advanced glycation end product inhibitor, OPB-9195. *Diabetologia* 42:579-588, 1999
59. Oldfield MD, Bach LA, Forbes JM, Nikolic-Paterson D, McRobert A, Thallas V, Atkins RC, Osicka T, Jerums G, Cooper ME: Advanced glycation end products cause epithelial-myofibroblast transdifferentiation via the receptor for advanced glycation end products (RAGE). *J Clin Invest* 108:1853-1863, 2001
60. Mott JD, Khalifah RG, Nagase H, Shield CF, III, Hudson JK, Hudson BG: Nonenzymatic glycation of type IV collagen and matrix metalloproteinase susceptibility. *Kidney Int* 52:1302-1312, 1997
61. Carey RM, Siragy HM: Newly Recognized Components of the Renin-Angiotensin System: Potential Roles in Cardiovascular and Renal Regulation. *Endocr Rev* 24:261-271, 2003
62. Lai KN, Leung JC, Lai KB, To WY, Yeung VT, Lai FM: Gene expression of the renin-angiotensin system in human kidney. *J Hypertens* 16:91-102, 1998
63. Zimpelmann J, Kumar D, Levine DZ, Wehbi G, Imig JD, Navar LG, Burns KD: Early diabetes mellitus stimulates proximal tubule renin mRNA expression in the rat. *Kidney Int* 58:2320-2330, 2000
64. Singh R, Alavi N, Singh AK, Leehey DJ: Role of angiotensin II in glucose-induced inhibition of mesangial matrix degradation. *Diabetes* 48:2066-2073, 1999
65. Wehbi GJ, Zimpelmann J, Carey RM, Levine DZ, Burns KD: Early streptozotocin-diabetes mellitus downregulates rat kidney AT2 receptors. *Am J Physiol Renal Physiol* 280:F254-F265, 2001
66. Abassi ZA, Ellahham S, Winaver J, Hoffman A: The Intrarenal Endothelin System and Hypertension. *News Physiol Sci* 16:152-156, 2001
67. Kedzierski RM, Yanagisawa M: Endothelin system: the double-edged sword in health and disease. *Annu Rev Pharmacol Toxicol* 41:851-876, 2001
68. Sakamoto H, Sasaki S, Nakamura Y, Fushimi K, Marumo F: Regulation of endothelin-1 production in cultured rat mesangial cells. *Kidney Int* 41:350-355, 1992
69. Karet FE, Davenport AP: Localization of endothelin peptides in human kidney. *Kidney Int* 49:382-387, 1996
70. Zoja C, Morigi M, Figliuzzi M, Bruzzi I, Oldroyd S, Benigni A, Ronco P, Remuzzi G: Proximal tubular cell synthesis and secretion of endothelin-1 on challenge with albumin and other proteins. *Am J Kidney Dis* 26:934-941, 1995
71. Liu BC, Sun J, Chen Q, Ma KL, Ruan XZ, Phillips AO: Role of connective tissue growth factor in mediating hypertrophy of human proximal tubular cells induced by angiotensin II. *Am J Nephrol* 23:429-437, 2003
72. Wolf G, Ziyadeh FN: Molecular mechanisms of diabetic renal hypertrophy. *Kidney Int* 56:393-405, 1999
73. Wang GX, Cai SX, Wang PQ, Ouyang KQ, Wang YL, Xu SR: Shear-Induced Changes in Endothelin-1 Secretion of Microvascular Endothelial Cells. *Microvasc Res* 63:209-217, 2002
74. Naicker S, Bhoola KD: Endothelins: vasoactive modulators of renal function in health and disease. *Pharmacol Ther* 90:61-88, 2001
75. Hocher B, Lun A, Priem F, Neumayer HH, Raschack M: Renal endothelin system in diabetes: comparison of angiotensin-converting enzyme inhibition and endothelin-A antagonism. *J Cardiovasc Pharmacol* 31:S492-S495, 1998
76. Shin SJ, Lee YJ, Lin SR, Tan MS, Lai YH, Tsai JH: Decrease of renal endothelin 1 content and gene

expression in diabetic rats with moderate hyperglycemia. *Nephron* 70:486-493, 1995
77. Iwase M, Doi Y, Goto D, Ichikawa K, Iino K, Yoshinari M, Fujishima M: Effect of nicardipine versus enalapril on plasma endothelin-1 in hypertensive patients with type 2 diabetes mellitus. *Clin Exp Hypertens* 22:695-703, 2000
78. Freedman BI, Tuttle AB, Spray BJ: Familial predisposition to nephropathy in African-Americans with non-insulin-dependent diabetes mellitus. *Am J Kidney Dis* 25:710-713, 1995
79. Seaquist ER, Goetz FC, Rich S, Barbosa J: Familial clustering of diabetic kidney disease. Evidence for genetic susceptibility to diabetic nephropathy. *N Engl J Med* 320:1161-1165, 1989
80. Pettitt DJ, Saad MF, Bennett PH, Nelson RG, Knowler WC: Familial predisposition to renal disease in two generations of Pima Indians with type 2 (non-insulin-dependent) diabetes mellitus. *Diabetologia* 33:438-443, 1990
81. Quinn M, Angelico MC, Warram JH, Krolewski AS: Familial factors determine the development of diabetic nephropathy in patients with IDDM. *Diabetologia* 39:940-945, 1996
82. Zanchi A, Moczulski DK, Hanna LS, Wantman M, Warram JH, Krolewski AS: Risk of advanced diabetic nephropathy in type 1 diabetes is associated with endothelial nitric oxide synthase gene polymorphism. *Kidney Int* 57:405-413, 2000
83. Araki Si, Ng DPK, Krolewski B, Wyrwicz L, Rogus JJ, Canani L, Makita Y, Haneda M, Warram JH, Krolewski AS: Identification of a Common Risk Haplotype for Diabetic Nephropathy at the Protein Kinase C-beta 1 (PRKCB1) Gene Locus. *J Am Soc Nephrol* 14:2015-2024, 2003
84. Tanaka N, Babazono T, Saito S, Sekine A, Tsunoda T, Haneda M, Tanaka Y, Fujioka T, Kaku K, Kawamori R, Kikkawa R, Iwamoto Y, Nakamura Y, Maeda S: Association of Solute Carrier Family 12 (Sodium/Chloride) Member 3 With Diabetic Nephropathy, Identified by Genome-Wide Analyses of Single Nucleotide Polymorphisms. *Diabetes* 52:2848-2853, 2003
85. Zhang H, Jia Y, Cooper JJ, Hale T, Zhang Z, Elbein SC: Common Variants in Glutamine:Fructose-6-Phosphate Amidotransferase 2 (GFPT2) Gene Are Associated with Type 2 Diabetes, Diabetic Nephropathy, and Increased GFPT2 mRNA Levels. *J Clin Endocrinol Metab* 89:748-755, 2004
86. Vardarli I, Baier LJ, Hanson RL, Akkoyun I, Fischer C, Rohmeiss P, Basci A, Bartram CR, Van Der Woude FJ, Janssen B: Gene for susceptibility to diabetic nephropathy in type 2 diabetes maps to 18q22.3-23. *Kidney Int* 62:2176-2183, 2002
87. Bowden DW, Colicigno CJ, Langefeld CD, Sale MM, Williams A, Anderson PJ, Rich SS, Freedman BI: A genome scan for diabetic nephropathy in African Americans. *Kidney Int* 66:1517-1526, 2004
88. Allen TJ, Cooper ME, Lan HY: Use of genetic mouse models in the study of diabetic nephropathy. *Curr Atheroscler Rep* 6:197-202, 2004
89. Fowell D, Mason D: Evidence that the T cell repertoire of normal rats contains cells with the potential to cause diabetes. Characterization of the CD4+ T cell subset that inhibits this autoimmune potential. *J Exp Med* 177:627-636, 1993
90. Zheng S, Noonan WT, Metreveli NS, Coventry S, Kralik PM, Carlson EC, Epstein PN: Development of Late-Stage Diabetic Nephropathy in OVE26 Diabetic Mice. *Diabetes* 53:3248-3257, 2004
91. Crawford SE, Stellmach V, Murphy-Ullrich JE, Ribeiro SM, Lawler J, Hynes RO, Boivin GP, Bouck N: Thrombospondin-1 is a major activator of TGF-beta1 in vivo. *Cell* 93:1159-1170, 1998
92. Murphy-Ullrich JE, Poczatek M: Activation of latent TGF-beta by thrombospondin-1: mechanisms and physiology. *Cytokine Growth Factor Rev* 11:59-69, 2000
93. Munger JS, Harpel JG, Gleizes PE, Mazzieri R, Nunes I, Rifkin DB: Latent transforming growth factor-beta: structural features and mechanisms of activation. *Kidney Int* 51:1376-1382, 1997
94. Kolm V, Sauer U, Olgemooller B, Schleicher ED: High glucose-induced TGF-beta 1 regulates mesangial production of heparan sulfate proteoglycan. *Am J Physiol* 270:F812-F821, 1996
95. Throckmorton DC, Brogden AP, Min B, Rasmussen H, Kashgarian M: PDGF and TGF-beta mediate collagen production by mesangial cells exposed to advanced glycosylation end products. *Kidney Int* 48:111-117, 1995
96. Hansch GM, Wagner C, Burger A, Dong W, Staehler G, Stoeck M: Matrix protein synthesis by glomerular mesangial cells in culture: effects of transforming growth factor beta (TGF beta) and platelet-derived growth factor (PDGF) on fibronectin and collagen type IV mRNA. *J Cell Physiol* 163:451-457, 1995
97. Ziyadeh FN, Sharma K, Ericksen M, Wolf G: Stimulation of collagen gene expression and protein synthesis in murine mesangial cells by high glucose is mediated by autocrine activation of transforming growth factor-beta. *J Clin Invest* 93:536-542, 1994
98. Baricos WH, Cortez SL, Deboisblanc M, Xin S: Transforming growth factor-beta is a potent inhibitor of extracellular matrix degradation by cultured human mesangial cells. *J Am Soc Nephrol* 10:790-795,

1999
99. Poncelet AC, Schnaper HW: Regulation of human mesangial cell collagen expression by transforming growth factor-beta1. *Am J Physiol* 275:F458-F466, 1998
100. Edwards DR, Murphy G, Reynolds JJ, Whitham SE, Docherty AJ, Angel P, Heath JK: Transforming growth factor beta modulates the expression of collagenase and metalloproteinase inhibitor. *EMBO J* 6:1899-1904, 1987
101. Kagami S, Kuhara T, Yasutomo K, Okada K, Loster K, Reutter W, Kuroda Y: Transforming growth factor-beta (TGF-beta) stimulates the expression of beta1 integrins and adhesion by rat mesangial cells. *Exp Cell Res* 229:1-6, 1996
102. Border WA, Okuda S, Languino LR, Ruoslahti E: Transforming growth factor-beta regulates production of proteoglycans by mesangial cells. *Kidney Int* 37:689-695, 1990
103. Border WA, Okuda S, Languino LR, Sporn MB, Ruoslahti E: Suppression of experimental glomerulonephritis by antiserum against transforming growth factor beta 1. *Nature* 346:371-374, 1990
104. Border WA, Noble NA, Yamamoto T, Harper JR, Yamaguchi Y, Piersbacher MD, Ruoslahti E: Natural inhibitor of transforming growth factor-beta protects against scarring in experimental kidney disease. *Nature* 360:361-364, 1992
105. Ziyadeh FN, Hoffman BB, Han DC, Iglesias-de la Cruz MC, Hong SW, Isono M, Chen S, McGowan TA, Sharma K: Long-term prevention of renal insufficiency, excess matrix gene expression, and glomerular mesangial matrix expansion by treatment with monoclonal antitransforming growth factor-beta antibody in db/db diabetic mice. *Proc Natl Acad Sci U S A* 97:8015-8020, 2000
106. Tang WW, Feng L, Loskutoff DJ, Wilson CB: Glomerular extracellular matrix accumulation in experimental anti-GBM Ab glomerulonephritis. *Nephron* 84:40-48, 2000
107. Datta PK, Reddy RS, Lianos EA: Effects of all-trans-retinoic acid (atRA) on inducible nitric oxide synthase (iNOS) activity and transforming growth factor beta-1 production in experimental anti-GBM antibody-mediated glomerulonephritis. *Inflammation* 25:351-359, 2001
108. Baelde HJ, Eikmans M, Van Vliet AI, Bergijk EC, De Heer E, Bruijn JA: Alternatively spliced isoforms of fibronectin in immune-mediated glomerulosclerosis: the role of TGF beta and IL-4. *J Pathol* 204:248-257, 2004
109. Iwano M, Kubo A, Nishino T, Sato H, Nishioka H, Akai Y, Kurioka H, Fujii Y, Kanauchi M, Shiiki H, Dohi K: Quantification of glomerular TGF-beta 1 mRNA in patients with diabetes mellitus. *Kidney Int* 49:1120-1126, 1996
110. Eikmans M, Baelde HJ, Hagen EC, Paul LC, Eilers PH, De Heer E, Bruijn JA: Renal mRNA levels as prognostic tools in kidney diseases. *J Am Soc Nephrol* 14:899-907, 2003
111. Yang CW, Hsueh S, Wu MS, Lai PC, Huang JY, Wu CH, Hu SA, Chen JF, Huang CC: Glomerular transforming growth factor-beta1 mRNA as a marker of glomerulosclerosis-application in renal biopsies. *Nephron* 77:290-297, 1997
112. Rastaldi MP, Tunesi S, Ferrario F, Indaco A, Zou H, Napodano P, D'Amico G: Transforming growth factor-beta, endothelin-1, and c-fos expression in necrotizing/crescentic IgA glomerulonephritis. *Nephrol Dial Transplant* 13:1668-1674, 1998
113. Niemir ZI, Stein H, Noronha IL, Kruger C, Andrassy K, Ritz E, Waldherr R: PDGF and TGF-beta contribute to the natural course of human IgA glomerulonephritis. *Kidney Int* 48:1530-1541, 1995
114. Kim TS, Kim JY, Hong HK, Lee HS: mRNA expression of glomerular basement membrane proteins and TGF-beta1 in human membranous nephropathy. *J Pathol* 189:425-430, 1999
115. Viklicky O, Matl I, Voska L, Bohmova R, Jaresova M, Lacha J, Lodererova A, Striz I, Teplan V, Vitko S: TGF-beta1 expression and chronic allograft nephropathy in protocol kidney graft biopsy. *Physiol Res* 52:353-360, 2003
116. Jain S, Mohamed MA, Sandford R, Furness PN, Nicholson ML, Talbot D: Sequential protocol biopsies from renal transplant recipients show an increasing expression of active TGF beta. *Transpl Int* 15:630-634, 2002
117. Sharma VK, Bologa RM, Xu GP, Li B, Mouradian J, Wang J, Serur D, Rao V, Suthanthiran M: Intragraft TGF-beta 1 mRNA: a correlate of interstitial fibrosis and chronic allograft nephropathy. *Kidney Int* 49:1297-1303, 1996
118. Shihab FS, Yamamoto T, Nast CC, Cohen AH, Noble NA, Gold LI, Border WA: Transforming growth factor-beta and matrix protein expression in acute and chronic rejection of human renal allografts. *J Am Soc Nephrol* 6:286-294, 1995
119. Eikmans M, Sijpkens YW, Baelde HJ, De Heer E, Paul LC, Bruijn JA: High transforming growth factor-beta and extracellular matrix mRNA response in renal allografts during early acute rejection is associated with absence of chronic rejection. *Transplantation* 73:573-579, 2002

120. Simon M, Grone HJ, Johren O, Kullmer J, Plate KH, Risau W, Fuchs E: Expression of vascular endothelial growth factor and its receptors in human renal ontogenesis and in adult kidney. *Am J Physiol* 268:F240-F250, 1995
121. Millauer B, Shawver LK, Plate KH, Risau W, Ullrich A: Glioblastoma growth inhibited in vivo by a dominant-negative Flk-1 mutant. *Nature* 367:576-579, 1994
122. Shweiki D, Itin A, Soffer D, Keshet E: Vascular endothelial growth factor induced by hypoxia may mediate hypoxia-initiated angiogenesis. *Nature* 359:843-845, 1992
123. Levy AP, Levy NS, Wegner S, Goldberg MA: Transcriptional Regulation of the Rat Vascular Endothelial Growth Factor Gene by Hypoxia. *J Biol Chem* 270:13333-13340, 1995
124. Mukhopadhyay D, Tsiokas L, Zhou XM, Foster D, Brugge JS, Sukhatme VP: Hypoxic induction of human vascular endothelial growth factor expression through c-Src activation. *Nature* 375:577-581, 1995
125. Kang DH, Yu ES, Yoon KI, Johnson R: The Impact of Gender on Progression of Renal Disease: Potential Role of Estrogen-Mediated Vascular Endothelial Growth Factor Regulation and Vascular Protection. *Am J Pathol* 164:679-688, 2004
126. Levy AP, Levy NS, Loscalzo J, Calderone A, Takahashi N, Yeo KT, Koren G, Colucci WS, Goldberg MA: Regulation of vascular endothelial growth factor in cardiac myocytes. *Circ Res* 76:758-766, 1995
127. Sato K, Yamazaki K, Shizume K, Kanaji Y, Obara T, Ohsumi K, Demura H, Yamaguchi S, Shibuya M: Stimulation by thyroid-stimulating hormone and Grave's immunoglobulin G of vascular endothelial growth factor mRNA expression in human thyroid follicles in vitro and flt mRNA expression in the rat thyroid in vivo. *J Clin Invest* 96:1295-1302, 1995
128. Williams B, Baker AQ, Gallacher B, Lodwick D: Angiotensin II increases vascular permeability factor gene expression by human vascular smooth muscle cells. *Hypertension* 25:913-917, 1995
129. Williams B, Quinn-Baker A, Gallacher B: Serum and platelet-derived growth factor-induced expression of vascular permeability factor mRNA by human vascular smooth muscle cells in vitro. *Clin Sci (Lond)* 88:141-147, 1995
130. Yamagishi S, Inagaki Y, Okamoto T, Amano S, Koga K, Takeuchi M, Makita Z: Advanced glycation end product-induced apoptosis and overexpression of vascular endothelial growth factor and monocyte chemoattractant protein-1 in human-cultured mesangial cells. *J Biol Chem* 277:20309-20315, 2002
131. Simon M, Rockl W, Hornig C, Grone EF, Theis H, Weich HA, Fuchs E, Yayon A, Grone HJ: Receptors of vascular endothelial growth factor/vascular permeability factor (VEGF/VPF) in fetal and adult human kidney: localization and [125I]VEGF binding sites. *J Am Soc Nephrol* 9:1032-1044, 1998
132. Baelde HJ, Eikmans M, Doran PP, Lappin DWP, De Heer E, Bruijn JA: Gene expression profiling in glomeruli from human kidneys with diabetic nephropathy. *Am J Kidney Dis* 43:636-650, 2004
133. Bortoloso E, Del Prete D, Dalla VM, Gambaro G, Saller A, Antonucci F, Baggio B, Anglani F, Fioretto P: Quantitave and qualitative changes in vascular endothelial growth factor gene expression in glomeruli of patients with type 2 diabetes. *Eur J Endocrinol* 150:799-807, 2004
134. de Vriese AS, Tilton RG, Elger M, Stephan CC, Kriz W, Lameire NH: Antibodies against vascular endothelial growth factor improve early renal dysfunction in experimental diabetes. *J Am Soc Nephrol* 12:993-1000, 2001
135. Singh AK, Gudehithlu KP, Pegoraro AA, Singh GK, Basheerudin K, Robey RB, Arruda JA, Dunea G: Vascular factors altered in glucose-treated mesangial cells and diabetic glomeruli. Changes in vascular factors impair endothelial cell growth and matrix. *Lab Invest* 84:597-606, 2004
136. Kang DH, Hughes J, Mazzali M, Schreiner GF, Johnson RJ: Impaired angiogenesis in the remnant kidney model: II. Vascular endothelial growth factor administration reduces renal fibrosis and stabilizes renal function. *J Am Soc Nephrol* 12:1448-1457, 2001
137. Masuda Y, Shimizu A, Mori T, Ishiwata T, Kitamura H, Ohashi R, Ishizaki M, Asano G, Sugisaki Y, Yamanaka N: Vascular endothelial growth factor enhances glomerular capillary repair and accelerates resolution of experimentally induced glomerulonephritis. *Am J Pathol* 159:599-608, 2001
138. Miyamoto K, Kitamoto Y, Tokunaga H, Takeya M, Ezaki T, Imamura T, Tomita K: Protective effect of vascular endothelial growth factor/vascular permeability factor 165 and 121 on glomerular endothelial cell injury in the rat. *Lab Invest* 84:1126-1136, 2004
139. Wada Y, Morioka T, Oyanagi-Tanaka Y, Yao J, Suzuki Y, Gejyo F, Arakawa M, Oite T: Impairment of vascular regeneration precedes progressive glomerulosclerosis in anti-Thy 1 glomerulonephritis. *Kidney Int* 61:432-443, 2002
140. Eremina V, Sood M, Haigh J, Nagy A, Lajoie G, Ferrara N, Gerber HP, Kikkawa Y, Miner JH, Quaggin SE: Glomerular-specific alterations of VEGF-A expression lead to distinct congenital and acquired renal

diseases. *J Clin Invest* 111:707-716, 2003
141. Bailey E, Bottomley MJ, Westwell S, Pringle JH, Furness PN, Feehally J, Brenchley PE, Harper SJ: Vascular endothelial growth factor mRNA expression in minimal change, membranous, and diabetic nephropathy demonstrated by non-isotopic in situ hybridisation. *J Clin Pathol* 52:735-738, 1999
142. Cipriani R, Sensi M, Gabriele A, Gatti A, Mandosi E, Di Mario U, Morano S: The impairment of renal function is not associated to altered circulating vascular endothelial growth factor in patients with Type 2 diabetes and hypertension. *Diabetes Nutr Metab* 17:90-94, 2004
143. Honkanen E, von Willebrand E, Koskinen P, Teppo AM, Tornroth T, Ruutu M, Gronhagen-Riska C: Decreased expression of vascular endothelial growth factor in idiopathic membranous glomerulonephritis: relationships to clinical course. *Am J Kidney Dis* 42:1139-1148, 2003
144. Boner G, Cox AJ, Kelly DJ, Tobar A, Bernheim J, Langham RG, Cooper ME, Gilbert RE: Does vascular endothelial growth factor (VEGF) play a role in the pathogenesis of minimal change disease? *Nephrol Dial Transplant* 18:2293-2299, 2003
145. Amore A, Conti G, Cirina P, Peruzzi L, Alpa M, Bussolino F, Coppo R: Aberrantly glycosylated IgA molecules downregulate the synthesis and secretion of vascular endothelial growth factor in human mesangial cells. *Am J Kidney Dis* 36:1242-1252, 2000
146. Kim NH, Jung HH, Cha DR, Choi DS: Expression of vascular endothelial growth factor in response to high glucose in rat mesangial cells. *J Endocrinol* 165:617-624, 2000
147. Treins C, Giorgetti-Peraldi S, Murdaca J, Van Obberghen E: Regulation of Vascular Endothelial Growth Factor Expression by Advanced Glycation End Products. *J Biol Chem* 276:43836-43841, 2001
148. Pertynska-Marczewska M, Kiriakidis S, Wait R, Beech J, Feldmann M, Paleolog EM: Advanced glycation end products upregulate angiogenic and pro-inflammatory cytokine production in human monocyte/ macrophages. *Cytokine* 28:35-47, 2004
149. Kim HS, Nagalla SR, Oh Y, Wilson E, Roberts CT, Jr., Rosenfeld RG: Identification of a family of low-affinity insulin-like growth factor binding proteins (IGFBPs): Characterization of connective tissue growth factor as a member of the IGFBPs-superfamily. *Proc Natl Acad Sci U S A* 94:12981-12986, 1997
150. Bradham DM, Igarashi A, Potter RL, Grotendorst GR: Connective tissue growth factor: a cysteine-rich mitogen secreted by human vascular endothelial cells is related to the SRC-induced immediate early gene product CEF-10. *J Cell Biol* 114:1285-1294, 1991
151. Igarashi A, Nashiro K, Kikuchi K, Sato S, Ihn H, Grotendorst GR, Takehara K: Significant correlation between connective tissue growth factor gene expression and skin sclerosis in tissue sections from patients with systemic sclerosis. *J Invest Dermatol* 105:280-284, 1995
152. Igarashi A, Nashiro K, Kikuchi K, Sato S, Ihn H, Fujimoto M, Grotendorst GR, Takehara K: Connective tissue growth factor gene expression in tissue sections from localized scleroderma, keloid, and other fibrotic skin disorders. *J Invest Dermatol* 106:729-733, 1996
153. Lasky JA, Ortiz LA, Tonthat B, Hoyle GW, Corti M, Athas G, Lungarella G, Brody A, Friedman M: Connective tissue growth factor mRNA expression is upregulated in bleomycin-induced lung fibrosis. *Am J Physiol Lung Cell Mol Physiol* 275:L365-L371, 1998
154. Frazier K, Williams S, Kothapalli D, Klapper H, Grotendorst GR: Stimulation of fibroblast cell growth, matrix production, and granulation tissue formation by connective tissue growth factor. *J Invest Dermatol* 107:404-411, 1996
155. Igarashi A, Okochi H, Bradham DM, Grotendorst GR: Regulation of connective tissue growth factor gene expression in human skin fibroblasts and during wound repair. *Mol Biol Cell* 4:637-645, 1993
156. Higgins DF, Biju MP, Akai Y, Wutz A, Johnson RS, Haase VH: Hypoxic induction of Ctgf is directly mediated by Hif-1. *Am J Physiol Renal Physiol* 287:F1223-F1232, 2004
157. Shimo T, Nakanishi T, Nishida T, Asano M, Sasaki A, Kanyama M, Kuboki T, Matsumura T, Takigawa M: Involvement of CTGF, a hypertrophic chondrocyte-specific gene product, in tumor angiogenesis. *Oncology* 61:315-322, 2001
158. Shimo T, Kubota S, Kondo S, Nakanishi T, Sasaki A, Mese H, Matsumura T, Takigawa M: Connective tissue growth factor as a major angiogenic agent that is induced by hypoxia in a human breast cancer cell line. *Cancer Lett* 174:57-64, 2001
159. Kondo S, Kubota S, Shimo T, Nishida T, Yosimichi G, Eguchi T, Sugahara T, Takigawa M: Connective tissue growth factor increased by hypoxia may initiate angiogenesis in collaboration with matrix metalloproteinases. *Carcinogenesis* 23:769-776, 2002
160. Ito Y, Aten J, Bende RJ, Oemar BS, Rabelink TJ, Weening JJ, Goldschmeding R: Expression of connective tissue growth factor in human renal fibrosis. *Kidney Int* 53:853-861, 1998

161. Suzuki D, Toyoda M, Umezono T, Uehara G, Zhang SY, Sakai T, Nishina M, Suga T, Endoh M, Yagame M, Sakai H: Glomerular expression of connective tissue growth factor mRNA in various renal diseases. *Nephrology* 8:92-97, 2003
162. Kanemoto K, Usui J, Nitta K, Horita S, Harada A, Koyama A, Aten J, Nagata M: In situ expression of connective tissue growth factor in human crescentic glomerulonephritis. *Virchows Arch* 444:257-263, 2004
163. Murphy M, Godson C, Cannon S, Kato S, Mackenzie HS, Martin F, Brady HR: Suppression subtractive hybridization identifies high glucose levels as a stimulus for expression of connective tissue growth factor and other genes in human mesangial cells. *J Biol Chem* 274:5830-5834, 1999
164. Wahab NA, Yevdokimova N, Weston BS, Roberts T, Li XJ, Brinkman H, Mason RM: Role of connective tissue growth factor in the pathogenesis of diabetic nephropathy. *Biochem J* 359:77-87, 2001
165. Riser BL, Denichilo M, Cortes P, Baker C, Grondin JM, Yee J, Narins RG: Regulation of connective tissue growth factor activity in cultured rat mesangial cells and its expression in experimental diabetic glomerulosclerosis. *J Am Soc Nephrol* 11:25-38, 2000
166. Weston BS, Wahab NA, Mason RM: CTGF mediates TGF-beta-induced fibronectin matrix deposition by upregulating active alpha5beta1 integrin in human mesangial cells. *J Am Soc Nephrol* 14:601-610, 2003
167. Adler SG, Kang SW, Feld S, Cha DR, Barba L, Striker L, Striker G, Riser BL, Lapage J, Nast CC: Glomerular mRNAs in human type 1 diabetes: biochemical evidence for microalbuminuria as a manifestation of diabetic nephropathy. *Kidney Int* 60:2330-2336, 2001
168. Wang S, Denichilo M, Brubaker C, Hirschberg R: Connective tissue growth factor in tubulointerstitial injury of diabetic nephropathy. *Kidney Int* 60:96-105, 2001
169. Makino H, Mukoyama M, Sugawara A, Mori K, Suganami T, Yahata K, Fujinaga Y, Yokoi H, Tanaka I, Nakao K: Roles of connective tissue growth factor and prostanoids in early streptozotocin-induced diabetic rat kidney: the effect of aspirin treatment. *Clin Exp Nephrol* 7:33-40, 2003
170. Twigg SM, Cao Z, McLennan SV, Burns WC, Brammar G, Forbes JM, Cooper ME: Renal connective tissue growth factor induction in experimental diabetes is prevented by aminoguanidine. *Endocrinology* 143:4907-4915, 2002
171. Koop K, Eikmans M, Baelde HJ, Kawachi H, De Heer E, Paul LC, Bruijn JA: Expression of podocyte-associated molecules in acquired human kidney diseases. *J Am Soc Nephrol* 14:2063-2071, 2003
172. Kawasaki ES, Clark SS, Coyne MY, Smith SD, Champlin R, Witte ON, McCormick FP: Diagnosis of chronic myeloid and acute lymphocytic leukemias by detection of leukemia-specific mRNA sequences amplified in vitro. *Proc Natl Acad Sci U S A* 85:5698-5702, 1988
173. Livak KJ, Flood SJ, Marmaro J, Giusti W, Deetz K: Oligonucleotides with fluorescent dyes at opposite ends provide a quenched probe system useful for detecting PCR product and nucleic acid hybridization. *PCR Methods Appl* 4:357-362, 1995
174. Chee M, Yang R, Hubbell E, Berno A, Huang XC, Stern D, Winkler J, Lockhart DJ, Morris MS, Fodor SP: Accessing genetic information with high-density DNA arrays. *Science* 274:610-614, 1996
175. Schena M, Shalon D, Heller R, Chai A, Brown PO, Davis RW: Parallel human genome analysis: microarray-based expression monitoring of 1000 genes. *Proc Natl Acad Sci U S A* 93:10614-10619, 1996

Chapter 2

Optimal method for RNA extraction from mouse glomeruli

H.J. Baelde, E.C. Bergijk, P.J. Hoedemaeker, E. de Heer, J.A. Bruijn

Department of Pathology, Leiden University Medical Center,
Leiden, The Netherlands

Nephrology Dialysis Transplantation 9(3):304-8, 1994

Abstract

Extraction of RNA has been described for rat and rabbit glomeruli but not for mouse glomeruli. Due to their small size, mouse glomeruli cannot be isolated by relatively simple sieving techniques. Based on recently reported methods for the isolation of mouse glomeruli, we developed an RNA isolation technique by performing comparative methodological studies. Two standard RNA extraction methods were compared. In addition in separate experiments the influence was studied of protease inhibitors and freezing and thawing of whole kidney prior to glomerular isolation, on the yield and degradation of RNA.

Therefore, kidneys were perfused with 10 ml 0.01 M PBS containing 1.25% Fe_3O_4 through the aorta. Kidneys were decapsulated and passed through a 75 µm metal screen. After pelletting and washing, tubes were placed against a magnet and pelleted glomeruli were washed three times. In a second experiment, protease inhibitors were added to the PBS. As a third method, kidneys were frozen before the isolation of glomeruli. From isolated glomeruli, RNA was extracted using either cesium chloride or lithium chloride method.

The yields of RNA (OD 260) were highest using the lithium chloride method. Hybridization of Northern blots of extracted RNA with cDNA probes showed the best results when RNA was extracted using the lithium chloride method, while the cesium chloride method led to considerable degradation of RNA. Freezing of kidney tissue prior to RNA extraction led to the virtual absence of any signal. We then applied this method successfully in an *in vivo* model of experimental lupus nephritis.

This is the first description of an optimal protocol for the extraction of RNA from mouse glomeruli. From our studies we conclude that the lithium chloride method is superior for the extraction of RNA from mouse glomeruli. Adding of protease inhibitors during glomerular isolation is superfluous and freezing of kidney tissue prior to the isolation of glomeruli leads to total degradation of RNA.

Introduction

In the majority of kidney diseases, the production of a number of proteins is severely altered in renal tissue. Measurement of mRNA steady-state levels has become widely accepted as a method to obtain information about the biosynthesis of proteins in cell cultures and tissues, in addition to RNA translation rates and post-translational protein maturation. Northern blot or slot/dot blot techniques can be used to determine mRNA steady-state levels for individual molecules in RNA extracted from whole-kidney tissue or isolated glomeruli. Extraction of RNA has been described for rat and rabbit glomeruli, but not for mouse glomeruli (1,2). Since the size of mouse glomeruli is similar to that of mouse tubules, mouse glomeruli cannot be isolated by relatively simple sieving techniques, which implicated that, so far, only total mouse kidney tissues have been used for the extraction of RNA (3-5), which not gave information about mRNA levels in the glomeruli apart, or microdissection techniques were used to isolate very small amounts of glomeruli which give RNA just sufficient for a single competitive polymerase chain reaction experiment (PCR)(6).

However, the need for an effective method for the purification of RNA from mouse glomeruli exists, since mice are widely used for a number of experimental models for renal disease. The recent development of a rapid purification method for mouse glomeruli (7-9) has opened the way to mouse glomerular RNA extraction rendering amounts of RNA sufficient to perform a number of tests, including northern blots, spot/dot blots, PCR or competitive PCR experiments.

In this study we compared three modified methods for the isolation of glomeruli, to determine the optimal conditions for obtaining intact RNA. First, we applied a procedure for the isolation of glomeruli from fresh mouse kidney tissue described earlier (9). Second, protease inhibitors were used to find out whether it is necessary to use these very toxic chemicals to prevent degradation of the glomerular cells by autolytic enzymes during the procedure. Glomerular cells must survive the procedure, since in intact cells RNA is protected from RNase which degrades RNA. It is impossible to use specific RNase inhibitors such as sodium dodecyl sulfate (SDS) or diethyl pyrocarbonate (DEPC) because they lyse the cells, which would make it impossible to isolate the glomeruli. The third method called for the freezing of kidney tissue prior to the isolation of glomeruli. In addition, two RNA isolation methods were compared, i.e., cesium chloride (CsCl) extraction, and lithium chloride (LiCl) extraction. Lastly, we used kidneys from mice suffering from chronic graft-versus-host disease, an experimental model for lupus nephritis (10-12), to assess the influence of glomerular destruction and progressive glomerulosclerosis on the efficiency of isolation of glomeruli, and the extraction of RNA from those glomeruli, to determine the applicability of our method to experimental models of renal disease.

Subjects and methods

Animals

DBA/2 and C57BL10 mice were originally obtained from Olac Ltd. (Bicester, Oxfordshire, UK). (C57BL10xDBA/2)F1 hybrids were bred and kept in our own facilities. For these experiments, use was made of 60 male (C57BL10xDBA/2)F1 hybrid mice.

Experimental design

Glomeruli were isolated in three different ways. First, the kidneys of ten mice were perfused with phosphate-buffered saline (PBS) followed by perfusion with 10 ml PBS containing 1.25% Fe_3O_4 (Aldrich Chemie N.V./S.A., Brussels, Belgium)(9). Kidneys were decapsulated and stored in cold PBS. When all mice had been perfused, the kidneys were pressed through a 75 µm mesh metal screen (Twente Metaalgaas B.V., Hengelo, The Netherlands) with a flatted glass pestle, washed with a jet of PBS and collected in a siliconized metal dish. The suspension was allowed to settle for 20 min at 4°C in siliconized conical 50-ml centrifuge tubes. The supernatant was then removed and the pellet (5 ml) was resuspended in PBS. After the third run the tube was placed against a magnet (Dynal MPC™6, Dynal AS, Oslo, Norway) for 20 s before the supernatant was removed. Next, the tube was removed from the magnetic field, the inner wall was washed with PBS, and the resuspended glomeruli were washed by repeating this procedure three times, each with a 20-seconds magnetic collection phase. After the last wash the resuspended glomeruli were pelleted by centrifugation (30 s, 1200 g), and the pellet was snap-frozen in CO_2 ice, before being stored at -70°C until use. The total procedure for ten mice was performed within 1.5 hours.

In a second experiment, the same procedure was used, but all PBS contained a cocktail of protease inhibitors: 0.1% NaN_3 (Merck, Darmstadt, Germay), 0.5 mM phenylmethylsulfonyl fluoride (Sigma Chemical Company, St. Louis, MO, USA), 2 mM benzamidine-HCl, (Sigma) and 50 mM ε-amino caproic acid (Sigma).

For the third procedure, we used the same method just described except that the kidneys were snap-frozen in CO_2 ice-cooled isopentane prior to isolation of glomeruli. Kidneys were thawed in PBS without protease inhibitors.

Extraction of RNA

RNA was extracted in two ways after each of these 3 procedures for the isolation of glomeruli. In the first extraction procedure, the frozen pellet of glomeruli was resuspended in 3 ml guanidine isothiocyanate solution and mixed quickly (Ultra-Thorrax T25, Janke & Kunkel, IKAr-Labortechnick, Tamson, Zoetermeer, The Netherlands) for 1 min. Iron oxide and debris were

removed by centrifugation for 5 min at 1500 g. The supernatant was loaded onto 1.3 ml of a 5.7 M CsCl solution in an ultracentrifuge tube and centrifuged at 90,000 g for 16 hours in a Beckmann Sw50Ti rotor (13). After centrifugation, the supernatant was removed and the pellet resuspended in 1 ml RNase free TES (10 mM Tris, 5mM EDTA, 1 % SDS) and precipitated o/n with 1/10 volume 3 M Na-acetate and 2.5 volume ethanol at -20°C. The amount of RNA was determined by measuring of the optical density at 260 nm.

With the second method, RNA was extracted according to a lithium chloride procedure (14). Glomeruli were resuspended in a mixture containing 3 M LiCl and 6 M urea, and mixed quickly. After overnight incubation at 4°C, the solution was centrifuged for 1 hour at 12,000 g. The pellet was resuspended in TES, followed by two phenol/chloroform extractions and an ethanol precipitation.

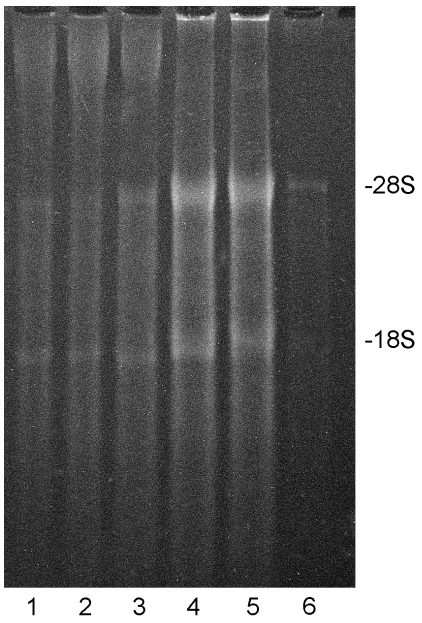

Figure 1. Ethidium bromide staining of the gel after electrophoresis. Lane 1 shows RNA extracted according to the CsCl method in combination with PBS. Lane 2 concerns RNA extracted according to the CsCl method in combination with protease inhibitors. Lane 3 refers to RNA extracted by the CsCl method after freezing of the kidneys. Lanes 4-6 represent the same glomeruli isolation methods as lanes 1-3 but in combination with LiCl RNA isolation method.

Northern blot analysis of RNA

The isolated RNA (20 µg/lane) was electrophoresed for 15 hours at 25V on a 1% agarose-formalin gel, stained with ethidium bromide to assess the quality of the RNA and blotted overnight to a Hybond™-C extra (Amersham, Little Chalfont, UK) membrane. After blotting, the membranes were rinsed with 3x SSC, air dried, and the RNA was baked on the membrane at 80°C for 4 hours.

cDNA probes and hybridization conditions

cDNA probes encoding for glyceraldehyde-3-phosphate dehydrogenase (GAPDH) or for collagen α1(IV) were labeled with ^{32}P with the use of a random primed labeling kit (Boerhinger Mannheim, Mannheim, Germany). The filters were pre-hybridized for 3 hours and hybridized o/n with the radio-(15)labeled probes at 65°C in 0.5 M $NaPO_4$ buffer (pH=7.0) containing 1 mM EDTA, 7% SDS, 1% bovine serum albumin and 50 µg/ml denatured salmon sperm DNA. The filters were washed twice with 2 x SSC and 0.1% SDS and twice with 0.2 x SSC and 1% SDS at 65°C. After being washed the filters were exposed to a Kodak XAR film (Eastman

Kodak, Rochester, New York, USA) at -70°C for 40 hours (GAPDH) or 10 days (Collagen α1(IV)).

Light microscopy.

For comparison of the percentages of sclerotic glomeruli in whole kidneys and in our preparation of glomeruli, the kidneys of a (C57BL10xDBA/2)F1 hybrid) mouse were perfused with iron oxide 12 weeks after the induction of chronic graft-versus-host disease as described in detail elsewhere(10). A sample of kidney tissue from this animal was fixed in 4% buffered formalin, embedded in paraffin, sectioned and stained with the Periodic acid-Schiff reaction for light-microscopical evaluation. Of the remaining renal tissue, the glomeruli were isolated, pelleted, and fixed in 1% glutaraldehyde and 4% formalin. The pellet was then embedded in Epon, sectioned, and stained with methylene blue for determination of the percentage of sclerotic glomeruli. For each of three tissue specimens at least 25 glomeruli were counted. Statistical analysis was performed with the unpaired Student's T-test.

Isolation method	OD260/280	Yield (μg)
CsCl - Method 1	>1.7	246
CsCl - Method 2	>1.7	266
CsCl - Method 3	>1.7	126
LiCl - Method 1	1.73	810
LiCl - Method 2	1.59	775
LiCl - Method 3	1.36	771

Table 1. Yields of RNA from mouse glomeruli using different methods. Method 1 is for RNA isolation from glomeruli isolated from fresh kidneys with the use of PBS. Method 2 is for RNA isolation from glomeruli isolated from fresh kidneys with the use of PBS containing protease inhibitors. Method 3 is used for RNA isolation from glomeruli isolated from frozen kidneys using PBS. (CsCl = cesium chloride RNA extraction, LiCl = lithium chloride RNA extraction).

Results

The glomerular magnetic suspensions contained no free fragments of tubuli, as was confirmed by light microscopy. Less then 10% of the glomeruli showed part of Bowman's capsule with a fragment of the proximal tubules attached. Yields of RNA are shown in Table I. RNA extraction according to the CsCl method rendered 200-300 μg RNA per twenty mouse kidneys either with or without protease inhibitors. The amounts of RNA isolated by the LiCl method were two to three times higher.

The quality of the RNA thus obtained was assessed by gel electrophoresis, as shown in Figure 1. RNA isolated according to the CsCl method showed two indistinct ribosomal bands (28S and 18S), and a smear in the top of the gel. LiCl isolation of RNA yielded two strong ribosomal bands. The 28S band was about twice as intense as the 18S ribosomal RNA band.

Hybridization of the membrane with a collagen α1(IV) cDNA probe gave a 6.8 kB band with the RNA isolated by the LiCl method from glomeruli isolated from fresh kidneys in PBS or in PBS containing the proteinase inhibitors (Figure 2, lanes 4 and 5). The other RNA preparations

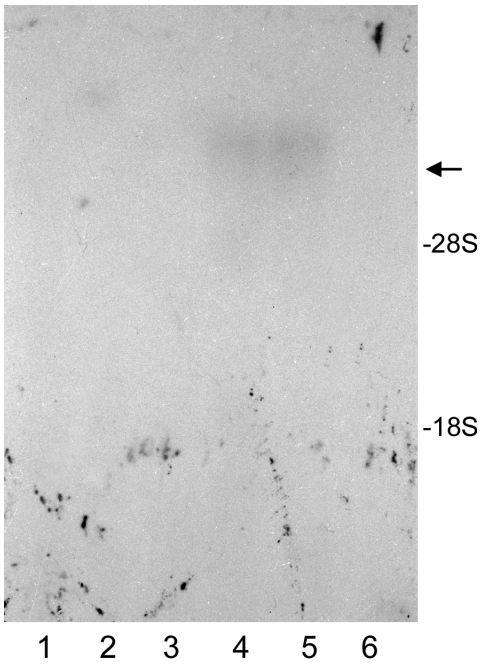

Figure 2. Hybridization of the filter with the collagen α1(IV) cDNA probe. Lane 1 represents RNA extracted by the use of the CsCl method in combination with PBS. Lane 2 refers to RNA extracted by the CsCl method in combination with protease inhibitors, lane 3 RNA extracted by the CsCl method after freezing of the kidneys. Lanes 4-6 represent the same glomeruli isolation methods as lanes 1-3 but in combination with the LiCl RNA isolation method.

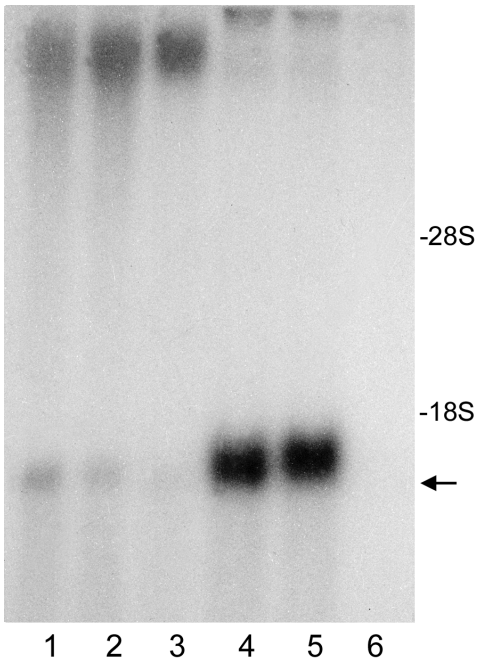

Figure 3. Hybridization of the filter with the GAPDH cDNA probe. Lane 1 represents RNA extracted by the CsCl method in combination with PBS, lane 2 RNA extracted by the CsCl method in combination with protease inhibitors, and lane 3 is RNA extracted by the CsCl method after freezing of the kidneys. Lanes 4-6 represent the same glomeruli isolation methods as lanes 1-3 but in combination with LiCl RNA isolation method.

failed to give a signal upon hybridization. Hybridization with a GAPDH cDNA probe resulted in an intense 1.3 kB band when the RNA was used that had been extracted according to the LiCl method in combination with the isolation of glomeruli from fresh kidneys with or without the use of proteinase inhibitors (Figure 3, lanes 4 and 5). The RNA extracted according to the CsCl method in combination with the isolation of glomeruli from fresh kidneys with or without proteinase inhibitors gave a weak 1.3 kB band and also a smear in the top of the membrane (Fig. 3, lanes 1 and 2). RNA extracted from glomeruli isolated from frozen kidneys did not give a visible signal.

Light-microscopical evaluation of the kidneys of animals with chronic graft-versus-host disease-related lupus nephritis showed focal and segmental glomerulosclerosis in 71.8% ± 4.1% (mean ± standard deviation of three counts, i.e., 25 glomeruli for each specimen) of the glomeruli.

In the isolated glomeruli preparation, 78.9% ± 7.6% of the glomeruli showed focal or segmental sclerosis. The difference between these two groups is not significant (p=0.225). Isolation of glomeruli from mice suffering from glomerulosclerosis gave the same or higher yields of glomeruli compared to isolation of glomeruli from normal mice. Moreover, the amounts of extracted total RNA for both groups were the same. Northern blots of RNA from these diseased mice showed intact RNA (16).

Discussion

In the present study we compared different methods for the isolation of glomeruli from mouse kidneys and different RNA isolation techniques to establish an optimal protocol for the extraction of RNA from mouse glomeruli. The time taken to isolate glomeruli was minimized which is crucial since ribonucleases may be released during the isolation procedure. Isolation of RNA from glomeruli according to the LiCl method yielded large amounts of RNA. Criteria for the intactness of this RNA were fulfilled: i.e., the ethidium bromide-stained gel showed no degradation products under the 18S ribosomal band, and the 28S band was about twice as intense as the 18S rRNA band. To evaluate the quality of the extracted RNA further, we performed hybridization with a cDNA probe coding for collagen a1(IV) mRNA. This probe is known to hybridize with a large mRNA transcript (6.8 kB) (17), that is relatively susceptible for degradation. Hybridization with this collagen a1(IV) cDNA probe yielded one distinct 6.8 kB band at the top of the blot just above the 28S ribosomal band, consistent with the localization of intact collagen α1(IV) mRNA (17). This indicates that no degradation of RNA had occurred during our extraction procedure, because degradation would have led to the presence of a smear under the 6.8 kB band of intact RNA. This also indicates, that during the approximate 1.5 h needed for glomeruli isolation the RNA is not degraded. This is probably due to the fact that the individual cells in the glomeruli stay intact, and that the use of protease inhibitors is not necessary for the isolation of intact RNA.

Extraction performed with the use of CsCl yielded smaller amounts of RNA. On a gel, the 28S and 18S ribosomal bands were not as prominent (Fig. 1, lanes 1 and 2), suggesting that part of the RNA had been degraded. This might explain why hybridization with the collagen α1(IV) probe did not give a signal and that with GAPDH only a weak signal (Fig. 3 lanes 1 and 2). The presence of a smear in the top of the gel and in the top of the blot after hybridization with the GAPDH cDNA probe might be due to contamination with DNA. With this CsCl extraction method too, no difference was found between glomeruli isolated with or without protease inhibitors.

Extraction of intact RNA from glomeruli isolated from frozen kidneys proved impossible. No signal was observed upon gel electrophoresis or after cDNA hybridization. Presumably, this

procedure leads to autolysis of glomerular cells and the release of RNase, which degraded the RNA during the glomeruli isolation. Therefore, the use of fresh kidney tissue is strongly advocated for the isolation of glomeruli and the subsequent extraction of glomerular RNA.

Extraction of poly A^+ mRNA, from isolated glomeruli, with the use of a commercially available kit (Fast track™ mRNA isolation kit, Version 2.1, Invitrogen corporation, San Diego, CA, USA) with oligo(dT) cellulose showed no signal after hybridization (data not shown) with the different probes. It might be expected that the iron particles used during the isolation of glomeruli might disturb mRNA isolation with this method because the iron particles were present throughout the isolation procedure. This in contrast with the other isolation methods in which they can be removed after centrifugation.

Finally, since the yield of RNA extraction may differ between normal and diseased kidneys, the influence of glomerular destruction on the efficiency of isolation of glomeruli was assessed to determine the applicability of our RNA extraction method to experimental models of renal disease. Interference with glomerular isolation due to the presence of glomerular sclerosis and capsule adhesion may lead to the extraction of a non-representative population of glomeruli and false mRNA steady-state levels, and should be excluded. To this end, we used end-stage kidneys from mice suffering from chronic graft-versus-host disease, an experimental model for lupus nephritis (10-12). Percentages of sclerosed glomeruli were similar in whole-kidneys and glomerular isolates, indicating that glomerular destruction does not affect our procedure for the determination of glomerular mRNA steady-state levels.

In sum, we have described here for the first time the optimal extraction procedure of RNA from glomeruli isolated from mouse kidneys. Based on our results, we advocate the use of fresh kidneys in combination with the LiCl RNA isolation method, which gave the highest yields and the best quality of RNA. We recently applied this method successfully in molecular biological studies on the development of glomerulosclerosis in experimental lupus nephritis in mice.

Acknowledgements

This work was supported by a grant from the Dutch Kidney Foundation (C92-1247). The authors thank Dr. B. Hogan (Vanderbilt University, Nashville, Tennessee, USA) for providing the cDNA coding for the α1 chain of type IV collagen.

References

1. Merritt SE, Killen PD, Phan SH, Wiggins RC: Analysis of α1 (I) procollagen α1 (IV) collagen, and β-actin mRNA in glomerulus and cortex of rabbits with experimental anti-glomerular basement membrane disease. *Lab Invest* 63:762-769, 1990
2. Okuda S, Languino LR, Ruoslahti E, Border WA: Elevated expression of transforming growth factor-β and proteoglycan production in experimental glomerulonephritis. Possible role in expansion of the mesangial extracellular matrix. *J Clin Invest* 86:453-462, 1990
3. Ebihara I, Killen PD, Laurie GW, Huang T, Yamada Y, Martin GR, Brown KS: Altered mRNA expression of basement membrane components in a murine model of polycystic kidney disease. *Lab Invest* 58(3):262-269, 1988
4. Doi T, Striker LJ, Kimata K, Peten EP, Yamada Y, Striker GE: Glomerulosclerosis in mice transgenic for growth hormone. Increased mesangial extracellular matrix is correlated with kidney mRNA levels. *J Exp Med* 173:1287-1290, 1991
5. Ledbetter S, Copeland EJ, Noonan D, Vogeli G, Hassell JR: Altered steady-state mRNA levels of basement membrane proteins in diabetic mouse kidneys and thromboxane synthase inhibition. *Diabetes* 39:196-203, 1990
6. Peten EP, Garcia-Perez A, Terada Y, Woodrow D, Martin BM, Striker GE, Striker LJ: Age-related changes in 1- and 2-chain type IV collagen mRNAs in adult mouse glomeruli: Competitive PCR. *Am J Physiol Renal,Fluid Electrolyte Physiol* 263:F951-F957, 1992
7. Gauthier VJ, Mannik M: A method for isolation of mouse glomeruli for quantitation of immune deposits. *Kidney Int* 33:897-899, 1988
8. Assmann KJM, Van Son JPHF, Koene RAP: Improved method for the isolation of mouse glomeruli. *J Am Soc Nephrol* 2:944-946, 1991
9. Baelde HJ, Bergijk EC, Bruijn JA: Isolation and characterization of mouse glomerular basement membrane. *J Clin Lab Immunol* 33:17-20, 1990
10. Bruijn JA, Elven van EH, Hogendoorn PCW, Corver WE, Hoedemaker PJ: Murine chronic graft-versus-host disease as a model for lupus nephritis. Animal model of human disease. *Am J Pathol* 130(3):639-641, 1988
11. Bergijk EC, Munaut C, Baelde JJ, Prins F, Foidart JM, Hoedemaeker PJ, Bruijn JA: A histologic study of the extracellular matrix during the development of glomerulosclerosis in murine chronic graft-versus-host disease. *Am J Pathol* 140:1147-1156, 1992
12. Bruijn JA, Bergijk EC, De Heer E, Fleuren GJ, Hoedemaeker PJ: Induction and progression of experimental lupus nephritis: Exploration of a pathogenetic pathway. *Kidney Int* 41:5-13, 1992
13. Chirgwin JM, Przybyla AE, MacDonald RJ, Rutter WJ: Isolation of biologically active ribonucleic acid from sources enriched in ribonucleases. *Biochemistry* 18:5294-5299, 1979
14. Auffray C, Rougeon F: Purification mouse Ig heavy chain mRNAs from total myeloma tumor RNA. *Eur J Biochem* 107:303-314, 1980
15. Church GM, Gilbert W: Genomic sequencing. *Proc Natl Acad Sci USA* 81:1991, 1984
16. Munaut C, Bergijk EC, Baelde JJ, Noel A, Foidart JM, Bruijn JA: A molecular biologic study of extracellular matrix components during the development of glomerulosclerosis in murine chronic graft-versus- host disease. *Lab Invest* 67:580-587, 1992
17. Kurkinen M, Bernard MP, Barlow DP, Chow LT: Characterization of 64-, 123- and 182-base-pair exons in the mouse α2(IV) collagen gene. *Nature* 317:177-179, 1985

Chapter 3

Distribution of fibronectin isoforms in human renal disease

A.I. Van Vliet, H.J. Baelde, L.J. Vleming, E de Heer, J.A. Bruijn

Department of Pathology, Leiden University Medical Center,
Leiden, The Netherlands

Journal of Pathology 193(2):256-62, 2001

Abstract

Fibronectin (FN) is an extracellular matrix component which appears in different isoforms, due to alternative mRNA splicing of the ED-A, ED-B, and IIICS regions, and subsequent posttranslational modifications. The FN isoforms, some of which occur specifically during foetal development and in fibrogenic diseases, have been reported to play a role in various biological functions, such as regulation of matrix assembly, adhesion, and proliferation. The contribution of these FN isoforms to the pathogenesis of chronic renal diseases, which are also fibrogenic disorders, is not well known. This study therefore examined the distribution of FN isoforms in renal diseases by immunohistochemistry, with a panel of isoform-specific monoclonal antibodies (mAbs), applied to 63 renal biopsies and 10 normal controls.

Normal kidneys contained total FN (mAb IST4) both in the mesangial and in the interstitial extracellular matrix (ECM), but only traces of ED-A-positive FN (mAb IST9), and no ED-B-positive FN (mAb BC1) or oncofoetal FN (mAb FDC6) were found in normal renal tissue. All patients with renal disease demonstrated an increased total FN staining of the interstitium and the mesangium. Periglomerular fibrotic lesions and fibrous crescents showed massive accumulation of total FN, whereas the amount of total FN in the ECM of obsolescent glomeruli was decreased, compared with that in normal mesangial ECM. Oncofoetal (FDC6), EDB-negative (mAb IST6), ED-A-positive, and ED-B-positive FN isoforms were found in glomerular ECM accumulations and in fibrous crescents. Tubulointerstitial fibrotic lesions predominantly contained the ED-A-positive FN isoform, whereas in globally sclerotic glomeruli, predominantly ED-B-positive FN was observed. The expression of FN isoforms was similar in all renal diseases studied.

These results show that in various renal diseases, oncofoetal (FDC6) FN and ED-A- and ED-B-positive isoforms of FN accumulate at locations of chronic lesions, independent of the etiology of the disease. The deposition of these isoforms in human renal tissue may play a role in the modulation of the immune response by attracting monocytes and lymphocytes to the injured kidney. Furthermore, because the ED-B-positive FN isoform is highly susceptible to proteolytic degradation, its accumulation may play a role in scar formation and tissue repair. ED-B-positive FN forms a temporary scaffold supporting the cells, which can easily be cleared by proteolytic degradation once new tissue has been produced at the site of injury.

Introduction

Glomerulosclerosis and interstitial fibrosis are severe complications of most glomerular and interstitial renal diseases, in which the accumulation of extracellular matrix (ECM) leads to impairment of the filtration function. In an experimental model for lupus nephritis in mice, we previously demonstrated that glomerulosclerotic lesions contain large amounts of the ECM component fibronectin (FN)(1). In addition, we found that the extent of glomerular FN deposition correlated with the severity of the glomerular structural abnormalities in several human renal diseases (2).

FN is a large adhesive glycoprotein which is involved in the regulation of adhesion, differentiation, migration, and cell proliferation, and it plays a role in blood coagulation, tissue repair, tumourigenicity, and opsonisation (3). FN is encoded by a single gene on chromosome 2, but post-transcriptional alternative splicing of the FN mRNA and post-translational modifications of the protein lead to the occurrence of multiple FN protein isoforms (3). Thus far, three regions of FN have been identified in which alternative splicing occurs: ED-A, ED-B, and IIICS. Both the ED-A and the ED-B regions code for a type III segment, which is either completely included or completely excluded at the protein level through alternative splicing of the FN mRNA. Alternative splicing of the IIICS region of FN mRNA is more complex, and results in five potential FN protein variants in humans. This has functional consequences with respect, for example, to migration and proliferation, because the IIICS domain bears recognition sites for integrins (4,5). In addition, inclusion of the ED-A and ED-B domains generates conformational changes in the structure of the protein, further influencing the affinity of FN for integrins and cells(6,7). Inclusion or exclusion of these various sites could therefore alter processes that depend on cell adhesion, cell proliferation, and matrix assembly. Likewise, changes in FN isoform expression in the glomerulus and the tubulointerstitium may modulate disease progression and outcome in patients suffering from renal disorders. We therefore investigated the distribution of the various FN isoforms in glomerulosclerotic lesions and in regions of tubulointerstitial fibrosis in several human renal diseases by immunohistochemical analysis.

Materials and methods

Patient selection

Kidney biopsies reported with any form of glomerulosclerosis in the period between January 1984 and December 1997 were selected from the archives of the Pathology Department at our centre. Only biopsies from which frozen material was available were included in the present study (n=63). All biopsies had been evaluated originally by routine light microscopic histological evaluation, in combination with the results of immunofluorescence and electron microscopy. The majority of the biopsies contained more than five glomeruli and corresponding interstitial regions for analysis. The patients' diagnoses and clinical characteristics are presented in Table 1. The biopsy from the 70-year-old male with minimal change disease contained one globally sclerosed glomerulus and was therefore included in the series. Control biopsies came from several sources and incorporated three pretransplantation biopsies from donated kidneys, two tumour nephrectomies, two post-mortem kidney biopsies from patients without renal dysfunction or histological abnormalities, and three kidney biopsies which had been taken on clinical indications but turned out to be normal.

Staining technique

The various FN isoforms were visualised with an indirect immunoperoxidase technique. We used the following primary monoclonal antibodies: IST-4 (8), specific for all FN isomers (total FN); IST-6 (8), which detects a FN isoform not containing ED-B; IST-9 (9), specific for ED-A-positive FN isoforms; BC-1 (10), specific for ED-B-positive FN; and FDC-6 (11), which reacts with an oncofoetal epitope on the IIICS region of FN (ATCC, HB-9018) (Figure 1). Specificities of these antibodies were determined earlier and described in detail elsewhere (8-11). In addition, a polyclonal goat anti-human FN (Sigma Immunochemicals, St Louis, MN, USA) was also used to detect total FN. The secondary antibodies were peroxidase-coupled rabbit anti-mouse IgG, and rabbit anti-goat IgG (Dako, Glostrup, Denmark).

Immunoperoxidase staining was performed on sequential frozen sections (4μm), which were mounted on glass slides. Tissue sections were defrosted and washed in phosphate buffered saline, then fixed in alcohol/acetone (50/50 vol/vol) for 5 minutes, followed by alcohol 100% for 10 minutes. After blocking of endogenous peroxidase in 0.3% H_2O_2 in methanol for 10 minutes, the sections were incubated with the primary antibodies for 1 hour. Subsequently, they were incubated with the appropriate secondary antibody for 30 minutes in the presence of 0.5% human IgG to prevent cross reactivity of the second antibody. Immunoreactivity was visualised by incubating with diaminobenzidine (DAB) and copper sulphate ($CuSO_4$). Counterstaining with hematoxylin was performed according to a standardized protocol. Pertinent

control stainings were performed.

Scoring technique

The sections of 63 patient biopsies and 10 control biopsies were evaluated by two experienced observers in a blinded fashion. Minor scoring differences were resolved by conference. The expression of the various FN isoforms was scored in normal mesangial matrix, glomerulosclerosis, obsolescent glomeruli, periglomerular regions, fibrous crescents, normal tubulointerstitial matrix, and tubulointerstitial matrix with interstitial fibrosis. Glomerulosclerosis was defined as matrix expansion and collapse of the glomerular capillary tuft. The average staining per biopsy was graded semi-quantitatively on a 4-point scale: 0 (absent), 1 (mild), 2 (moderate), and 3 (abundant). These scoring values mainly represent the size of the areas positive for the various isoforms, because the staining intensity did not vary significantly.

Statistical analysis

Scores are presented as means ± standard deviations (SD). The significance of differences in the various comparisons was determined by non-parametric analysis (Wilcoxon signed-rank test) with an appropriate post-hoc procedure. A p-value ≤ 0.05 was considered statistically significant.

Table 1. Clinical characteristics of all patients [a]

	No. of patients	Age (years)	Sex (f/m)	Serum creatinine (μmol/l)
Minimal change disease	1	70	1/0	
Membranous nepropathy	3	62.3 ± 13.3	3/0	228.3 ± 121.5
IgA nephropathy	13	50.1 ± 18.3	9/4	192.5 ± 98.6
Proliferative glomerulonephritis	6	63.6 ± 18.9	3/3	413.8 ± 380.5
Pauciimmune glomerulonephritis	1	55	0/1	388
Lupus nephritis	6	41.8 ± 15.2	1/5	141.8 ± 85.5
Diabetic nephropathy	8	61.8 ± 8.2	6/2	331.0 ± 280.1
Transplant glomerulosclerosis	9	45.6 ± 10.6	8/1	290.6 ± 215.2
Amyloidosis	1	40	1/0	371
Light chain deposit disease	1	42	1/0	498
Focal segmental glomerulosclerosis	14	48.1 ± 15.6	7/7	419.7 ± 289.5
Total	63	47.4 ± 21.2	40/23	281.7 ± 261.8

[a] Data are presented as mean ± SD.

Results

Distribution of FN isoforms

The distribution of FN isoforms in renal diseases was studied by immunohistochemistry, using a panel of isoform-specific monoclonal antibodies (mAbs) that were applied to 63 renal biopsies with a variety of diseases, with 10 normal controls. The results are shown in Figure 2 and Table 2.

In normal kidneys, total FN (i.e. the polyclonal Ab against FN and the mAb IST4) was found in the mesangial and the interstitial ECM, the periglomerular regions, intermediate sized blood vessels, and peritubular capillaries (Figure 2A). The staining patterns of both antibodies did not differ significantly, so the combined results of mAb IST4 and the polyclonal Ab against FN are presented in Table 2 (column 'total FN'). Only traces of ED-A-positive FN (mAb IST9, Figure 2B) were visible in the normal mesangium, the interstitial matrix, and in interstitial blood vessels; the periglomerular region stained positive for this isoform in only a few cases. Normal controls expressed neither ED-B-positive FN (mAb BC1), nor oncofoetal FN (mAb FDC6). The marker IST6, detecting a FN isoform lacking the ED-B domain, showed abundant staining of the normal mesangial and interstitial matrix. Periglomerular areas and blood vessels also showed a strong expression of this FN isoform.

In all patient groups (Figures 2C-H, Table 2), areas of glomerulosclerosis and those with interstitial fibrosis showed a significant increase in total FN staining in comparison with those in normal controls (Figure 2C). Because no statistically significant differences in the expression of the various FN isoforms were found between any of the patient groups (Table 1), the results

Figure 1. Epitope mapping of the employed panel of FN isoform-specific mAbs. Schematic representation of one FN protein subunit. Indicated are the ED-A, ED-B, and IIICS regions, which can be included in or excluded from the protein by alternative splicing of the FN pre-mRNA. The sites of specificity of the mAbs used are depicted. Rectangles represent homologous type I repeats, circles represent homologous type II repeats and squares represent homologous type III repeats. IST4, mAb detecting all FN isoforms; IST6, mAb detecting a FN isoform which does not include ED-B; IST9, mAb specific for ED-A-positive FN isoforms; BC1, mAb specific for ED-B-positive FN isoforms (Note that mAb BC1 is specific for ED-B-containing FN even though the epitope recognised is localised on repeat III-7); FDC6, mAb which detects an oncofoetal epitope on the IIICS region of FN.

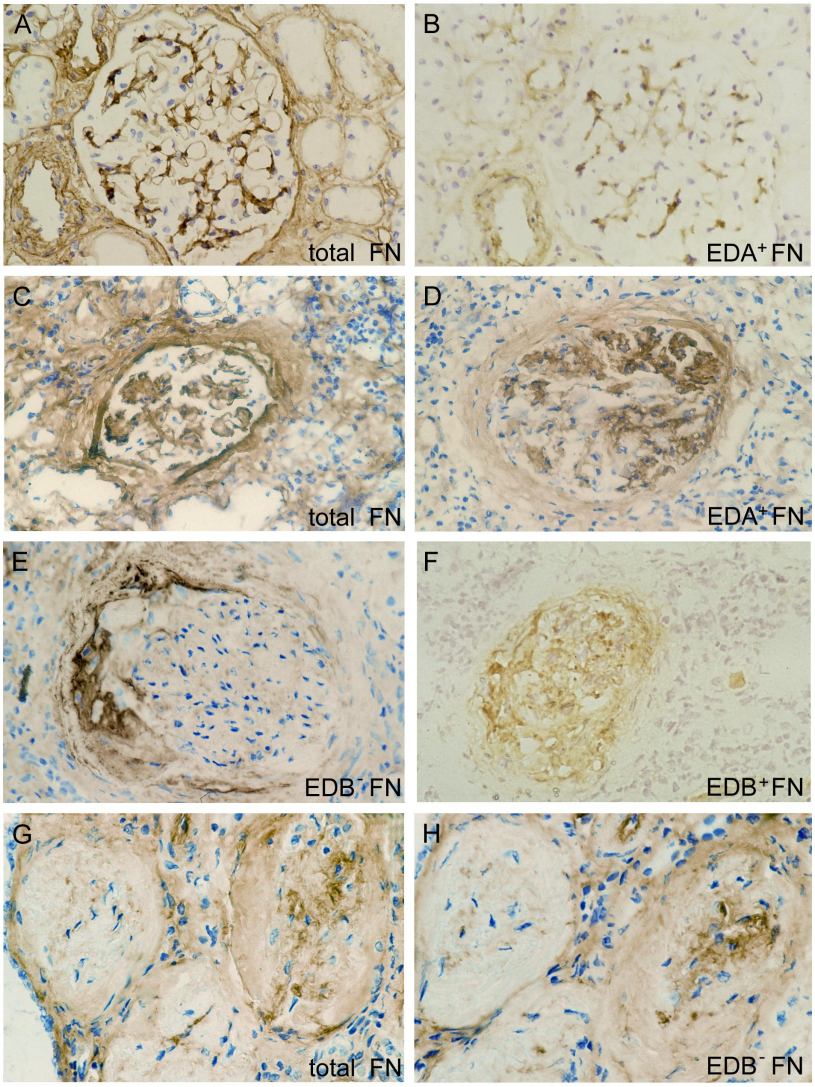

Figure 2. Representative micrographs illustrating the localisation of FN isoforms in normal and diseased renal tissues at specific lesions as determined by immunohistochemistry. Figures A and B show renal tissue of a normal control biopsy, stained with antibodies detecting total FN (A, IST4) and ED-A-positive FN (B, IST9). Figures C (total FN; IST4) and D (ED-A-positive FN; IST9) show renal tissue from a patient with focal and segmental glomerulosclerosis and periglomerular fibrosis. Increased staining for total FN (C) and ED-A-positive FN (D) is observed in the segmental sclerotic lesions, periglomerularly, and to some extent in the tubulointerstitium. Figures E and F show the distribution of ED-B-negative FN (E, IST6) and ED-B-positive FN (F, BC1) in glomeruli of a patient with diabetic nephropathy. The periglomerular region, but not the glomerular tuft, contains ED-B-negative FN (E*). De novo* expression of ED-B-positive FN is seen in the mesangial area (F). Figures G and H show obsolescent glomeruli with variable staining for total FN (G, IST4) and ED-B-negative FN (H, IST6) in a patient with focal and global sclerosis. Both markers show staining in remnant of capillary tuft (glomerulus in right-hand side in G and H), and practically no staining in globally sclerotic glomerulus (left-hand side in G and H).

Table 2. Fibronectin isoforms in renal biopsies [a]

	Total FN	ED-B$^-$ FN (IST6)	ED-A$^+$ FN (IST9)	ED-B$^+$ FN (BC1)	Oncofetal FN (FDC6)
1. Normal mesangial matrix	2.41	2.39	0.35	0.001	0.01
2. Glomerulosclerosis	**2.88**[b]	**2.86**[b]	**2.16**[b]	**0.44**[b]	**0.42**[b]
3. Fibrous crescents	2.65	3.00	3.14	1.79	1.75
4. Obsolescent glomeruli	**1.91**[c]	**1.90**[c]	1.04	**0.14**[b]	0.16
5. Normal periglomerular region	2.00	2.00	0.20	0.001	0.001
6. Periglomerular fibrosis	2.20	**2.27**[d]	**1.17**[d]	0.13	0.22
7. Normal tubulointerstitial matrix	2.12	2.18	0.90	0.001	0.001
8. Interstitial fibrosis	**2.43**[e]	**2.55**[e]	**1.38**[e]	0.01	0.01

[a] *P*-values < 0.05 were considered significant.
[b] Significant increase in the amount of staining compared to normal mesangial matrix (area 1).
[c] Significant decrease in the amount of staining compared to normal mesangial matrix (area 1).
[d] Significant increase in the amount of staining compared to normal periglomerular regions (area 5).
[e] Significant increase in the amount of staining compared to normal tubulointerstitial matrix (area 7)

are presented for the entire group as a whole (Table 2). Periglomerular (fibrotic) regions and fibrous crescents also showed an abundant expression of total FN. In contrast, the amount of total FN in the ECM of obsolescent glomeruli was significantly decreased as compared to that in normal mesangial ECM (Figure 2G). ED-A- and ED-B-positive FN isoforms (mAbs IST9 and BC1, respectively) were found in significantly increased amounts in glomerulosclerotic lesions (Figures 2D and F). Fibrous crescents contained rather high amounts of the ED-A- and ED-B-positive FN isoforms. Obsolescent glomeruli still contained increased amounts of ED-B-positive FN as compared to normal mesangial ECM, but not of ED-A-positive FN isoforms. The fibrotic periglomerular regions in patient biopsies showed a marginal increase in staining for the ED-A-positive FN isoform compared with the periglomerular regions of normal controls. ED-B-positive FN was practically absent in this location**.** In areas with interstitial fibrosis, ED-A-positive FN was present in significantly increased amounts, whereas there was no ED-B-positive FN deposited in the fibrotic interstitium. The isoform of FN lacking the ED-B domain (mAb IST6) was abundantly expressed in glomerulosclerotic lesions, in fibrous crescents, and in regions of periglomerular and interstitial fibrosis (Figure 2E). In obsolescent glomeruli with end-stage sclerotic lesions this was the major FN isoform expressed (Figure 2H). The oncofoetal isoform of FN that is recognized by the mAb FDC6 showed a significantly increased expression in fibrous crescents and glomerulosclerotic lesions as compared to normal controls.

Discussion

Most chronic human kidney diseases are characterised by an accumulation of ECM resulting in glomerulosclerosis and tubulointerstitial fibrosis, both of which compromise renal function. In addition to a disturbed balance between ECM synthesis and degradation, intramolecular alterations of ECM molecules may also play a role in fibrogenesis. Increased deposition of the ECM component FN in the glomerulus has been shown to play a role in the development of end-stage renal failure. FN is encoded by a single gene, but post-transcriptional alternative splicing and post-translational modifications give rise to the occurrence of multiple FN protein isoforms (3), whose production is regulated in a cell- and tissue-specific manner. It is known that the various isoforms of FN have different biological functions, and that it is not only a change in the amount of FN deposited at a specific location that may play a role in disease progression (12); a change in the ratio between the various isoforms may also contribute to the development of fibrotic disease. We investigated the distribution of the various FN isoforms in several human renal diseases by immunohistochemical analysis.

In normal glomeruli, total FN and all FN-isoforms investigated, except for ED-B-positive and oncofoetal FDC6-positive FN, were present in the mesangium. In cases of glomerular matrix expansion in glomerulosclerosis, a significant increase was found in all FN isoforms investigated. In contrast, in obsolescent glomeruli the amounts of all isoforms investigated had decreased, especially in globally sclerotic lesions, although marginal staining was sometimes seen in remnants of the capillary tuft. This may possibly result from a replacement of FN by other ECM components in late stages of glomerular disease. Indeed, it is known from other studies that FN provides a provisional ECM during injury and forms a foundation for the deposition of additional ECM proteins such as collagen and laminin (13-16).

In areas of glomerulosclerosis, obsolescent glomeruli, and interstitial fibrosis, an absolute increase of both ED-A- and ED-B-positive FN isoforms was seen. Inclusion of the ED-A sequence in the FN molecule has been extensively studied, both *in vitro* and *in vivo* (17-21). Deposition of an ED-A-positive FN isoform, as we see in abnormal tubulointerstitium and regions of glomerular matrix expansion, may have functional consequences. Inclusion of the ED-A region in the protein leads to conformational changes that alter the affinity of the central cell-binding domain (7). Deposition of this FN isoform can thus lead to a more efficient attraction of cells to the ECM in the kidney and may well be part of a tissue repair process.

Whereas most authors report on the expression of the ED-A-positive FN isoform, we observed a decrease in the ratio of the ED-A- over the ED-B-positive FN isoforms, in the comparison of obsolescent glomeruli to normal controls. The observation that the amount of ED-B-positive FN isoforms is relatively and absolutely increased, may have important biological

consequences. *In vitro* studies have shown that inclusion of the ED-B region in FN changes the activational status of cells by enhancing adhesion and spreading (22). *In vitro* studies have also shown that FN isoforms containing the ED-B region are more sensitive to proteolytic attack by cathepsin D (23). Our results show that deposition of this FN isoform is independent of the type of renal disease, and we speculate that it plays a role in tissue repair mechanisms and scar formation similar to what has been described for wound healing (24). The ED-B-positive FN molecules form a temporary scaffold supporting the surrounding cells and attract other (inflammatory) cells. However, since the ED-B-positive FN molecules are highly susceptible to proteolytic attack, the newly formed scaffold can be easily cleared once new tissue has been produced, as mentioned above.

In all cases, there was a large amount of ED-A- and ED-B-positive FN isoforms deposited in fibrous crescents, indicating the presence of significant amounts of these otherwise scarcely present FN isoforms. These findings are in line with earlier results from Assad et al., who described the presence of ED-A- and ED-B-positive FN isoforms in crescents of a small group of patients with segmental glomerulonephritis (25). Likewise, in the animal model of anti-GBM nephritis in rats, embryonic FN isoforms containing the EIII-A and EIII-B regions (rodent homologues for the ED-A and ED-B regions) were shown to be the main FN isoforms synthesized at the site of fibrous crescent formation (17). Interestingly, these locally produced EIII-A- and EIII-B-positive rat FN isoforms have been suggested to play a role in scarring in the anti-GBM model by providing a transitional matrix that is involved in mesangial cell migration, proliferation, and the formation of a stable ECM (17), comparable to the mechanism described above for the glomerular lesions.

In our present study, regions of interstitial fibrosis showed an accumulation of total FN, FN lacking the ED-B region, and of the FN isoform containing the ED-A region. With very few exceptions, the tubulointerstitium was always negative for the ED-B-positive FN isoform. Similarly, FN lacking the ED-B region and ED-A-positive FN were increased in areas of periglomerular fibrosis. Thus, during the development of immunologically mediated renal diseases the tubulointerstitial tissue expresses high levels of the ED-A- positive and ED-B-negative (IST6) FN isoforms, as was reported earlier in wound healing and during embryogenesis (26).

Taken together, our results show an increase in the total amount of FN deposited in the glomerulus and the tubulointerstitial compartment of patients, compared with normal control biopsies. In addition, we found that the relative amounts of oncofoetal (FDC6), ED-A-, and ED-B-positive FN isoforms increased to different extent, as a result of which the ratios changed between the various FN isoforms deposited in the ECM. In particular, the increase of the ED-B-positive variant was considerably stronger than that of ED-A-positive FN in both glomerulo-

sclerosis and interstitial fibrosis (Table 2). This is in concert with results from earlier *in vitro* studies, which showed that the ED-A and ED-B regions are under separate regulatory control with respect to splicing of their mRNAs (27). These changes in FN isoform deposition may influence the biological properties of the glomerular and tubulointerstitial matrix. Our results show that in renal diseases the oncofoetal (FDC6), ED-A-, and ED-B-positive FN isoforms are upregulated at specific locations within the renal tissue, suggesting a specific pathogenic role for these FN isoforms during disease development. The expression of the FN isoforms at distinct locations within the glomerulus and tubulointerstitium was similar in all renal diseases studied. Further studies are currently directed at the identification of the cellular source of the fibronectin isoforms. Our results support the concept that the development of glomerulosclerosis and interstitial fibrosis, leading to progressive loss of kidney function, results from a final common pathway independent of the original etiology.

References

1. Bergijk EC, Baelde HJ, De Heer E, Killen PD, Bruijn JA: Specific accumulation of exogenous fibronectin in experimental glomerulosclerosis. *J Pathol* 176:191-199, 1995
2. Vleming LJ, Baelde JJ, Westendorp RGJ, Daha MR, Van Es LA, Bruijn JA: The glomerular deposition of PAS positive material correlates with renal function in human kidney diseases. *Clin Nephrol* 47:158-167, 1997
3. Hynes RO: Fibronectins. New York, Springer Verlag, 1990, pp 1-538
4. Komoriya A, Green LJ, Mervic M, Yamada SS, Yamada KM, Humphries MJ: The minimal essential sequence for a major cell-specific adhesion site (CS1) within the alternatively spliced IIICS domain of fibronectin is Leu-Asp-Val. *J Biol Chem* 266:15075-15079, 1991
5. Humphries MJ, Komoriya A, Akiyama SK, Olden K, Yamada KM: Identification of two distinct regions of the type III connecting segment of human plasma fibronectin that promote cell type-specific adhesion. *J Biol Chem* 262:6886-6892, 1987
6. Carnemolla B, Leprini A, Allemanni G, Saginati M, Zardi L: The inclusion of the type III repeat ED-B in the fibronectin molecule generates conformational modifications that unmask a cryptic sequence. *J Biol Chem* 267:24689-24692, 1992
7. Manabe R, Oh-e N, Maeda T, Fukuda T, Sekiguchi K: Modulation of cell-adhesive activity of fibronectin by the alternatively spliced EDA segment. *J Cell Biol* 139:295-307, 1997
8. Zardi L, Carnemolla B, Siri A, Santi L, Accolla RS: Somatic cell hybrids producing antibodies specific for human fibronectin. *Int J Cancer* 25:325-329, 1980
9. Borsi L, Carnemolla B, Castellani P, Rosellini C, Vecchio D, Allemani G, Chang SE, Taylor-Papadimitriou J, Pande H, Zardi L: Monoclonal antibodies in the analysis of fibronectin isoforms generated by alternative splicing of mRNA precursors in normal and transformed human cells. *J Cell Biol* 104:595-600, 1987
10. Carnemolla B, Balza E, Siri A, Zardi L, Nicotra MR, Natali PG: A tumor-associated fibronectin isoform generated by alternative splicing of messenger RNA precursors. *J Cell Biol* 108:1139-1148, 1989
11. Matsuura H, Hakomori S: The oncofetal domain of fibronectin defined by monoclonal antibody FDC-6: its presence in fibronectins from fetal and tumor tissues and its absence in those from normal adult tissues and plasma. *Proc Natl Acad Sci USA* 82:6517-6521, 1985
12. Romberger DJ: Fibronectin. *Int J Biochem Cell Biol* 29:939-943, 1997

13. Van de Water L: Mechanisms by which fibrin and fibronectin appear in healing wounds: Implications for Peyronie's disease. *J Urol* 157:306-310, 1997
14. Dixon FJ, Burns J, Dunnill MS, McGee J: Distribution of fibronectin in normal and diseased human kidneys. *J Clin Pathol* 33:1021-1028, 1980
15. McDonald JA: Extracellular matrix assembly. *Annu Rev Cell Biol* 4:183-207:183-207, 1988
16. Ignotz RA, Massague J: Transforming growth factor-beta stimulates the expression of fibronectin and collagen and their incorporation into the extracellular matrix. *J Biol Chem* 261:4337-4345, 1986
17. Nickeleit V, Zagachin L, Nishikawa K, Peters JH, Hynes RO, Colvin RB: Embryonic fibronectin isoforms are synthesized in crescents in experimental autoimmune glomerulonephritis. *Am J Pathol* 147:965-978, 1995
18. Barnes JL, Torres ES, Mitchell RJ, Peters JH: Expression of alternatively spliced fibronectin variants during remodeling in proliferative glomerulonephritis. *Am J Pathol* 147:1361-1371, 1995
19. Viedt C, Bürger A, Hänsch GM: Fibronectin synthesis in tubular epithelial cells: Up-regulation of the EDA splice variant by transforming growth factor β. *Kidney Int* 48:1810-1817, 1995
20. Alonso J, Gómez-Chiarri M, Ortíz A, Serón D, Condom E, López-Armada MJ, Largo R, Barat A, Egido J: Glomerular up-regulation of EIIIA and V120 fibronectin isoforms in proliferative immune complex nephritis. *Kidney Int* 50:908-919, 1996
21. Bürger A, Wagner C, Viedt C, Reis B, Hug F, Hänsch GM: Fibronectin synthesis by human tubular epithelial cells in culture: effects of PDGF and TGF-β on synthesis and splicing. *Kidney Int* 54:407-415, 1998
22. Hashimoto-Uoshima M, Yan YZ, Schneider G, Aukhil I: The alternatively spliced domains EIIIB and EIIIA of human fibronectin affect cell adhesion and spreading. *J Cell Sci* 110:2271-2280, 1997
23. Zardi L, Carnemolla B, Siri A, Petersen TE, Paolella G, Sebastio G, Baralle FE: Transformed human cells produce a new fibronectin isoform by preferential alternative splicing of a previously unobserved exon. *EMBO J* 6:2337-2342, 1987
24. Brown LF, Dubin D, Lavigne L, Logan B, Dvorak HF, Van de Water L: Macrophages and fibroblasts express embryonic fibronectins during cutaneous wound healing. *Am J Pathol* 142:793-801, 1993
25. Assad L, Schwartz MM, Virtanen I, Gould VE: Immunolocalization of tenascin and cellular fibronectins in diverse glomerulopathies. *Virchows Arch* 63:307-316, 1993
26. Laitinen L, Vartio T, Virtanen I: Cellular fibronectins are differentially expressed in human fetal and adult kidney. *Lab Invest* 64:492-498, 1991
27. Paolella G, Henchcliffe C, Sebastio G, Baralle FE: Sequence analysis and in vivo expression show that alternative splicing of ED-B and ED-A regions of the human fibronectin gene are independent events. *Nucleic Acids Res* 16:3545-3557, 1988

Chapter 4

Alternatively spliced isoforms of fibronectin in immune-mediated glomerulosclerosis: the role of TGF-beta and IL-4

H.J. Baelde, M. Eikmans, A.I. van Vliet, E.C. Bergijk, E. de Heer, J.A. Bruijn

Department of Pathology, Leiden University Medical Center,
Leiden, The Netherlands

Journal of Pathology 204(3):248-57, 2004

Abstract

Fibronectin (FN) is the main extracellular matrix component in glomerulosclerotic lesions. Different FN isoforms exists, which result from alternative splicing at the EDA and EDB regions of FN mRNA. Increased inclusion of EDA and EDB, which can be elicited by TGF-β, may be conducive to the development of glomerulosclerosis (GS). TGF-β and IL-4 have previously been shown to play a role in the development of GS.

We investigated the mRNA splicing patterns for EDA+ and EDB+ fibronectin *in vivo* in various experimental sclerotic glomerulopathies, *in vitro* in rat mesangial cells (MC) that were stimulated by TGF-β or transfected with IL-4, and in human kidney biopsies with GS from patients with various kidney diseases.

Glomerular FN mRNA demonstrated inclusion of both ED regions in rats with anti-Thy1 nephritis or chronic serum sickness and in mice with anti-GBM glomerulonephritis. Inclusion of both the EDA and EDB regions was associated with glomerular TGF-β expression. In contrast, in mice with Th2-mediated graft-versus-host disease, a model for lupus nephritis, the FN transcripts included neither the EDA, nor the EDB region, and renal TGF-β expression was absent. Compared to normal MC in culture, MC transfected with IL-4 produced lower amounts of FN and demonstrated less EDA inclusion, while MC that had been treated with TGF-β showed increased production of FN and more EDA inclusion. Renal biopsies from patients with renal diseases, except those taken from patients with lupus nephritis, showed higher TGF-β levels, higher FN levels, and more EDA inclusion than controls.

TGF-β might be a key player in the development of GS by inducing local FN production and alternative splicing of FN mRNA. In lupus glomerulonephritis, in which the involvement of TGF-β in GS is less prominent, Th2 cytokines such as IL-4 probably account for increased intrarenal collagen synthesis and subsequent FN accumulation from the circulation. We conclude that in lupus nephritis neither alternative FN splicing, nor a high transcription level of TGF-β appears to be a general prerequisite for the development of GS.

Introduction

Injury to the kidney can result in chronic progressive renal failure with glomerulosclerosis, accompanied by excessive accumulation of extracellular matrix (ECM) components. Several studies in humans and animal models have shown increased deposition of fibronectin (FN) in glomerulosclerotic lesions (1-5). Accumulation of FN in the glomeruli may be caused by both increased local gene transcription and specific accumulation from the circulation (6).

The glycoprotein FN plays an important role in several biological processes including: maintenance of normal cell morphology, cell migration, cell differentiation, cell remodeling during embryogenesis, and wound healing (7-9). Three distinct splicing sites have been identified in the mRNA of the fibronectin molecule (10,11), which may be spliced-in or spliced-out in a tissue-specific and developmental stage-specific manner (12,13): the extra domain A (EDA), the extra domain B (EDB), and the type III connecting segment (IIICS or V) region. Increased inclusion of EDA-encoding fragments in fibronectin mRNA is observed in tissue during embryonic development (14) and at the margins of healing wounds (9,15), suggesting that the appearance of EDA+ and EDB+ fibronectin mRNA in the tissue is associated with a high rate of remodeling.

In the normal kidney, in both humans and rodents, the FN that contains the EDA domain is present in only small amounts in the mesangium, while the EDB containing FN is not detectable at the protein level. Alterations in the amount and localization of FN protein isoforms which contain the EDA and EDB domains have been found in both human diseases and experimental models (1,2,16-18).

A number of cytokines have been found to mediate the pathological process that leads to glomerulosclerosis. The cytokine TGF-β plays a causal role in the pathogenesis of glomerulosclerosis in the anti-Thy1 model by increasing the production of matrix molecules (19). TGF-β also affects splicing of FN (20,21). IL-4 may also play a role in the induction of quantitative and qualitative alterations in matrix composition, which occurs during the development of glomerulosclerosis. IL-4 expression is increased in various types of glomerulonephritis (22). *In vivo* studies showed that IL-4 plays a role in the development of glomerulosclerosis in GVHD mice (23).

In the current study, the splicing pattern of the FN EDA and EDB regions at the mRNA level was examined *in vivo* in several experimental models of immune complex glomerulonephritis, and it was examined *in vitro* in rat mesangial cells that had either been stimulated by TGF-β or transfected with IL-4. These data were also compared with the mRNA levels for fibronectin, EDA+ and EDB+ fibronectin, and TGF-β in human kidney biopsies from patients with glomerulosclerosis.

Materials and methods

In vivo animal studies

Animal models of nephritis-induced glomerulosclerosis.
Anti-Thy-1 nephritis (αThy1) was induced in female Lewis rats as described elsewhere (24). Animals were sacrificed at day 2, 6, and 14. Chronic serum sickness (CSS) was induced in Wistar rats as has been described elsewhere (25). These rats developed a membranous glomerulopathy with focal and segmental glomerulosclerosis (26). The time points at which the proteinuria reached a level of 800 mg/24 hr was considered week 0 of the experiment for each rat. Animals were sacrificed at week –3, 0, 5, and 20. Anti-glomerular basement membrane nephritis (αGBM) was induced in 12-weeks-old female C57BL/10 mice through injection of rabbit anti-GBM antibodies (a generous gift of Dr. K.J.M. Assmann, Dept. of Pathology, University Hospital Nijmegen, The Netherlands). The antibody was prepared as described before (27). Animals were sacrificed at day 0 (1hr after injection), 5, and 14. Animals developed glomerulonephritis and glomerulosclerosis within 14 days. Lupus nephritis was induced with the chronic Graft-versus-Host disease (GVHD) model by injecting 8-week-old female (C57BL/10 x DBA/2) F1 hybrids with a single-cell suspension of DBA/2 donor cells, as described before (28). These mice developed immune-complex glomerulonephritis, which was followed by glomerulosclerosis 8 to 10 weeks after induction of the disease. Animal care and experimentation were in accordance with legislation on animal experiments as determined by the Dutch Veterinary Inspection.

Glomerular RNA isolation
Rat glomeruli were isolated with the differential sieving technique (29). Mouse glomeruli were isolated with iron-oxide perfusion followed by magnetic extraction (30). RNA was isolated with TRIzol® reagent (Invitrogen, Paisley, Scotland, UK) according to the instructions of the manufacturer.

Reverse transcriptase-polymerase chain reaction (RT-PCR) for EDA and EDB fibronectin
cDNA was prepared using AMV reverse transcriptase RT (Roche, Germany), according to the prescription of the manufacturer, and the PCR was performed as described (31). DNA fragments were analyzed by electrophoresis and the radioactivity of each PCR product was visualized with a Phosphor Imager 445 SI (Molecular Dynamics, Sunnyvale, CA).

Immunohistochemistry

Immunofluorescence studies were performed on frozen kidney tissue from rats with CSS and from mice with GVHD to detect the presence of TGF-β1. Cryostat sections were incubated for 30 minutes at room temperature with a polyclonal rabbit antibody against human TGF-β1 (32).

***In vitro* studies**

Culture and transfection of rat MC

Glomeruli were isolated from 10-weeks old Lewis/MAA rats by the differential sieving method (29) and MC were cultured in RPMI 1640 medium supplemented with 20% heat inactivated FCS. The full-length rat IL-4 cDNA sequence from the plasmid pBABE-IL4, a generous gift of Dr. Wesseling from the University of Rotterdam, was subcloned into the expression vector pHβApr-1, which contains a β-actin promoter and a neomycin-resistance gene. This construct was introduced *in vitro* into rat MC with Fugene (Roche, Germany). Transfectants were tested for IL-4 production with ELISA according to the instructions of the manufacturer (Pharmingen, CA). Mesangial cells that had been transfected with the empty vector pHβApr-1 were used as a control.

Experimental design of in vitro studies with MC

IL-4 and mock-transfected MC were grown to near confluence. After growth-arrest for 18 hours in RPMI medium without serum, the cells were kept in growth-arrest state for another for 24 or 48 hours and the supernatants were collected for analysis. Total RNA was extracted. Cell lysates were harvested from cells that had been incubated for 48 hours by adding 5 ml lysisbuffer (1% triton X-100, 62.5 mM EDTA and 50 mM Tris/PBS). As a positive control for the alternative splicing of FN mRNA, untransfected cells were also cultured with 100 pM TGF-ß (Sigma, St. Louis, MO).

Soluble fibronectin (s-FN) and cell-associated fibronectin (c-FN) was measured with an ELISA. In brief, microtiter plates were coated with goat-anti-human FN (Sigma, St. Louis, MO). Rabbit-anti-mouse FN (1:2500) was applied to detect the bound FN, and anti-rabbit-HRP (DAKO, Demark) was used as a second step. A serial dilution of mouse FN (Gibco BRL, MD) was used as a standard.

Dot blot analysis, as previously described (33), was performed to measure the amount of FN mRNA. The hybridized filters were analyzed with a Phosphor Imager 445 SI (Molecular Dynamics, Sunnyvale, CA).

TGF-β mRNA levels were measured with real-time PCR using an Abi Prism 7700™ (Perkin

and Elmer). GAPDH was used as a housekeeping gene. Primer and TaqMan® Probe sequences are summarized in Table 1. Details concerning the real-time PCR protocol have been described elsewhere (34).

Studies on human biopsies

Biopsy material

The alternative splicing pattern of EDA and EDB FN was measured in human biopsies to compare the results obtained from the animal models and cultured mesangial cells. Twenty-four renal biopsies with glomerulosclerosis in at least 10% of the glomeruli were selected from the archives of the Pathology department at our hospital center. These biopsy specimens had been obtained from 24 patients (Table 2). As controls, renal tissue from five kidneys that had been obtained at autopsy, two biopsies from transplanted kidneys without histological abnormalities, and five cadaveric donor kidneys, not used for transplantation, were analyzed. These kidneys demonstrated normal function and histology. As a disease control, three transplanted kidneys with acute rejection were used as an additional group. Patient studies were approved by the LUMC ethical committee.

RT-PCR for TGF-β, total fibronectin, EDA, and EDB

RNA was extracted from the cortical tissue of frozen biopsy tissue from each patient with the aid of the Trizol® (Gibco BRL) method (35). Real-time PCR was used to quantify the mRNA levels of TGF-β, fibronectin, and the housekeeping molecule GAPDH. Primer and probe sequences can be found in Table 1.

Table 1. Primer and Taqman® probe sequences.

Gene	Species	Forward primer	Reverse primer	Taqman® probe	Label
EDA	Rat/mouse	TTGATTTCTTTCATTGGTCCTGTCTT	AAACAGAAATGACCATTGAAGGTTTG		
EDB	Rat/mouse	TGACATCAGAAGAATCAAAACCAGTT	TTACACTGTCAAAGATGACAAGGAAA		
TGF-ß	Rat	CACCGGAGAGCCCTGGATA	TTCCAACCCAGGTCCTTCCT	ACTACTGCTTCAGCTCCACAGAGAAGAACTGC	TET
GAPDH	Rat	ACCACCAACTGCTTAGCCCC	CACAGCCTTGGCAGCACC	TGGAAGGGCTCATGACCACAGTCCA	TET
Fibronectin	Human	GGAGAATTCAAGTGTGACCCTCA	AGGCAACGTGTTACGATGATGGGAAGACAT	TGCCACTGTTCTCCTACGTGG	TET
TGF-ß	Human	CCCAGCATCTGCAAAGCTC	GTCAATGTACAGCTGCCGCA	ACACCAACTATTGCTTCAGCTCCACGGA	TET
GAPDH	Human	TTCCAGGAGCGAGATCCCT	CACCCATGACGAACATGGG	CCCAGCCTTCTCCATGGTGGTGAA	FAM
EDA	Human	AAACAGAAATGACTATTGAAGGCTTG	AAACAGAAATGACTATTGAAGGCTTG		
EDB	Human	ATTACTCGTTATAGAATTACCACAACC	TAATATCAGAAAAGTCAATGCCAGTTG		

Statistics

Statistical analysis for comparison between groups was performed with unpaired Student's T-tests.

Results

In vivo animal studies

Development of renal disease

After induction of αThy1 nephritis, proteinuria started to develop at day 3. Mesangial cell proliferation and mesangial matrix expansion were visible after 6 days, and mesangial sclerosis was observed at day 14 (36). Induction of CSS has been shown to result in the development of membranous nephropathy (26). At the most severe stage of CSS (week 0) protein excretion of the rats reached a level of 800 mg/24 hours. In the following weeks, the protein levels gradually decreased to 400 mg/ 24 hours. In week 15 mesangial matrix expansion and thickening of the GBM were observed. At a later stage (from week 20) the development of focal and segmental glomerulosclerosis was observed. Induction of αGBM nephritis in mice leads to the development of proteinuria, mesangial cell proliferation, and finally glomerulosclerosis on day 14. GvHD, a model for human lupus nephritis, was induced in F1 hybrid mice, leading to the development of class V lupus nephritis. Albuminuria started to develop in week 4. From week 6 onwards, mice showed glomerular hypercellularity and membranous nephritis, leading to the development of

Table 2. Characteristics of controls and patient groups

Diagnosis	No.	Age (years) [b]	Sex (f/m)	Serum creat (μM) [b]
Normal controls	12	50.0 ± 22.8	7/5	87 ± 20
Acute transplant rejection	3	49.7 ± 7.8	1/2	377 ± 340
Lupus nephritis	3	36.3 ± 9.1	3/0	90 ± 37
Other chronic diseases				
IgA nephropathy	7	49.6 ± 11.4	1/6	200 ± 110
FSGS [a]	5	45.8 ± 9.9	2/3	489 ± 412
Diabetic nephropathy	5	63.2 ± 5.1	1/4	378 ± 338
Proliferative GN	4	61.5 ± 18.9	2/2	266 ± 100
Total	21	54.19 ± 13.2	6/15	318 ± 262

[a] FSGS: Focal and segmental glomerulosclerosis, GN: Glomerulonephritis
[b] Data are presented as means ± SD

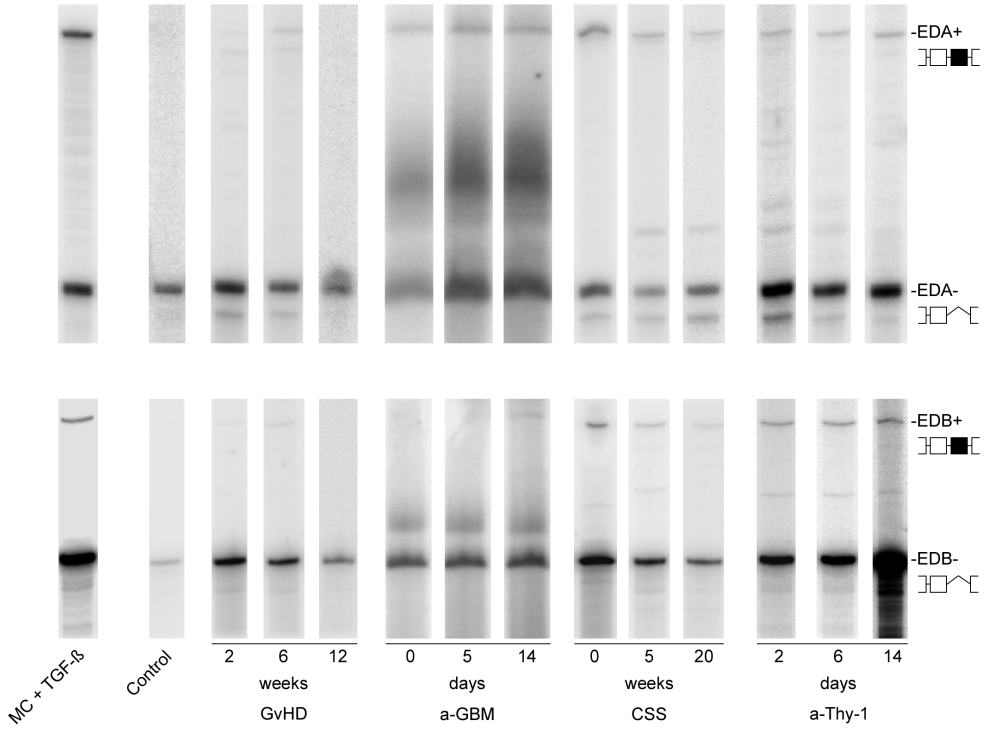

Figure 1. *Inclusion and exclusion patterns of the EDA and EDB domains in FN mRNA. Upper panel of the figure shows RT-PCR results for in- or exclusion of the EDA domain in FN mRNA, while the lower panel shows the results for the EDB region. A control sample of mouse mesangial cells cultured in the presence of TGF-β showed inclusion of both the EDA and the EDB domains in the FN mRNA, while normal mice did not express the oncofetal domains EDA and EDB. Induction of αGBM gave rise to an inclusion of the EDB domain in the FN mRNA at day 14, and an inclusion of EDA at days 0, 5, and 14. Induction of GvHD in mice did not lead to an inclusion of EDA or EDB region. Rats with αThy1 or CSS expressed both the oncofetal FN domains EDA and EDB.*

focal and segmental glomerulosclerosis from week 8 onwards.

Splicing patterns of FN mRNA in experimental models of glomerulonephritis

We performed an RT-PCR, with primers flanking the EDA or EDB region, on glomerular mRNA isolated from mice and rats at several time points after induction of the disease. The 526 bp amplification product corresponded to FN mRNA, which included the EDA region, while the 256 bp product corresponded to EDA-negative FN mRNA. Inclusion of the EDB region in the FN mRNA corresponded to the 640 bp product, and the 367 bp amplification product represented EDB-negative FN mRNA. Figure 1 shows the results of the RT-PCR experiments. A control sample of mouse mesangial cells that had been cultured in the presence of 100 pM TGF-β showed inclusion of the EDA and the EDB domains in the FN mRNA. Normal mice did not

express the oncofetal domains EDA and EDB. Induction of αGBM nephritis resulted in inclusion of the EDA domain in the FN mRNA on days 0, 5, and 14 and in inclusion of EDB on day 14. However, induction of GvHD in mice had no effect on the splicing pattern of FN mRNA (no inclusion of EDA and EDB). Induction of CSS or αThy1 in rats also resulted in oncofetal EDA and EDB-positive FN mRNA in glomeruli. These results are summarized in Table 2.

Immunohistochemistry for TGF-ß

In the rat model of CSS, TGF-β positive cells were observed in the glomerulus for 2 to 3 weeks prior to the most severe stage of the disease (Figure 2A). These TGF-β positive cells were not ED1 positive. The role of TGF-β in αThy1 disease and αGBM nephritis has been extensively described in the literature. Border et al. (19) have shown that TGF-β plays a role in the development of αThy1 disease. An important role for TGF-ß has also been described in anti-GBM nephritis (37,38). In the GVH model in the mice, no positive cells for TGF-β could be detected at any stage of the disease. Fig. 2B shows the results for week 6.

Table 3. Overview of the involvement of TGF-ß and the FN EDA/B splicing pattern in the different animal models, cultured mesangial cells, and human biopsies.

	TGF-ß	**EDA +**	**EDB +**
Animal model:			
GVHD	=	=	=
α-GBM	↑	↑	=/↑
α-Thy-1	↑↑	↑	↑
CSS	↑	↑	↑
Mesangial cells:			
IL-4 overexpr.[1]	↓	↓	=
Exogenous TGF-ß (100 pM)[2]	=	↑	↑
Human biopsies:			
Acute rejection	↑	↑	=
Lupus nephritis	=	=	=
Other chronic diseases	↑	↑	=

[1]IL-4 transfected rat mesangial cells. [2]TGF-ß means rat mesangial cells stimulated with TGF-ß. ↑ indicates increased expression compared to controls, ↓ indicates decreased expression compared to controls, = indicates no differences compared to controls.

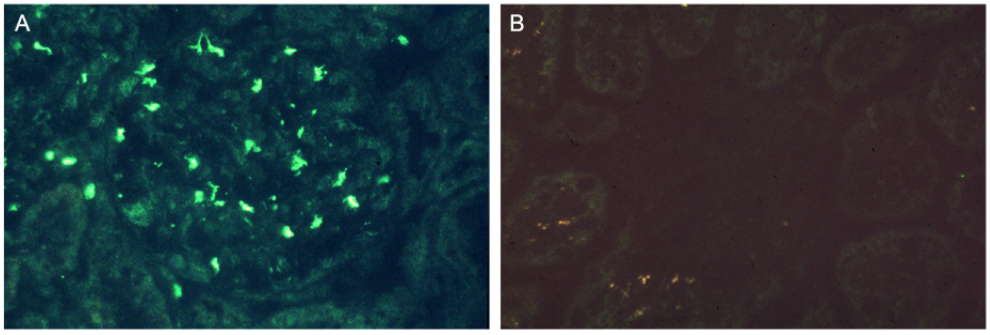

Figure 2. Expression of TGF-β1 positive cells in rats with CSS. Immunohistochemical staining of kidney sections for TGF-β1 showed expression of positive cells 2 and 3 weeks prior to the most severe stage of the disease (week 0)of CSS (Fig. A). Figure B shows a kidney section stained for TGF-ß six weeks after induction of GVHD.

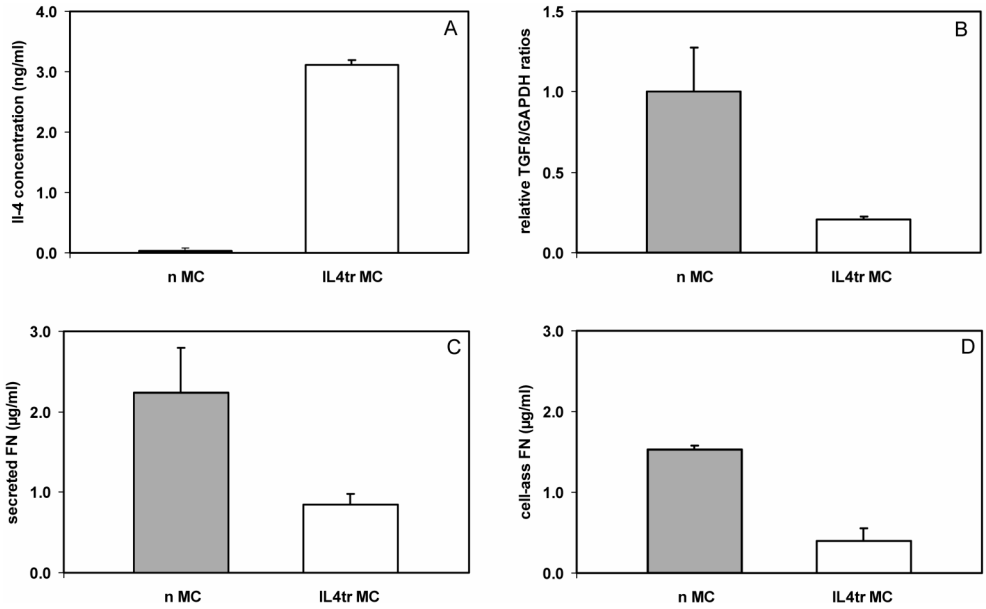

Figure 3. Measurements on cultured mesangial cells. Normal mesangial cells (nMC) cultured for 24 hours showed no production of IL-4 as measured by ELISA. IL-4 transfected mesangial cells (IL4tr MC) showed an increased production of the cytokine as compared to normal mesangial cells (A) ($P<0.01$). Mesangial cells were cultured for 24 hours and TGF-β1 mRNA levels were measured by RT- PCR. IL-4 transfected mesangial cells (IL4tr MC) showed a significant decrease in TGF-β1 mRNA production as compared to normal mesangial cells (nMC) in culture (B) ($P<0.01$). The production of secreted-FN (C) and cell-associated FN (D) of mesangial cells in culture was measured by ELISA. IL-4 transfected cells showed a significant decreased production of both secreted and cell-associated FN, as compared to normal mesangial cells ($P<0.01$).

In vitro studies

IL-4 overexpression in mesangial cells

Rat mesangial cells were transfected with IL-4 to investigate the role of IL-4 in the alternative splicing of FN. Normal mesangial cells in culture do not produce detectable amounts of IL-4 measured by ELISA, whereas mesangial cells transfected with the full-length rat IL-4 gene show an increased production of IL-4 (Fig 3A). Incubation of normal rat B cells with culture supernatant from IL-4 transfected cells resulted in an increased expression of MHC class II antigens (data not shown), indicating that the produced IL-4 is biologically active.

In IL-4 overexpressing mesangial cells, TGF-β1 mRNA levels were 5 times lower ($P<0.01$) than those in normal mesangial cells (Fig. 3B) The production of soluble fibronectin (s-FN) and cell-associated fibronectin (c-FN) was significantly reduced in IL-4 transfected mesangial cells (Fig. 3 C and D). The amount of total FN mRNA that was measured with dot blot analysis showed a significant decrease in cultured cells that had been transfected with IL-4 in comparison to mock-transfected mesangial cells (Fig.4A). IL-4 overexpression also influenced the splicing pattern of FN mRNA. After 24 hours of culture a significant decrease was seen in EDA+ FN mRNA levels. There was no significant effect of IL-4 over-expression on EDB+ FN mRNA levels (Figs. 4B and C).

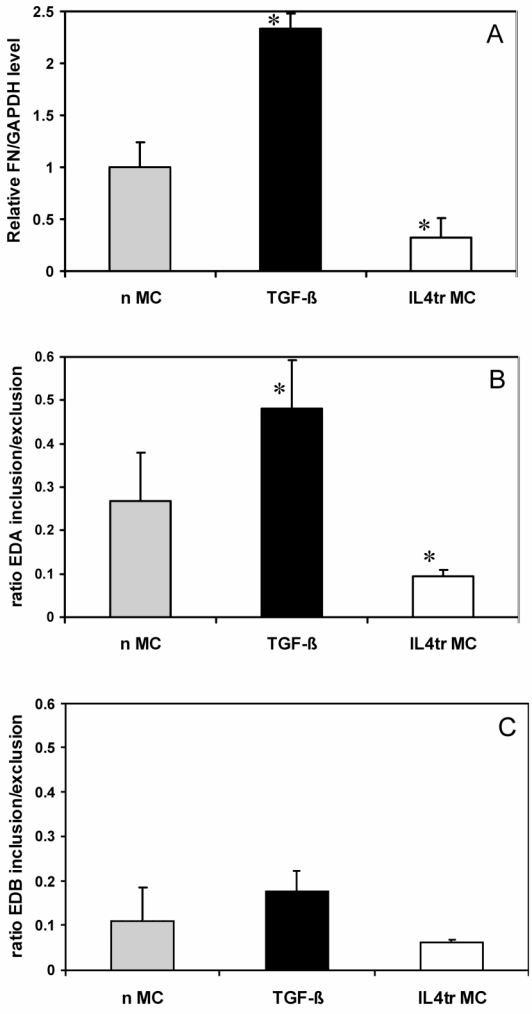

Figure 4. FN mRNA measurement on cultured mesangial cells. The amount of FN mRNA produced during 24 hours culture of mesangial cells was measured by dot blot analysis. IL-4 transfected cells produced significant lower levels of FN mRNA(A) while TGF-β stimulated MC showed an increase. Relative levels of FN mRNA containing the EDA and EDB domains were determined by rt-PCR. There was a significant decrease in the production of EDA+ FN mRNA in IL-4 transfected mesangial cells compared to normal mesangial cells in culture. TGF-ß stimulated MC showed a significant increase in EDA inclusion. The relative amounts of EDB positive FN mRNA remained unchanged both in IL-4 transfected and in TGF-β stimulated MCs (*$P<0.05$ compared to normal MCs).

Studies on human biopsies

mRNA levels in normal and diseased tissue

To validate the results obtained from the animal models, TGF-β mRNA levels, fibronectin mRNA levels, and the EDA+/EDA- mRNA ratio were measured in renal cortical tissue. Based on the findings of the animal studies, where the GVH model was the only model showing no increase of TGF-β and no inclusion of EDA at any time point of the disease, the patients with lupus nephritis were considered a separate group for the analysis. The other chronic renal disease entities were treated as one group. The relative TGF-β mRNA levels were 1.0 ± 0.4 for the controls, 2.2 ± 1.0 ($P<0.05$) for the patients with acute rejection, 1.1 ± 0.7 (P = NS) for the patients with lupus nephritis, and 1.7 ± 0.7 ($P<0.05$) for the patients with other chronic renal diseases (Figure 5A). The relative fibronectin mRNA levels were 1.0 ± 0.5, 2.5 ± 1.4 ($P<0.01$), 2.1 ± 2.1 (P = NS), and 3.1 ± 2.3 ($P < 0.05$), respectively (Figure 5B). The percentage of EDA+ mRNA in these groups were 22.8 ± 13.3, 41.3 ± 6.5 ($P < 0.05$), 19.4 ± 13.3 (P = NS), and 34.0 ± 11.8 ($P < 0.05$), respectively (Figure 5C). The percentage of EDB+ mRNA was less than 5 % in all groups (data not shown).

A correlation between the fibronectin mRNA level and the EDA+/EDA- mRNA ratio ($r = 0.48$, $P < 0.005$) was observed. The TGF-β mRNA level did not correlate with either the fibronectin mRNA level or the EDA+/EDA- mRNA ratio.

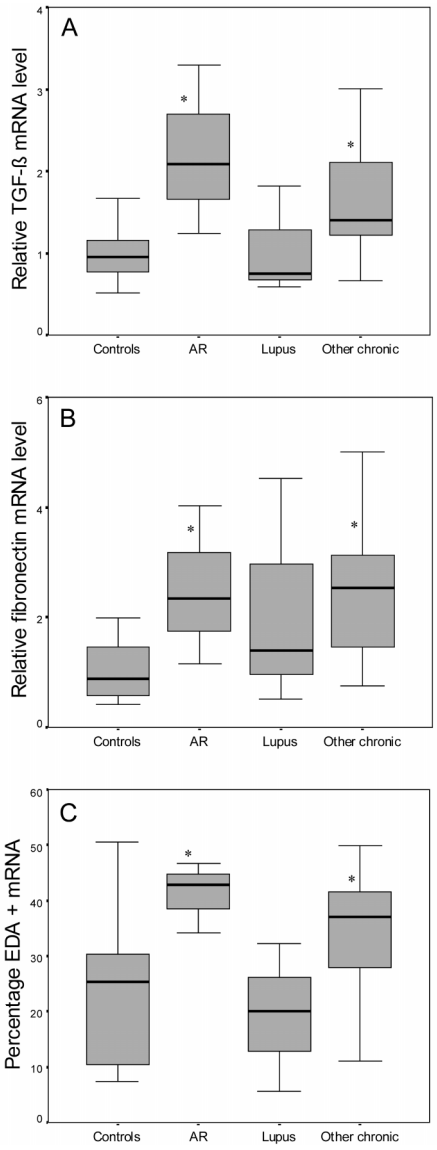

Figure 5. Relative mRNA levels in patients. (A) TGF-β mRNA levels, (B) fibronectin mRNA levels, and (C) the percentage EDA+ FN mRNA in renal cortical tissue from normal controls (n = 12), from patients with acute transplant rejection (n = 3), from patients with lupus nephritis (n = 3), and from patients with chronic renal disease (n = 21). Data are represented as means ± standard error of the mean. (*$P<0.05$ compared to controls)

Discussion

Most chronic human kidney diseases are characterized by an accumulation of ECM resulting in glomerulosclerosis and tubulo-interstitial fibrosis. The concept has been proposed that the development of these lesions, which is accompanied by progressive loss of kidney function, results from a final common pathway in a manner that is independent of the original etiology (1). However, the initiating mechanisms which precede to this final common pathway may vary. In patients with glomerulosclerosis the presence of EDA positive FN in the glomerulus has been demonstrated (1). It remains to be established whether all glomerulosclerotic lesions require the involvement of the same inducing and mediating factors. Since matrix proteins can modify the behavior of mesangial cells (39), the presence of particular FN isoforms in the mesangial matrix, as well as their amount and persistence during glomerular injury, may determine the evolution of either healing or scarring processes.

The aim of the present study was to investigate the splicing patterns of the EDA and EDB regions of FN in various glomerulopathies, and to elucidate the role of TGF-β1 and IL-4 in this process. The *in vivo* studies showed that splicing of FN mRNA is differentially regulated in αThy1, CSS, αGBM, and GVHD. Both acute and chronic disease in rats showed inclusion of the EDA and EDB regions. An increase in EDA and EDB containing FN isoforms was only observed in the acute model of αGBM disease in mice. TGF-β might be responsible for the presence of FN isoforms that contain EDA. Previous studies have described that TGF-β is capable of inducing EDA+ fibronectin synthesis (13,16,20,40,41). We presented data showing the presence of TGF-β early in the development of CSS. Border et al. (19) have shown that TGF-β plays a role in the development of glomerulosclerosis in αThy1 nephritis. The same is true for the αGBM model, in which TGF-β is involved in the development of the disease (42). Inclusion of EDA or EDB within the FN molecule was not detected in GVHD mice, a model in which TFG-β positive cells in the glomeruli or an increased glomerular mRNA level of TGF-β could not be found at any stage of the disease. In summary, results from various experimental models show that levels of TGF-β are associated with the extent of EDA and EDB inclusion.

The effect of IL-4 and TGF-β was investigated *in vitro* to achieve a better understanding of the effects of cytokines on FN transcription and splicing at the EDA region. Evidence for the involvement of IL-4 in the pathogenesis of glomerulonephritis has been provided by several investigators who have shown that intrinsic human glomerular cells express mRNA for both IL-4 and IL-4 receptor (22), and that IL-4 expression is upregulated in various types of GN. In crescentic GN, early IL-4 treatment was shown to reduce proteinuria and inflammation (43). Our results demonstrated that overexpression of IL-4 in cultured mesangial cells led to a reduction of the amount of EDA+ FN mRNA. Also, a reduced overall production of FN by decreased FN

transcription was observed in IL-4 transfected MC. The decreased EDA inclusion might be explained by the significant decrease in TGF-β mRNA production found in IL-4 overexpressing cells. Decreased TGF-β1 serum levels (44) were observed in mice with constitutive transgenic expression of IL-4. These results suggest that IL-4 may play a role in the induction of quantitative and qualitative alterations in matrix composition, during the development of glomerulosclerosis.

Chronic GHVD was the only model tested in which we could not find an indication for a role for TGF-β and EDA inclusion. We wanted to investigate whether these findings could be confirmed in human glomerulosclerosis. Therefore, we measured the mRNA levels of fibronectin and the ratio between EDA+ and EDA- mRNA in controls and diseased renal tissue. We also analyzed TGF-β mRNA levels in these tissues. The renal biopsies with glomerulosclerosis were divided into two subgroups. One group consisted of patients suffering from lupus nephritis, which corresponded to the GHVD model in the mice, while the other group consisted of various other chronic kidney diseases. TGF-β, fibronectin mRNA, and the EDA+/EDA- mRNA ratio were significantly increased in patients with renal disease in comparison to the controls. In contrast, patients with lupus nephritis did not show a significant increase in TGF-β, FN, and EDA+/EDA- in comparison to controls, which corroborates the experimental models. The steady-state level of fibronectin mRNA correlates with the EDA+/EDA- mRNA ratio, indicating that the increased fibronectin mRNA observed in chronic disease is mainly EDA positive.

The question remains what triggers the development of GS in mice with GVHD-induced lupus nephritis and in patients with lupus nephritis. In an earlier study we have shown that in these mice the accumulation of FN protein during the sclerotic phase of the disease is not a result of an increased FN production but a result of specific trapping of plasma fibronectin from the circulation (45). Circulating FN was shown to bind through its heparin binding site to integrin α5β1, which was upregulated in glomeruli in the later stage of the disease (6). IL-4 has been found to induce upregulation of ß1-integrins in lung fibroblasts (46). Therefore, EDA negative FN from the circulation might be trapped in the kidney through binding to integrins, of which the expression is induced by IL-4. In addition, mice with constitutive transgenic expression of IL-4 show progressive glomerulosclerosis with mesangial accumulation of collagens type I, IV, and V. Seven-day-old IL-4-transgenic animals showed early renal fibrotic changes in the absence of immune deposits or TGF-β1 upregulation (44). Treatment of these mice with IL-4 neutralizing antibody prevented renal disease (47). It has also been found that IL-4 is capable of activating the human type I collagen promoter in lung fibroblasts and may thus contribute to lung fibrosis (48). In addition, NZM.2410 mice rendered deficient in STAT6, a transcription factor involved in the production and function of type 2 cytokines, are completely protected from the development of glomerulosclerosis(49). The renoprotective effects of ACE inhibitors in lupus nephritis may be explained in part by their negative action on IL-4 and IL-10

production (50). From our study we conclude that alternative splicing of the EDA domain of FN mRNA is correlated with the presence of TGF-β. The results suggest that TGF-β is a key player in the development of GS by inducing FN production and alternative FN mRNA splicing. On the other hand, we showed that *in vitro* TGF-β and IL-4 have opposing effects with respect to spicing at the EDA region of FN. In lupus glomerulonephritis, in which the role of TGF-β in GS is less prominent, type 2 cytokines such as IL-4 probably predominate in the induction of collagen synthesis and FN accumulation from the circulation, which leads to increased matrix accumulation and glomerulosclerosis. Therefore, neither alternative FN splicing, nor a high transcription level of TFG-β appears to be a general prerequisite for the development of GS.

Acknowledgements

We thank Jan van der Ploeg, Michel Mulders, Leontine van der Wel and Monique L. Scholtes for excellent technical assistance. This work was in part supported by the Royal Dutch Academy of Science.

Refereces

1. Van Vliet A, Baelde HJ, Vleming LJ, De Heer E, Bruijn JA: Distribution of fibronectin isoforms in human renal disease. *J Pathol* 193:256-262, 2001
2. Assad L, Schwartz MM, Virtanen I, Gould VE: Immunolocalization of tenascin and cellular fibronectins in diverse glomerulopathies. *Virchows Arch B Cell Pathol Incl Mol Pathol* 63:307-316, 1993
3. Abrass CK, Adcox MJ, Raugi GJ: Aging-associated changes in renal extracellular matrix. *Am J Pathol* 146:742-752, 1995
4. Vleming LJ, Baelde JJ, Westendorp RGJ, Daha MR, Van Es LA, Bruijn JA: The glomerular deposition of PAS positive material correlates with renal function in human kidney diseases. *Clin Nephrol* 47:158-167, 1997
5. Bergijk EC, Munaut C, Baelde JJ, Prins F, Foidart JM, Hoedemaeker PJ, Bruijn JA: A histological study of the extracellular matrix during the development of glomerulosclerosis in murine chronic graft-versus-host disease. *Am J Pathol* 140:1147-1156, 1992
6. Van Vliet AI, van Alderwegen IE, Baelde HJ, De Heer E, Bruijn JA: Fibronectin accumulation in glomerulosclerotic lesions: self-assembly sites and the heparin II binding domain. *Kidney Int* 61:481-489, 2002
7. Ruoslahti E: Fibronectin and its receptors. *Annu Rev Biochem* 57:375-413, 1988
8. Oyama F, Murata Y, Suganuma N, Kimura T, Titani K, Sekiguchi K: Patterns of alternative splicing of fibronectin pre-mRNA in human adult and fetal tissues. *Biochem* 28:1428-1434, 1989
9. Ffrench-Constant C, Van De WL, Dvorak HF, Hynes RO: Reappearance of an embryonic pattern of fibronectin splicing during wound healing in the adult rat. *J Cell Biol* 109:903-914, 1989
10. Kornblihtt AR, Umezawa K, Vibe-Pedersen K, Baralle FE: Primary structure of human fibronectin: differential splicing may generate at least 10 polypeptides from a single gene. *EMBO J* 4:1755-1759, 1985
11. Schwarzbauer JE, Patel RS, Fonda D, Hynes RO: Multiple sites of alternative splicing of the rat fibronectin gene transcript. *EMBO J* 6:2573-2580, 1987
12. Pagani F, Zagato L, Vergani C, Casari G, Sidoli A, Baralle FE: Tissue-specific splicing pattern of fibronectin messenger RNA precursor during development and aging in rat. *J Cell Biol* 113:1223-1229, 1991
13. Magnuson VL, Young M, Schattenberg DG, Mancini MA, Chen DL, Steffensen B, Klebe RJ: The alternative splicing of fibronectin pre-mRNA is altered during aging and in response to growth factors. *J Biol Chem* 266:14654-14662, 1991
14. Ffrench-Constant C, Hynes RO: Alternative splicing of fibronectin is temporally and spatially regulated in the chicken embryo. *Development* 106:375-388, 1989
15. Brown LF, Dubin D, Lavigne L, Logan B, Dvorak HF, Van De WL: Macrophages and fibroblasts express embryonic fibronectins during cutaneous wound healing. *Am J Pathol* 142:793-801, 1993
16. Nickeleit V, Zagachin L, Nishikawa K, Peters JH, Hynes RO, Colvin RB: Embryonic fibronectin isoforms are synthesized in crescents in experimental autoimmune glomerulonephritis. *Am J Pathol* 147:965-978, 1995
17. Barnes JL, Torres ES, Mitchell RJ, Peters JH: Expression of alternatively spliced fibronectin variants during remodeling in proliferative glomerulonephritis. *Am J Pathol* 147:1361-1371, 1995
18. Alonso J, Gómez-Chiarri M, Ortíz A, Serón D, Condom E, López-Armada MJ, Largo R, Barat A, Egido J: Glomerular up-regulation of EIIIA and V120 fibronectin isoforms in proliferative immune complex nephritis. *Kidney Int* 50:908-919, 1996
19. Border WA, Okuda S, Languino LR, Sporn MB, Ruoslahti E: Suppression of experimental glomerulonephritis by antiserum against transforming growth factor beta 1. *Nature* 346:371-374, 1990
20. Viedt C, Burger A, Hansch GM: Fibronectin synthesis in tubular epithelial cells: up-regulation of the EDA splice variant by transforming growth factor beta. *Kidney Int* 48:1810-1817, 1995
21. Balza E, Borsi L, Allemanni G, Zardi L: Transforming growth factor β regulates the levels of different fibronectin isoforms in normal human cultured fibroblasts. *FEBS Lett* 228:42-44, 1988
22. Furusu A, Miyazaki M, Koji T, Abe K, Ozono Y, Harada T, Nakane PK, Hara K, Kohno S: Involvement of IL-4 in human glomerulonephritis: an in situ hybridization study of IL-4 mRNA and IL-4 receptor mRNA. *J Am Soc Nephrol* 8:730-741, 1997
23. de Wit D, van Mechelen M, Zanin C, Doutrelepont JM, Velu T, Gerard C, Abramowicz D, Scheerlinck

JP, De Baetselier P, Urbain J: Preferential activation of Th2 cells in chronic graft-versus-host reaction. *J Immunol* 150:361-366, 1993
24. Bagchus WM, Hoedemaeker PJ, Rozing J, Bakker WW: Glomerulonephritis induced by monoclonal anti-Thy 1.1 antibodies. A sequential histological and ultrastructural study in the rat. *Lab Invest* 55:680-687, 1986
25. Bergijk EC, Baelde HJ, De Heer E, Killen PD, Bruijn JA: Role of the extracellular matrix in the development of glomerulosclerosis in experimental chronic serum sickness. *Exp Nephrol* 3:338-347, 1995
26. Hogendoorn PCW, Bruijn JA, Gelok EWA, Van den Broek LJ, Fleuren GJ: Development of progressive glomerulosclerosis in experimental chronic serum sickness. *Nephrol Dial Transplant* 5:100-109, 1990
27. Schrijver G, Bogman MJ, Assmann KJM, De Waal RMW, Robben HCM, Van Gasteren H, Koene RA: Anti-GBM nephritis in the mouse: role of granulocytes in the heterologous phase. *Kidney Int* 38:86-95, 1990
28. Bruijn JA, Van Elven EH, Hogendoorn PCW, Corver WE, Hoedemaeker PJ, Fleuren GJ: Murine chronic graft-versus-host disease as a model for human lupus nephritis. *Am J Pathol* 130:639-641, 1988
29. Bowman C, Peters DK, Lockwood CM: Anti-glomerular basement membrane autoantibodies in the Brown Norway rat: detection by a solid-phase radioimmunoassay. *J Immunol Methods* 61:325-333, 1983
30. Baelde JJ, Bergijk EC, Hoedemaeker PJ, De Heer E, Bruijn JA: Optimal method for RNA extraction from mouse glomeruli. *Nephrol Dial Transplant* 9:304-308, 1994
31. Bergijk EC, Baelde HJ, Kootstra CJ, De Heer E, Killen PD, Bruijn JA: Cloning of the mouse fibronectin V-region and variation of its splicing pattern in experimental immune complex glomerulonephritis. *J Pathol* 178:462-468, 1996
32. De Heer E, Pas O, Prins F, Van der Wal AM, Van Diemen-Steenvoorde R, Boersma W, Bruijn JA: The major TGF-β1 synthesizing cells in rats with anti-Thy-1 neprhitits are intrinsic mesangial cells [Abstract]. J Am Soc Nephrol 4:946, 1993
33. Van Vliet AI, van Alderwegen IE, Baelde HJ, De Heer E, Killen PD, Kalluri RK, Bruijn JA, Bergijk EC: Differential expression of collagen type IV alpha-chains in the tubulointerstitial compartment in experimental chronic serum sickness nephritis. *J Pathol* 189:279-287, 1999
34. Eikmans M, Baelde HJ, De Heer E, Bruijn JA: Effect of age and biopsy site on extracellular matrix mRNA and protein levels in human kidney biopsies. *Kidney Int* 60:974-981, 2001
35. Eikmans M, Baelde HJ, De Heer E, Bruijn JA: Processing renal biopsies for diagnostic mRNA quantification: improvement of RNA extraction and storage conditions. *J Am Soc Nephrol* 11:868-873, 2000
36. Aben JA, Hoogervorst DA, Paul LC, Borrias MC, Noble NA, Border WA, Bruijn JA, De Heer E: Genes expressed by the kidney, but not by bone marrow-derived cells, underlie the genetic predisposition to progressive glomerulosclerosis after mesangial injury. *J Am Soc Nephrol* 14:2264-2270, 2003
37. Tang WW, Feng L, Loskutoff DJ, Wilson CB: Glomerular extracellular matrix accumulation in experimental anti-GBM Ab glomerulonephritis. *Nephron* 84:40-48, 2000
38. Datta PK, Reddy RS, Lianos EA: Effects of all-trans-retinoic acid (atRA) on inducible nitric oxide synthase (iNOS) activity and transforming growth factor beta-1 production in experimental anti-GBM antibody-mediated glomerulonephritis. *Inflammation* 25:351-359, 2001
39. Alonso J, Mampaso F, Martin A, Palacios I, Egido J: Changes in the pattern of fibronectin mRNA alternative splicing in acute experimental mesangioproliferative nephritis. *Lab Invest* 79:185-194, 1999
40. Bürger A, Wagner C, Viedt C, Reis B, Hug F, Hänsch GM: Fibronectin synthesis by human tubular epithelial cells in culture: Effects of PDGF and TGF-β on synthesis and splicing. *Kidney Int* 54:407-415, 1998
41. Van der Velde-Zimmermann D, Verdaasdonk MAM, Rademakers LHPM, De Weger RA, Van den Tweel JG, Joling P: Fibronectin distribution in human bone marrow stroma: Matrix assembly and tumor cell adhesion via α5β1 integrin. *Exp Cell Res* 230:111-120, 1997
42. Kanamaru Y, Nakao A, Mamura M, Suzuki Y, Shirato I, Okumura K, Tomino Y, Ra C: Blockade of TGF-beta signaling in T cells prevents the development of experimental glomerulonephritis. *J Immunol* 166:2818-2823, 2001
43. Cook HT, Singh SJ, Wembridge DE, Smith J, Tam FW, Pusey CD: Interleukin-4 ameliorates crescentic

glomerulonephritis in Wistar Kyoto rats. *Kidney Int* 55:1319-1326, 1999
44. Ruger BM, Hasan Q, Erb KJ, Davis PF: Progression of renal disease in interleukin-4 transgenic mice: involvement of transforming growth factor-beta. *Int J Exp Pathol* 80:113-123, 1999
45. Bergijk EC, Baelde HJ, De Heer E, Killen PD, Bruijn JA: Specific accumulation of exogenous fibronectin in experimental glomerulosclerosis. *J Pathol* 176:191-199, 1995
46. Doucet C, Brouty-Boye D, Pottin-Clemenceau C, Jasmin C, Canonica GW, Azzarone B: IL-4 and IL-13 specifically increase adhesion molecule and inflammatory cytokine expression in human lung fibroblasts. *Int Immunol* 10:1421-1433, 1998
47. Ruger BM, Erb KJ, He Y, Lane JM, Davis PF, Hasan Q: Interleukin-4 transgenic mice develop glomerulosclerosis independent of immunoglobulin deposition. *Eur J Immunol* 30:2698-2703, 2000
48. Buttner C, Skupin A, Rieber EP: Transcriptional activation of the type I collagen genes COL1A1 and COL1A2 in fibroblasts by interleukin-4: analysis of the functional collagen promoter sequences. *J Cell Physiol* 198:248-258, 2004
49. Singh RR, Saxena V, Zang S, Li L, Finkelman FD, Witte DP, Jacob CO: Differential Contribution of IL-4 and STAT6 vs STAT4 to the Development of Lupus Nephritis. *J Immunol* 170:4818-4825, 2003
50. De Albuquerque DA, Saxena V, Adams DE, Boivin GP, Brunner HI, Witte DP, Singh RR: An ACE inhibitor reduces Th2 cytokines and TGF-beta1 and TGF-beta2 isoforms in murine lupus nephritis. *Kidney Int* 65:846-859, 2004

Chapter 5

Fibronectin accumulation in glomerulosclerotic lesions: self-assembly sites and the heparin II binding domain

A.I. van Vliet, I.E. van Alderwegen, H.J. Baelde, E. de Heer, J.A. Bruijn

Department of Pathology, Leiden University Medical Center,
Leiden, The Netherlands

Kidney International 61(2):481-9, 2002

Abstract

Glomerulosclerosis is a severe complication of many immunologically mediated kidney diseases, eventually resulting in loss of renal function. In chronic graft-versus-host disease (GvHD) in mice, a model for human lupus nephritis, the end-stage sclerotic lesions were previously shown to contain large amounts of fibronectin (FN). This study investigated a domain-specific accumulation process of circulating plasma FN (pFN) in sclerotic lesions.

GvHD mice were injected with FITC-conjugated pFN or pFN-fragments, with or without heparin pre-incubation. pFN-fragments were generated by digestion of FN by Cathepsin D, after which the fragments were separated on a heparin affinity column. Thus, two batches of fragments were obtained with either low or high affinity for heparin.

FN accumulation was accompanied by an up-regulated expression of integrin $\alpha 5\beta 1$, the FN receptor, in the periphery of sclerotic lesions. pFN-FITC injected into GvHD mice was trapped in sclerotic glomeruli within 24 hrs. Both heparin and non-anti-coagulant heparin blocked the accumulation of pFN-FITC, indicating that the protective effect of heparin in the trapping of FN is independent of its anticoagulant properties, and probably results from preventing direct binding of FN in the sclerotic lesions.

To investigate whether FN binds in the glomerulus via the heparin-binding regions, pFN-fragments were generated and injected into GvHD mice. Whereas the fraction with high affinity for heparin did not accumulate in the sclerotic glomeruli, the fraction with low affinity for heparin did. Partial sequencing of the isolated peptides showed that in the glomerulus fibronectin does not bind via the heparin II binding region.

We hypothesize that the protective effect of heparin treatment may be the result of steric hindrance of the specific binding sites, that is, the $I_{1\text{-}5}$ and/or III_1 self-assembly sites of FN.

Introduction

Accumulation of extracellular matrix (ECM) molecules in the glomerulus leads to the development of glomerulosclerosis, which is a prominent feature of many immunologically mediated renal diseases. Glomerulosclerosis, together with tubulointerstitial fibrosis, causes irreversible end-stage renal damage with poor patient prognosis. Vleming et al. reported that of a number of matrix molecules in a variety of human renal diseases, only the amount of intraglomerular fibronectin (FN) deposition correlates with the severity of glomerular structural abnormalities, and inversely with renal function (1).

FN is a large adhesive glycoprotein, that is widely distributed as cellular FN (cFN) in the ECM of various tissues and on cell surfaces, and as soluble plasma FN (pFN) in the circulation. FN is involved in the regulation of cell adhesion, differentiation, migration, and proliferation. This multifunctional protein consists of a dimer of two disulfide-bonded subunits, each with a molecular weight of approximately 220 kD, that contain binding sites for heparin, collagen, DNA, integrins, and FN itself (2,3). In the normal kidney FN is located in the mesangium, the glomerular basement membrane (GBM), Bowman's capsule and the tubular basement membrane (TBM)(4). FN has a crucial role in the organization of ECM components, and is considered to play a key part in the pathogenesis of some glomerulonephritides, where the molecule is present in increased amounts in the expanded mesangium (5,6).

Chronic Graft-versus-Host disease (GvHD) in mice is an experimental model for human systemic lupus erythematosus (SLE), in which a transfer of donor lymphocytes into F1-hybrid recipients causes uncontrolled B-cell activation with production of autoantibodies (7). This results in an immune complex glomerulonephritis, resembling human lupus nephritis (8). Both in the GvHD model and in human renal diseases, the end-stage glomerulosclerotic lesions consist mainly of FN, which accumulates as a result of specific trapping of pFN from the circulation rather than through *de novo* synthesis (9). The mechanism by which the specific accumulation of pFN in the sclerotic lesions takes place is still unknown. FN accumulation may result from its involvement in the blood coagulation system, or via direct binding of pFN to cells or other ECM components in the damaged glomerulus.

Because the accumulation of FN in the end-stage glomerulosclerotic lesions may be the result of an activation of the coagulation cascade, we studied the effect of heparin on the glomerular accumulation of FITC-labeled pFN in the GvHD model. Heparin is a sulfated glycosaminoglycan, closely related to heparan sulfate, with a long history in the treatment of patients with thrombotic diseases. Many ECM components, such as fibronectin, laminin, thrombospondin and different types of collagen, can bind to heparin. In addition to its anti-coagulant function, heparin has an impact on interactions that involve matrix organization, cell

adhesion, proliferation, and cytokine action (reviewed by (10)). With regard to the kidney, heparin was shown to have an anti-proliferative effect on cultured vascular smooth muscle cells, epithelial cells, and mesangial cells (11-14). In several models, e.g. renal ablation, MRL/*lpr* mice, puromycine aminonucleoside-induced nephrotic syndrome, and anti-Thy 1.1 nephritis in the rat, administration of heparin diminishes proteinuria and hypertension, and decelerates the progression of renal insufficiency and glomerulosclerosis *in vivo* (15-19).

Our results show that both heparin and N-desulfated heparin can block accumulation of injected pFN-FITC and specific Cathepsin-induced FN fragments in glomerulosclerotic lesions. These results provide evidence for a domain-specific accumulation process in the accumulation of circulating FN in sclerotic lesions.

Materials and methods

Animals

DBA/2 and C57BL/10*DBA/2 F1 hybrid mice were purchased from Harlan BV (Horst, The Netherlands). Female DBA/2 mice aged 7 to 8 weeks served as donors of lymphocytes in the induction of GvHD. Eight to 10 week-old female F1 hybrids served as recipients of lymphocytes. GvHD was induced in 61 experimental F1 hybrid mice. Eleven age- and sex-matched normal F1 hybrid mice (NF1) were used as controls. The numbers of animals used for each experiment are detailed in the results section.

Induction of disease

GvHD was induced in F1 hybrid mice as described previously (20). In brief, single cell suspensions were prepared from DBA/2 spleens, lymph nodes, and thymi in Hanks' balanced salt solution (HBSS). The total number of cells and the proportion of vital cells were determined by Trypan blue staining. The suspensions were mixed, and injected intravenously in F1 recipients on days 0, 3, 7, and 10. Each dose of $25*10^6$ viable DBA/2 cells in 0.25 ml HBSS was composed of approximately 60% spleen cells, 30% thymocytes, and 10% lymph-node cells.

Accumulation experiments

All accumulation experiments were performed 10-12 weeks after the induction of GvHD, since specific trapping of pFN in the glomerulosclerotic lesions has been shown to occur at this timepoint. GvHD mice were injected intravenously with 500 µg FITC-conjugated mouse pFN with or without 250 U (non-anti-coagulant) heparin. This is approximately 15% of the normal total plasma FN content of a mouse as estimated by a quantitative sandwich-ELISA technique (unpublished results). Where appropriate, pFN and either heparin or non-anti-coagulant heparin

were incubated together for 1 h at 37°C before injection, after which the solution was spun down for 30 sec to remove FITC-crystals. pFN-heparin complexes remained soluble during the incubation and centrifugation step.

pFN-fragments were obtained as detailed below. Accumulation experiments with the pFN-fragments were performed with 250 μg of the FITC-conjugated low-affinity pFN fraction or 125 μg of the FITC-conjugated high-affinity pFN fraction, with or without 250 U heparin. The amounts of injected FITC-conjugated pFN-fragments were adjusted to equimolar amounts of molecules as compared to total pFN molecules injected in previous experiments. As controls, NF1 hybrid mice were injected intravenously with either pFN or one of the pFN fragments with or without pre-incubation with heparin.

Follow-up of F1 mice

The urine albumin content of the GvHD F1 mice was determined at two-weekly intervals, starting 2 weeks before disease induction. Animals were kept in urine-collection cages for 18 h with free access to water and food. The albumin levels were assessed by rocket electrophoresis against rabbit anti-mouse albumin, with albumin as a standard (Sigma Chemical Corporation, St.Louis, MN, USA) (20).

Groups of three experimental mice were sacrificed at week 0, 2, 4, 6, 8, 10, and 12 of GvHD. After perfusion with PBS, the kidneys were removed. For light microscopic examination with periodic acid-Schiff (PAS) reagent and phosphotungstic acid haematoxylin (PTAH), a part of the kidney tissue was fixed in 10% buffered formalin, dehydrated, and then embedded in Paraplast (Amstelstad, Amsterdam, The Netherlands). The remaining tissue was frozen in CO_2 ice-cooled isopentane and stored at –70°C until further use. Immunohistochemistry was performed with a fluorescein-isothiocyanate (FITC)-conjugated rat anti-mouse CD49e monoclonal antibody (Pharmingen, San Diego, CA, USA) to detect the integrin α5 chain. The FITC-conjugated rabbit anti-mouse CD49d monoclonal antibody (anti-integrin α4 chain) was a generous gift of Dr. E. Ruoslahti (Cancer Research Center, La Jolla, CA, USA). Fluorescence intensity was scored semi-quantitatively on a scale from 0 to 3+, in which 0 represented no staining and 3+ reflected a very strong staining. The slides were scored in a double-blinded fashion by two observers independently of each other, using a Leitz fluorescence microscope. Representative examples of the scoring are shown in figure 1.

Eighteen hours after the injection of pFN or pFN-fragments, groups of mice were sacrificed. The numbers of animals used for each experiment are detailed in the results section. After perfusion with PBS, the kidneys were removed and stored for light and fluorescence microscopy as described above. The amount accumulation of pFN or pFN-fragments was scored semi-quantitatively on a scale from 0 to 3+, in which 0 represented no accumulation and 3+ reflected

a very strong accumulation. The slides were scored in a double-blinded fashion by two observers independently of each other, using a Leitz fluorescence microscope. Representative examples of the scoring are shown in figure .

pFN isolation and purification of pFN fragments

pFN was isolated from normal mouse plasma, in the presence of 30 mM citrate as an anti-coagulant. The plasma was dialyzed overnight against PBS/10 mM EDTA at 4°C. The plasma was spun down at 3,000g for 20 min. to remove protein aggregates, after which the supernatant was circulated over a gelatin-Sepharose 4B affinity column for 2 h. The column was rinsed with PBS/10 mM EDTA. pFN was eluted from the column with 6 M urea in 0.1 M citric acid/50 mM Tris pH 4.7. The eluate was dialyzed overnight against PBS/10 mM EDTA at 4°C before labeling with FITC (21). For preparation of pFN fragments 10 mg of affinity-purified pFN was dialyzed overnight against 50 mM sodium acetate/50 mM NaCl/10 mM EDTA pH 6.4. Addition of a 10% solution of glacial acetic acid was used to adjust the pH of the dialysate to 3.5. Digestion with Cathepsin D (Sigma-Aldrich N.V./S.A., Bornem, The Netherlands) was performed for 18 h at 37°C in a weight ratio of FN:Cathepsin D = 200:1. Adjusting the pH to 7 with 2.5 M Tris (pH 9) terminated the reaction. The digested pFN solution was tested by SDS-PAGE, under reducing conditions, before purification of the fragments.

The heparin-Sepharose 4B affinity column was equilibrated with 20 mM Tris/50 mM NaCl/ 10 mM EDTA/5 mM Caproic acid/0.2 mM PMSF pH 7.4. The digested pFN was allowed to bind to the column by recirculation of the effluent, followed by the washing with three column volumes of equilibration buffer. The pFN fragments were eluted by a discontinuous gradient subsequently consisting of 0.25 M, 0.6 M and 1 M NaCl in equilibration buffer. The separate fractions were analyzed by SDS-PAGE under reducing conditions, dialyzed overnight against PBS/10 mM EDTA at 4°C, and labeled with FITC (21). Fractions were concentrated and washed by high-pressure diafiltration in a Centricon (Amicon), and stored at –20°C until further use.

Preparation of non-anti-coagulant heparin

Heparin (Organon Teknika Nederland BV, Boxtel, The Netherlands) was converted into N-desulfated non-anti-coagulant heparin according to the procedure of Inoue and Nagasawa (22). In brief, sodium-heparin salt dissolved in 0.1 M HCl was converted into a pyridin-heparin salt on a DOWEX column (Pharmacia, Uppsala, Sweden). Desulfation was performed by using dimethyl sulfoxide/5% methanol. Activated partial thromboplastin time (aPTT) was performed according to the manufacturers protocol (Boehringer, Mannheim, Germany). N-desulfated non-anti-coagulant heparin had no effect on the clotting time. In an ELISA under isotonic conditions, non-anti-coagulant heparin and anti-coagulant heparin were found to have comparable binding

capacities to pFN (unpublished results).

Statistical analysis

Results are presented as means ± SD where indicated, and were analyzed using the Chi-square test. $P \leq 0.05$ was considered statistically significant.

Results

Clinical course of GvHD

Four weeks after the induction of GvHD, mice developed abnormal proteinuria. Albuminuria reached the highest levels at week 12 (results not shown). At this timepoint the majority of the animals developed ascites and edema. Light-microscopy of kidney sections of GvHD mice showed a lupus type of nephritis, complicated by focal and segmental glomerulosclerosis starting 10 weeks after the induction of the disease (Fig. 1), confirming earlier results (20). Furthermore, PTAH staining showed fibrin deposited in sclerotic regions, suggesting that the coagulation pathway may be involved in the development of glomerulosclerosis in GvHD (results not shown).

Altered expression of integrins that specifically bind to FN may well lead to enhanced binding of pFN in the glomerulosclerotic lesions. Immunohistochemistry showed that both the integrin chains α4 and α5 were expressed in minimal amounts in the glomeruli of NF1 mice (fluorescence intensity +/-, diffuse pattern). The expression of the integrin α4 did not alter during the development of GvHD. However, from week 6 on we observed increased amounts of the α5 integrin chain in the periphery of sclerotic lesions (segmental staining, fluorescence intensity 3+, Fig. 1). Control staining with an irrelevant non-immune IgG showed no fluorescence pattern in NF1 or GvHD mice.

pFN isolation and purification of pFN fragments

Figure 2 shows the results of SDS-PAGE analysis of isolated pFN and pFN fragments under reducing conditions. Total pFN was isolated by affinity chromatography and has a molecular weight of 220 kD (lane B). Incubation of pFN with Cathepsin D for 18 hr led to complete digestion of pFN (lane C). Digestion for a longer period of time or at a higher protein/proteinase ratio did not provide any additional FN fragmentbands. Incubation for a shorter period showed incomplete digestion of FN, leaving remains of the 220 kD total FN band in the SDS-PAGE gel (results not shown). Purification of the pFN fragments on a heparin affinity column revealed two separate fractions that could be eluted from the column with 0.25 M NaCl in an equilibration

buffer (lane D) and with 1 M NaCl (lane E) respectively. No fragments could be eluted with 0.6 M NaCl. The fraction with low affinity for heparin contains a specific pFN fragment with an apparent MW of 120 kD (lane D) and a mixture of additional bands with an apparent MW around 100 kD. The fraction with high affinity for heparin contains a specific pFN fragment with an apparent MW of 60 kD (lane E) and also a mixture of additional bands with an apparent MW around 100 kD. No pFN protein bands were visible in the gel below the 60 kD band.

Although the mouse FN protein sequence (Swissprot: FINC_mouse, 2477aa) shows more than 80% homology with the human FN protein sequence (Swissprot: FINC_human, 2386aa), the digestion of mouse FN with Cathepsin D generated several different fragments (120 kD, 60 kD, and 100 kD) than digestion of human FN (70 kD gelatin bindin domain, 27 kD N-terminal heparin binding domain, 40 kD collagen binding domain, 120 kD cell binding domain, and 55-65 kD C-terminal heparin binding domain (23,24)). Results of N-terminal sequencing of the fractions revealed that the protein-sequence of the 60 kD high-affinity fragment started at residue 1704 (AQNRNGESQP). This fragment thus includes the high-affinity heparin II binding domain. Repeated N-terminal sequencing of the low-affinity fraction suggests that the N-terminus of the 120 kD fragment was located near the low-affinity heparin-binding domain, but we were not able to find one unequivocal starting point for the sequence. The 100 kD proteins in both samples were not identical to each other, but the 100 kD protein fragment in the low-affinity fraction shared sequence homology with the 120 kD pFN fragment, while the 60 kD pFN fragment shared sequence homology with the 100 kD protein fragment in the high-affinity fraction. Figure 3 shows a proposed schematic drawing of the FN protein sequence indicating the proposed locations of the FN fragments.

Both heparin and N-desulfated non-anti-coagulant heparin prevent binding of pFN to glomerulosclerotic lesions

FITC-conjugated pFN injected intravenously into mice 10-12 weeks after induction of GvHD accumulated in the glomerulosclerotic lesions (n=9, fluorescence intensity 3+, Fig. 4A). The segmental fluorescent staining pattern was comparable to the occurrence of PAS-positive glomerulosclerotic lesions. This accumulation was not observed in NF1 mice (n=2), confirming earlier results by Bergijk et al. (9). Ex vivo pre-incubation of pFN-FITC with heparin resulted in a significantly reduced accumulation of pFN-FITC upon injection ($p < 0.05$). Hardly any fluorescence signal was detectable in 4 out of 5 animals with GvHD (Fig. 4B, fluorescence intensity +/-). Injection of pFN pre-incubated with non-anti-coagulant, N-desulfated heparin also prevented the accumulation of pFN-FITC in the glomerular lesions ($p < 0.05$). Five GvHD mice showed no accumulation, while only 2 animals had a weak fluorescent staining of 1+. There was no statistically significant difference between the accumulation of pFN-FITC pre-

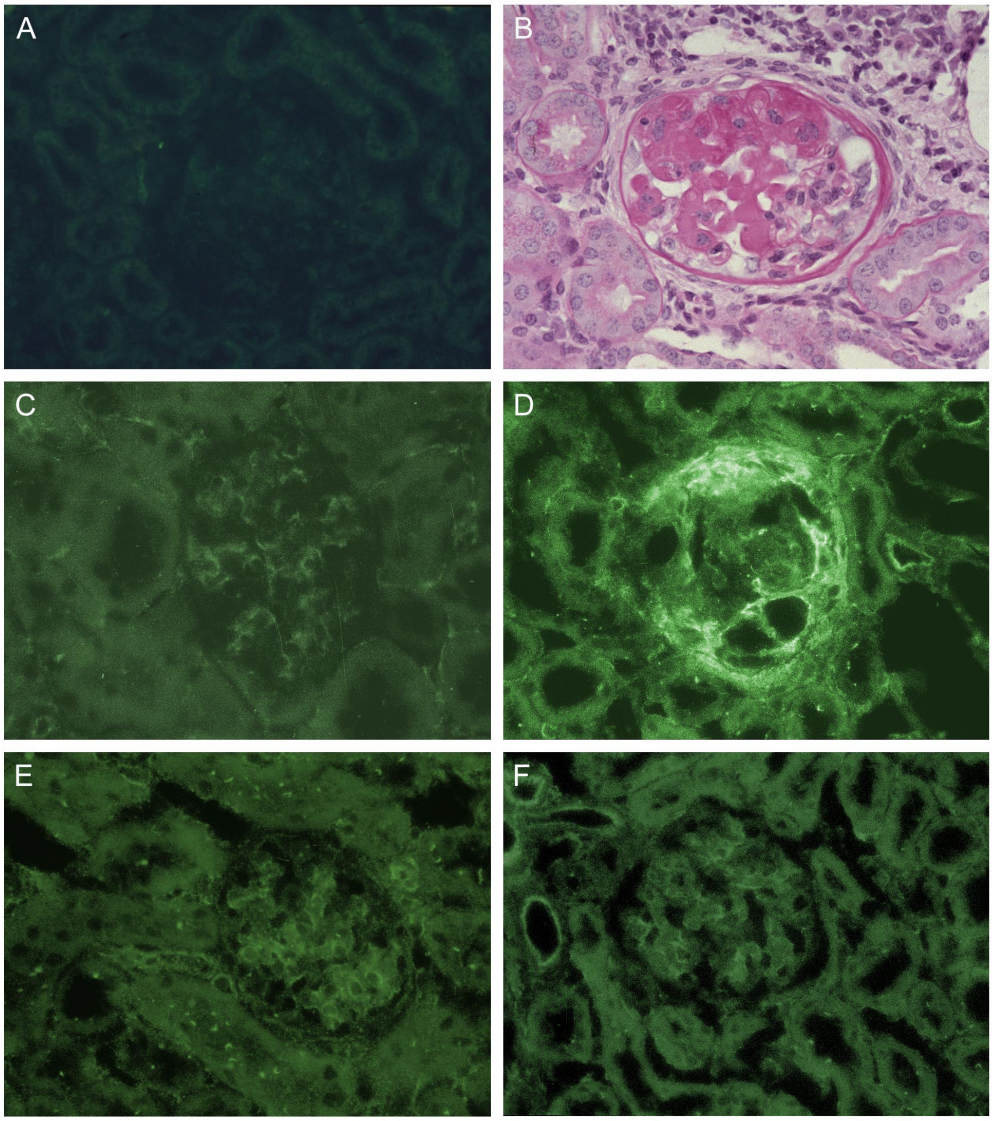

Figure 1. (Immuno-)histochemical staining of renal tissue. Figure A shows a control staining with a non-immune IgG antibody. Figure B is a PAS staining of a mouse glomerulus 10 weeks after the induction of GvHD, showing extensive glomerulosclerosis. The integrin α5 chain is expressed in minimal amounts in a glomerulus of a NF1 mouse (C). Increased expression of the integrin α5 chain is visible in the periphery of the glomerulosclerotic lesion 8 weeks after the induction of GvHD (D). The integrin α4 chain was expressed in trace amounts in glomeruli of NF1 mice (E). The expression of the integrin α4 chain did not alter during GvHD (Fig. F, GvHD week10).

treated with heparin or non-anti-coagulant heparin. Results of the accumulation experiments are summarized in Table 1.

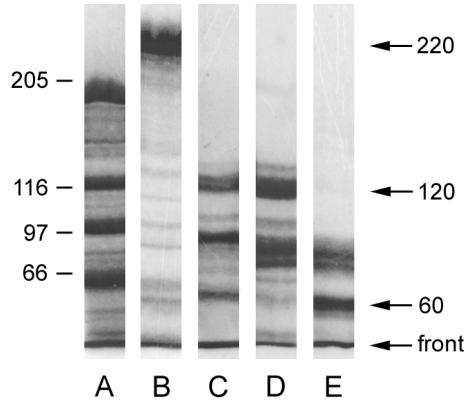

Figure 2. Polyacrylamide gel electrophoresis under reducing conditions of plasma-fibronectin isolated from normal mouse plasma using a gelatin-Sepharose 4B affinity column. Lane A represents molecular weight markers. Lane B contains total FN with an apparent MW of 220 kD. Lane C shows Cathepsin D induced fragments of total FN. There is no 220 kD FN band left after enzymatic digestion. Affinity purification of the fragment-mixture, on a heparin-Sepharose 4B column, resulted in a low-affinity fraction containing a specific 120 kD FN fragment (Lane D) and a high-affinity fraction containing a specific 60 kD FN fragment (Lane E). The low-affinity fraction (120kD) was completely depleted of the 60 kD band, while the high-affinity fraction (60 kD) did not contain any 120 kD FN fragments. Additional pFN fragments with an apparent MW of about 100 kD are present in both fractions.

pFN binding in glomerulosclerotic lesions does not occur via the high-affinity binding site for heparin

Intravenous injection of the FITC-conjugated pFN fraction with low affinity for heparin resulted in intense segmental staining of glomeruli from 8 out of 11 mice with GvHD at week 10 (fluorescence intensity 2+, Fig. 4C). This accumulation did not occur when the low-affinity fraction was injected in NF1 mice (n=3). Ex vivo incubation of the low-affinity pFN-FITC fraction with heparin inhibited its accumulation in the glomerulus of GvHD mice (n=2). The FITC-conjugated pFN fraction with high affinity for heparin did not accumulate in the glomerulus of GvHD mice at week 10 (n=10, Fig. 4D), nor of NF1 mice (n=3). There was no statistically significant difference between the accumulation of the low-affinity fraction and the accumulation of total pFN-FITC, but there was a strong difference between the accumulation of total pFN-FITC and the accumulation of the high-affinity fraction ($p < 0.02$)

Discussion

Circulating pFN, which is produced by the liver, accumulates in glomerulosclerotic lesions at a late stage in GvHD (9). This dimeric glycoprotein is known to play a role in a variety of cellular processes, immune complex clearance, and wound healing. Several domains within the FN molecule may be involved in the specific binding to the sclerotic lesion. The actual accumulation of pFN may result from 1) direct binding to other ECM components in the damaged glomerulus, 2) direct binding to beta-1 integrins on cell surfaces, 3) involvement of the coagulation system, or 4) binding to itself by polymerization via self-assembly sites into insoluble fibrils, or from a combination of these mechanisms.

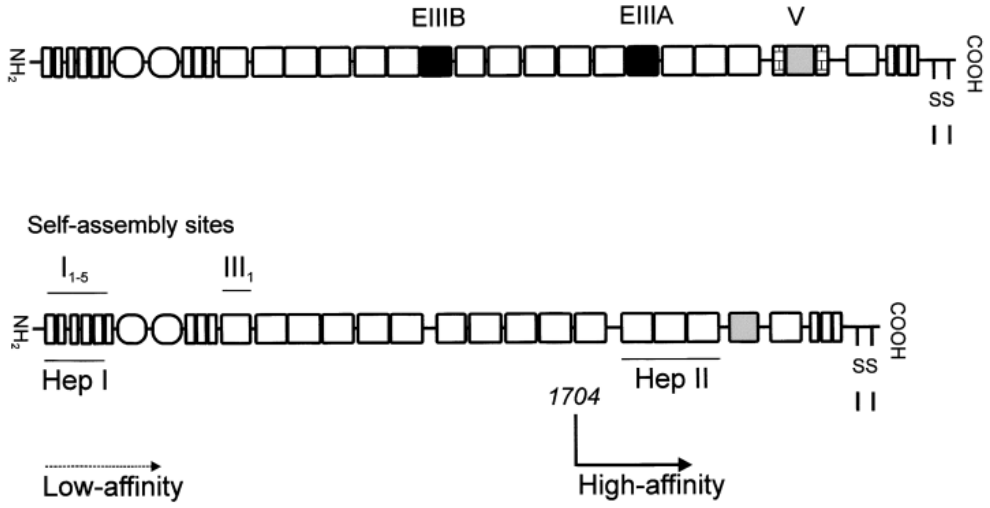

Figure 3. Schematic drawing of the total FN protein sequence (top) and the pFN protein sequece (bottom), with the proposed locations of the FN fragments involved in the accumulation of FN in glomerulosclerotic lesions. Indicated are the EIIIA, EIIIB and V regions, which can be included in or excluded from the protein by alternative splicing of the FN pre-mRNA. Rectangles represent homologous type I repeats, circles represent homologout type II repeats, and squares represent homologous type III repeats. The protein sequence of the high-affinity fraction starts at residue 1704 (homology repeat III_{11}), just before the high-affinity heparin-binding domain (Hep II). The N-terminus of the low-affinity fraction is suggested to be located near the low-affinity heparin-binding domain (Hep I, homology repeat I_{1-5}).

Firstly, FN can bind to other ECM molecules, such as collagen and laminin, that are produced and deposited in the kidney to maintain a stable matrix. Alterations in the ECM turnover that may contribute to the accumulation of FN have been described to precede the development of glomerulosclerosis in the GvHD model (25). Secondly, stabilization of the tissue is also obtained

Table 1. Summary of FN accumulation experiments 10-12 weeks after induction of GvHD.*

	Pre-incubation with		
Administration of	Buffer	Heparin	N-desulfated heparin
Total pFN	+++ (n = 9)	+/- (n = 5)	+/- (n = 5)
High-affinity pFN fraction	0 (n = 10)	0 (n = 2)	nd
Low-affinity pFN fraction	++ (n = 11)	0 (n = 2)	nd

* Results are scored semi-quantitatively on a scale from 0 to +++, in which 0 represents no accumulation of FITC-conjugated pFN or pFN fragments, and +++ reflects very strong accumulation in the glomerulosclerotic lesions, as determined by direct immunofluorescence. Abbreviations are: ND, not determined; N, number of animals.

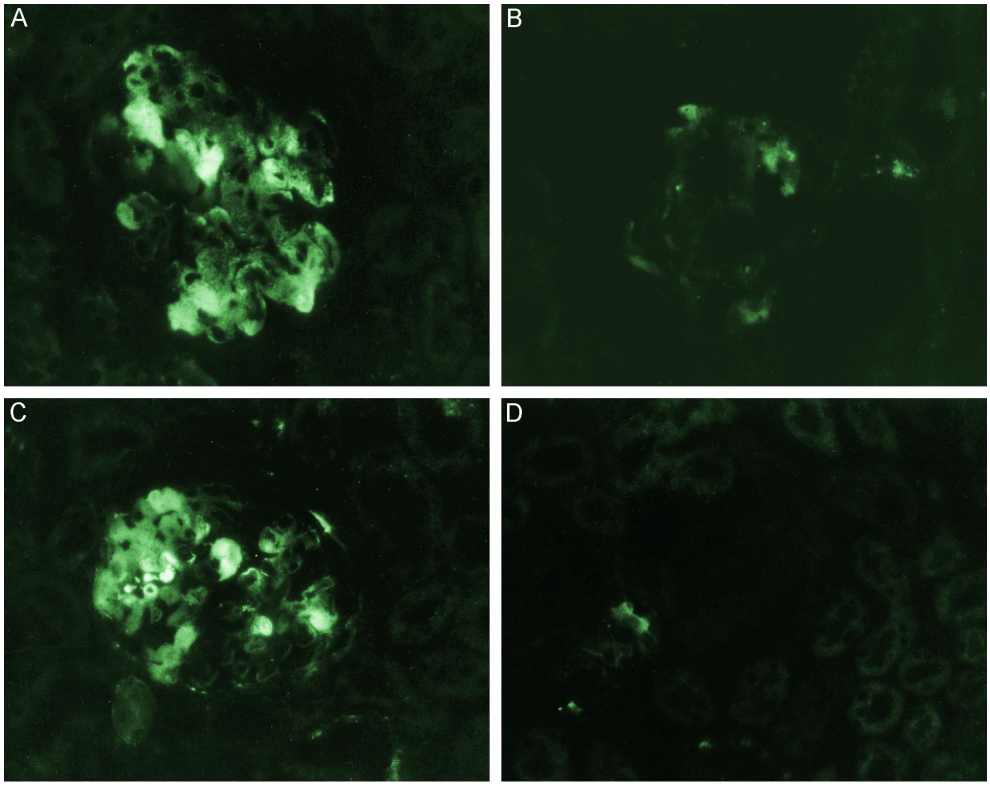

Figure 4. Immunofluorescence micrographs of mouse glomeruli 10 weeks after the induction of GvHD, and 18 h after injection with pFN-FITC (A), pFN-FITC pre-incubated with heparin (B), low-affinity pFN-FITC fraction (C), or high-affinity pFN-FITC fraction (D). Injection of the low-affinity pFN fraction pre-incubated with heparin shows a significantly reduced pattern of accumulation, comparable to the pattern shown in figure B.

by the cell-to-cell and cell-to-substrate attachments via integrin receptors. FN has two major integrin binding sites. The first binding site is an RGD (Arg-Gly-Asp) sequence in the central cell binding domain which is recognized by $\alpha 5\beta 1$ integrins. The second binding site, recognized by $\alpha 4\beta 1$ integrins, is an LDV (Leu-Asp-Val) sequence located in the alternatively spliced V-region. This study shows an increase in the expression of the $\alpha 5$ integrin chain in areas surrounding the glomerulosclerotic lesions (Fig. 1). This altered integrin expression in the glomerulus during the course of the disease may lead to enhanced binding of pFN.

A third mechanism that may participate in the accumulation of pFN in the glomerulus, is activation of the coagulation system. PTAH staining showed deposition of fibrin in the glomerulosclerotic lesions during the development of GvHD, indicating an activation of the coagulation cascade during the induction of the disease. Therapeutical intervention in the coagulation cascade can be achieved by treating the mice with heparin. We earlier performed an

experiment that investigated whether heparin treatment in a late stage of GvHD could significantly affect the development of glomerulosclerosis in vivo (Abstract; Bergijk EC, *et al*. *J Am Soc Nephrol* 6:892, 1995). Seven weeks after induction of GvHD the glomeruli showed mesangial matrix expansion and thickening of the GBM. From this moment on, mice (N=5/group) were treated with different doses of heparin (20 or 40 U/24h). High dose treatment significantly diminished the development of fibronectin-containing end-stage sclerotic lesions in 50-80% of the animals at week 11 of the disease. This points toward the involvement of the coagulation cascade in the process of FN-accumulation leading to the development of end-stage sclerotic lesions. However, to our surprise, treatment of mice with N-desulfated non-anti-coagulant heparin showed a similar effect. This indicates that the protective effect of heparin in the trapping of FN in the glomerulosclerotic lesions is independent of the anti-coagulant properties of heparin. We then hypothesized that heparin treatment directly interferes with FN accumulation by binding to FN, i.e., without participation of the coagulation system.

FN has been shown to contain two heparin-binding sites. The high-affinity heparin II binding domain located at the carboxyterminal site of FN (III_{12-14}) has a dual function. The heparin II binding domain is thought to interact with cell surface glycosaminoglycans to facilitate cell adhesion and spreading (26,27), but it also plays an important role in matrix assembly (28), probably via interactions with I_{1-5}. In addition to the high-affinity heparin II binding domain, FN also has a low-affinity binding domain for heparin (heparin I binding domain) located on $I_{1-5.}$ The heparin I domain is also involved in matrix assembly and, in particular, FN self-assembly (29,30).

To test the possible involvement of either of the heparin-binding sites of FN in its glomerular accumulation, we performed an experiment in which we injected GvHD mice with pFN-FITC pre-incubated with heparin or N-desulfated heparin. Our results show that pre-incubation with heparin prevents FN accumulation in the sclerotic lesions. Similar results were obtained using N-desulfated non-anti-coagulant heparin (Table 1). This suggests the involvement of either one of the heparin binding sites of FN in its glomerular accumulation. To investigate whether FN binds to the glomerulus via its high- or low-affinity heparin-binding domain, FN was digested with Cathepsin D, after which the fragments were separated on a heparin affinity column. Thus, two batches of FN fragments were obtained with either low or high affinity for heparin, respectively. The 100 kD fragments present in both fractions appeared to have no functional effect during the accumulation experiments. Further molecular dissection of these fragments will be required to obtain conclusive evidence for their non-involvement.

In contrast to our expectation, the fraction with FN fragments containing the high- affinity heparin II binding domain did not accumulate in the sclerotic glomeruli, whereas the FN fraction containing the low-affinity binding site for heparin (heparin I binding domain) did. The

accumulation of the latter fraction could be inhibited by pre-incubation with heparin (Table I), suggesting that FN does not bind to the glomerulus via its high-affinity heparin-binding region, but probably via its low-affinity heparin-binding domain, or via a site nearby. In the latter case, we hypothesize that the protective effect of heparin treatment could result from steric hindrance of the specific binding site, or heparin might act via other unknown mechanisms. Therefore, we conclude that i) the protective effect of heparin is independent of its anti-coagulant properties, suggesting that the coagulation cascade is not involved in the trapping of FN in the sclerotic lesion, ii) the process of glomerulosclerosis is not mediated via the heparin II binding site of FN, and iii) the site involved in the accumulation of FN in the glomerulus is located on or near the heparin I binding site.

A final remark concerns the possible functional involvement of the heparin I binding site in the glomerular accumulation and stabilization of FN in the diseased glomeruli. As mentioned above, it is known that the heparin I binding domain contains a self-assembly site which is instrumental in polymerization of FN into insoluble FN fibrils (29,30). Self-assembly of FN dimers into insoluble fibrils is thought to involve primarily interactions between the first five type I (I_{1-5}) repeats located on the low-affinity heparin I binding domain, and the first type III (III_1) repeat located nearby (31-34). Treatment of purified FN in solution with an III_1-C fragment resulted in the appearance of FN multimers, called superfibronectin, which resemble matrix fibrils (35). It has been suggested that this self-assembly site of FN is protected from spontaneous polymerization by keeping it cryptic, and that it is only unmasked in response to either physiological stimuli, or to tissue repair reactions. Based on these observations and ours, we hypothesize that self-assembly of soluble pFN after binding to FN molecules already present in the glomerular ECM contributes to the observed accumulation of FN during the development of glomerulosclerosis in a late stage of GvHD.

In conclusion, our results provide evidence for progressive accumulation of FN in glomerulosclerotic lesions in our model via its low-affinity heparin binding site or a site nearby. This may involve a self-assembly process involving the first five type I (I_{1-5}) repeats, or the first type III (III_1) repeat, or both. However, the extent to which this self-assembly process is preceded by initial binding of FN to either ECM or beta 1 integrins requires further investigation.

Acknowledgments

The authors thank Jan van der Ploeg and Michel Mulders for excellent technical assistance. We also thank Dr. I.M. Bajema for critically reading this manuscript.

References

1. Vleming LJ, Baelde JJ, Westendorp RGJ, Daha MR, Van Es LA, Bruijn JA: The glomerular deposition of PAS positive material correlates with renal function in human kidney diseases. *Clin Nephrol* 47:158-167, 1997
2. Hynes R: Molecular biology of fibronectin. *Annu Rev Cell Biol* 1:67-90, 1985
3. Ruoslahti E: Fibronectin and its receptors. *Annu Rev Biochem* 57:375-413, 1988
4. Dixon FJ, Burns J, Dunnill MS, McGee J: Distribution of fibronectin in normal and diseased human kidneys. *J Clin Pathol* 33:1021-1028, 1980
5. Altunkova I, Minkova V, Belovezhdov N: Role of fibronectin in immune glomerulonephritis. *Nephron* 63:438-444, 1993
6. Ikeya M, Nagase M, Honda N: Intraglomerular distribution of fibronectin in primary glomerular disease. *Clin Nephrol* 24:53-59, 1985
7. Via CS, Shearer GM: T-cell interactions in autoimmunity: insights from a murine model of graft-versus-host disease. *Immunol Today* 9:207-213, 1988
8. Bruijn JA, Van Elven EH, Hogendoorn PCW, Corver WE, Hoedemaeker PJ, Fleuren GJ: Murine chronic graft-versus-host disease as a model for human lupus nephritis. *Am J Pathol* 130:639-641, 1988
9. Bergijk EC, Baelde HJ, De Heer E, Killen PD, Bruijn JA: Specific accumulation of exogenous fibronectin in experimental glomerulosclerosis. *J Pathol* 176:191-199, 1995
10. Lindahl U, Lidholt K, Spillmann D, Kjellén L: More to “heparin” than anticoagulation. *Thromb Res* 75:1-32, 1994
11. Reilly CF, Kindy MS, Brown KE, Rosenberg RD, Sonenshein GE: Heparin prevents vascular smooth muscle cell progression through the G1 phase of the cell cycle. *J Biol Chem* 264:6990-6995, 1989
12. Adler S: Inhibition of rat glomerular visceral epithelial cell growth by heparin. *Am J Physiol* 255:F781-6, 1988
13. Groggel GC, Marinides GN, Hovingh P, Hammond E, Linker A: Inhibition of rat mesangial cell growth by heparan sulfate. *Am J Physiol* 258:F259-65, 1990
14. Wang ZQ, Liang KH, Pahl MV, Vaziri ND: Effect of heparin on mesangial cell growth and gene expression of matrix proteins. *Nephrol Dial Transplant* 13:3052-3057, 1998
15. Olson JL: Role of heparin as a protective agent following reduction of renal mass. *Kidney Int* 25:376-382, 1984
16. Van Bruggen MCJ, Walgreen B, Rijke TPM, Corsius MJAMM, Assmann KJM, Smeenk RJT, Van Dedem GWK, Kramers K, Berden JHM: Heparin and heparinoids prevent the binding of immune complexes containing nucleosomal antigens to the GBM and delay nephritis in MRL/lpr mice. *Kidney Int* 50:1555-1564, 1996
17. Diamond JR, Karnovsky MJ: Nonanticoagulant protective effect of heparin in chronic aminonucleoside nephrosis. *Ren Physiol* 9:366-374, 1986
18. Floege J, Eng E, Young BA, Couser WG, Johnson RJ: Heparin suppresses mesangial cell proliferation and matrix expansion in experimental mesangioproliferative glomerulonephritis. *Kidney Int* 43:369-380, 1993
19. Burg M, Ostendorf T, Mooney A, Koch K-M, Floege J: Treatment of experimental mesangioproliferative glomerulonephritis with non-anticoagulant heparin: therapeutic efficacy and safety. *Lab Invest* 76:505-516, 1997
20. Bergijk EC, Munaut C, Baelde JJ, Prins F, Foidart JM, Hoedemaeker PJ, Bruijn JA: A histological study of the extracellular matrix during the development of glomerulosclerosis in murine chronic graft-versus-host disease. *Am J Pathol* 140:1147-1156, 1992
21. The TH, Feltkamp TE: Conjugation of fluorescein isothiocyanate to antibodies. I. Experiments on the conditions of conjugation. *Immunol* 18:865-873, 1970
22. Inoue Y, Nagasawa K: Selective N-desulftion of heparin with dimethyl sulfoxide containing water or methanol. *Carbohydrate Res* 46:87-95, 1976
23. Homandberg GA, Erickson JW: Model of fibronectin tertiary structure based on studies of interactions between fragments. *Biochem* 25:6917-6925, 1986
24. Click EM, Balian G: Domain structure of human plasma and cellular fibronectin. Use of a monoclonal antibody and heparin affinity to identify three different subunit chains. *Biochem* 24:6685-6696, 1985
25. Bergijk EC, van Alderwegen IE, Baelde HJ, De Heer E, Funabiki K, Miyai H, Killen PD, Kalluri RK,

Bruijn JA: Differential expression of collagen IV isoforms in experimental glomerulosclerosis. *J Pathol* 184:307-315, 1998

26. McCarthy JB, Skubitz APN, Zhao Q, Yi X, Mickelson DJ, Klein DJ: RGD-independent cell adhesion to the carboxy-terminal heparin-binding fragment of fibronectin involves heparin-dependent and -independent activities. *J Cell Biol* 110:777-787, 1990
27. Jalkanen S, Jalkanen M: Lymphocyte CD44 binds the COOH-terminal heparin-binding domain of fibronectin. *J Cell Biol* 116:817-825, 1992
28. Bultmann H, Santas AJ, Peters DMP: Fibronectin fibrillogenesis involves the heparin II binding domain of fibronectin. *J Biol Chem* 273:2601-2609, 1998
29. McKeown-Longo PJ, Mosher DF: Interaction of the 70,000-mol-wt amino-terminal fragment of fibronectin with the matrix-assembly receptor of fibroblasts. *J Cell Biol* 100:364-374, 1985
30. Quade BJ, McDonald JA: Fibronectin's amino-terminal matrix assembly site is located within the 29-kDa amino-terminal domain containing five type I repeats. *J Biol Chem* 263:19602-19609, 1988
31. Hocking DC, Sottile J, McKeown-Longo PJ: Fibronectin's III-1 module contains a conformation-dependent binding site for the amino-terminal region of fibronectin. *J Biol Chem* 269:19183-19187, 1994
32. Morla A, Ruoslahti E: A fibronectin self-assembly site involved in fibronectin matrix assembly: reconstruction in a synthetic peptide. *J Cell Biol* 118:421-429, 1992
33. Sechler JL, Takada Y, Schwarzbauer JE: Altered rate of fibronectin matrix assembly by deletion of the first type III repeats. *J Cell Biol* 134:573-583, 1996
34. Aguirre KM, McCormick RJ, Schwarzbauer JE: Fibronectin self-association is mediated by complementary sites within the amino-terminal one-third of the molecule. *J Biol Chem* 269:27863-27868, 1994
35. Morla A, Zhang Z, Ruoslahti E: Superfibronectin is a functionally distinct form of fibronectin. *Nature* 367:193-196, 1994

Chapter 6

Gene expression profiling in glomeruli from human kidneys with diabetic nephropathy

H.J. Baelde[1], M. Eikmans[1], P.P. Doran[2], D.W.P. Lappin[2],

E. de Heer[1], J.A. Bruijn[1]

[1]Department of Pathology, Leiden University Medical Center, Leiden, The Netherlands

[2]Department of Medicine and Therapeutics, Mater Misericordiae Hospital, University College Dublin and Dublin Molecular Medicine Centre, Dublin, Ireland

American Journal of Kidney Diseases 43(4):636-50, 2004

Abstract

Diabetic nephropathy is a frequent complication in patients with diabetes mellitus. To find improved intervention strategies in this disease, it is necessary to investigate the molecular mechanisms that are involved. To obtain more insight in the processes that lead to diabetic nephropathy, mRNA expression profiles of diabetic glomeruli and glomeruli from healthy individuals were compared.

Two morphologically normal kidneys and two kidneys from patients with diabetic nephropathy were used for the study. Glomerular RNA was hybridized in duplicate on Human Genome U95Av2 Arrays (Affymetrix®). Several transcripts were further tested in independent patient groups and at the protein level by immunohistochemistry.

Ninety-six genes were upregulated in the diabetic glomeruli, whereas 519 genes were downregulated. The list of over expressed genes in diabetic nephropathy includes aquaporin 1, calpain 3, hyaluronoglucosidase, and platelet/endothelial cell adhesion molecule (PECAM-1). The list of downregulated genes includes bone morphogenetic protein 2 (BMP-2), vascular endothelial growth factor (VEGF), fibroblast growth factor 1 (FGF-1), insulin-like growth factor binding protein (IGFPB-2), and nephrin. A decrease in VEGF and nephrin could be validated at the protein level and also at the mRNA level in renal biopsies of 5 additional diabetes patients.

In conclusion, the results of oligonucleotide microarray analyses on control and diabetic glomeruli are presented and discussed in their relation to vascular damage, mesangial matrix expansion, proliferation, and proteinuria. Our findings suggest that progression of diabetic nephropathy might result from a diminished tissue repair capability.

Introduction

Diabetic nephropathy (DN) is a major cause of morbidity in patients with type II diabetes (1). One of the earliest clinical signs of diabetic nephropathy is microalbuminuria, which often progresses towards proteinuria (2). Characteristic features associated with diabetic nephropathy include hyperfiltration, followed by a decrease in the glomerular filtration rate (GFR), glomerular hypertrophy, progressive expansion of the mesangial matrix, and thickening of the glomerular and tubular basement membranes (3,4). These features may precede the development of glomerulosclerosis and interstitial fibrosis, and eventually the onset of end-stage renal disease.

Little is known about the molecular mechanisms leading to end-stage renal disease in diabetic nephropathy. While the role of many genes in progressive renal diseases has been described (5,6), their interrelationship remains largely unclear. With the completion of the human genome project and the development of microarray technology it is now possible to simultaneously screen the RNA expression of thousands of genes in healthy and diseased organs, or in parts of them. Although gene profiling studies have been described recently in animal models for diabetic nephropathy (7), microarray studies on isolated glomeruli from human diabetic kidneys have not yet been reported.

In this study, we investigated the gene expression profile of glomerular RNA from patients suffering from type II diabetes mellitus, and glomerular RNA from individuals with normal renal function and histology.

Material and Methods

Patients

Cadaveric donor kidneys were obtained from Eurotransplant. These kidneys were unsuitable for transplantation for technical or morphological reasons (Table 1). We used glomeruli from two control kidneys, and from two kidneys from patients with diabetes mellitus type II. Diabetic nephropathy was histologically confirmed by Periodic acid-Schiff (PAS) stained paraffin sections. Pathologic criteria for diabetic nephropathy include glomerular hypertrophy, diffuse mesangial and focal nodular glomerulosclerosis, arteriolar hyalinosis, and focal and segmental glomerulosclerosis, hyaline drops between Bowman's capsule and epithelial cells, and interstitial fibrosis. Nodular glomerulosclerosis, arteriolar hyalinosis are characteristic for diabetic nephropathy, and present in the diabetic kidneys that we have used for this study.

Isolation of glomeruli

Glomeruli were isolated as described earlier (8). In brief, fresh cortical tissue was first pressed with a flattened glass pestle through a 212 μm pore diameter metal sieve and then through a

150µm pore diameter metal sieve. Glomeruli were rinsed from the surface of the 150 µm sieve with ice-cold phosphate buffered saline (PBS), transferred to a tube and pelleted for 1 min at 1200Xg. The supernatant was removed and the glomeruli were frozen at -70°C until RNA isolation. The purity of the glomerular suspension was controlled by light-microscopy and was at least 90%.

RNA isolation

Glomerular RNA was isolated using a combination of two RNA isolation procedures. Glomerular tissue (500mg) was dissolved in 5 ml Trizol® and homogenized with an ultra-turrax (Janke & Kunkel) for 1 min. After adding 1ml chloroform and mixing for 1 min, the suspension was centrifuged at 15,000g for 10 min. The RNA was precipitated with isopropanol. The pellet was air-dried and dissolved in 100 µl MilliQ and further purified with an RNeasy Mini column (QIAGEN GmbH, Germany), according to the instructions of the manufacturer.

Table 1. Characteristics of the patients.

	Control 1	Control 2	Diabetes 1	Diabetes 2
Retinopathy	no	no	yes	yes
Duration of diabetes type 2 (years)	-	-	> 5	>5
Age (years)	29	70	55 years	63 years
Gender	Male	Male	Male	Male
Serum Creatinin (mg/dL)[1]	0.68	unknown	1.14	unknown
Serum Glucose(mg/dL)[1]	133	128	326	unknown
Urine glucose[1]	negative	negative	++	++
Urine Protein[1]	negative	trace	+	+/-
GFR(mL/min)[1]	181	unknown	78	unknown
Perfusion fluid	UW[2]	UW[2]	UW[2]	UW[2]
Cold ischemia time (hours)	32	33	26	32
Dopamine (µg/kg BW/min)	3	0.2 (Norepinephrine)	2	3
Known other drugs	-	-	Insulin	Insulin
Cause of death	ICB[3]	ICB[3]	ICB[3]	ICB[3]
Reason of refusal	Lesion upper arterial pole	Arteriosclerosis	DN	DN
Percentage of sclerotic glomeruli	<1%	<1%	33%	24%
Percentage of interstitial fibrotic area	< 5%	< 5%	25-50%	25-50%

[1] Levels within last 24 hours of donation, [2] University of Wisconsin solution, [3] Intracerebral bleeding.

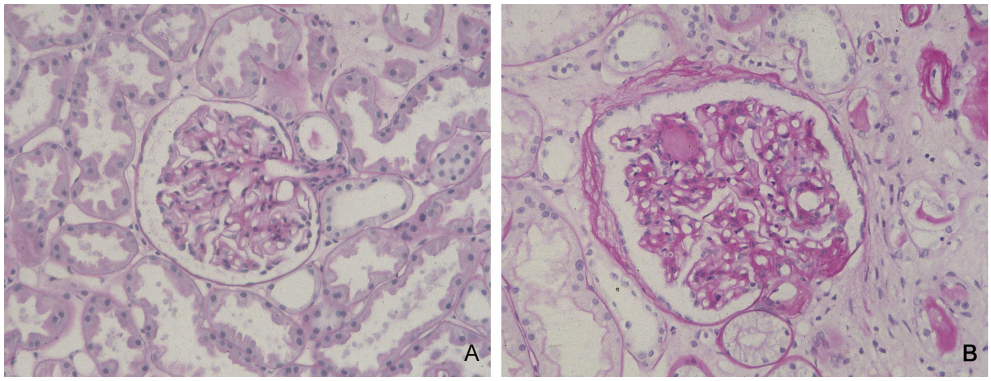

Figure 1. Light microscopic pictures of a glomerulus from a control kidney (A) and a representative glomerulus from a diabetic kidney (B). The diabetic kidneys show glomerular hypertrophy, diffuse mesangial and focal nodular glomerulosclerosis, and arteriolar hyalinosis. (PAS staining, original magnification 200x)

To assess the quality of the RNA, 2 µg of RNA was applied on a 1% agarose-formalin gel. Electrophoresis was performed for 3 h at 50 V. The gel was stained with ethidium bromide.

Microarray hybridization

Hybridizations were performed on the Human Genome U95Av2 Array (Affymetrix® Santa Clara, CA, USA). This array contains ~12,000 sequences characterized previously in terms of function or disease association. Ten µg of total RNA from isolated glomeruli of each kidney was converted to complementary (c)DNA, double stranded (ds)DNA, and transcribed *in vitro* according to the instructions of the manufacturer. After hybridization, the microchips were scanned and analyzed with Affymetrix® Microarray Suite 5.0 software. To normalize the data from different microarray experiments, the expression levels of all genes on the chip were scaled to a standard value and the mean of the scaling factors was calculated. This value served as the normalization factor for all genes represented on the different microarray chips. To obtain normalized expression values, the expression levels for each gene was multiplied with the normalization factor. Statistics behind this method can be found in the Microarray Suite User's Guide, Version 5.0, which is available at http://www.affymetrix.com/support/technical/manuals.affx. To determine the inter-assay variation, the labeling procedure and hybridization for one of the controls and one of the diabetic glomerular samples were performed in duplicate. A total of six chips were hybridized, three with control RNA, and three with RNA from diabetic glomeruli.

Confirmation of microarray data by real-time PCR

We performed real-time polymerase chain reaction (PCR) (9), in combination with the Taqman

probe technique, for three genes to confirm the data obtained with the microarray analyses. RNA (1µg) was converted to cDNA using avian myeloblastosis virus (AMV) reverse transcriptase (Roche Applied Science). The transcription levels for nephrin, transforming growth factor-beta (TGF-β), and vascular endothelial growth factor (VEGF) were determined and corrected to a panel of five different housekeeping genes, i.e., glyceraldehyde-phosphate-dehydrogenase (GAPDH), beta-2 microglobulin (B2M), hypoxanthine phosphoribosyl transferase (HPRT), porphobilinogen deaminase (PBGD) and TATA box-binding protein (TBP), as described by Vandesomple et al. (10). The primer and probe sequences are summarized in Table 2. To calculate the relative mRNA levels we measured the threshold cycle (Ct) values of a standard curve with a known amount of total RNA. For each housekeeping gene the relative amount of the samples were calculated by linear regression analysis from their standard curve. The relative values of each of the 5 different household genes of the controls were adjusted to one by dividing the samples by the mean of all samples. After this correction the mean of the 5 different housekeeping genes was calculated. The relative expression level of VEGF, TGF-ß and nephrin was calculated by dividing the value of the gene by the mean of the different household genes. The relative values were set to one for the controls.

We also measured the relative mRNA levels for VEGF, TGF-ß and nephrin in microdissected glomeruli of 5 renal biopsies from patients with diabetic nephropathy according the method of Specht et al. (11). In brief, 4 µm frozen sections were put on a polyethylene foil coated slide. To microdissect the glomeruli, we used the PALM Laser-MicroBeam System (P.A.L.M., Wolfratshausen, Germany). RNA from the micro-dissected glomeruli was isolated with the TRIzol method as described above. All 5 diabetic patients were suffering diabetes type II for at least 5 years with retinopathy and DN. Renal biopsies of these patients showed glomerular

Table 2. Primer and Taqman® probes sequences.

	Forward primer	Reverse primer	Taqman® probe	Reporter
TGF-β	CCCAGCATCTGCAAAGCTC	GTCAATGTACAGCTGCCGCA	ACACCAACTATTGCTTCAGCTCCACGGA	FAM
VEGF	AAACCCTGAGGGAGGCTCC	TACTTGCAGATGTGACAAGCCG	CCTCCTGCCCGGCTCACCGC	TET
Nephrin	AGGACCGAGTCAGGAACGAAT	CTGTGAAACCTCGGGAATAAGACA	TCAGAGCTCCACGGTCAGCACAACAG	TET
GAPDH	TTCCAGGAGCGAGATCCCT	CACCCATGACGAACATGGG	CCCAGCCTTCTCCATGGTGGTGAA	TET
B2M	TGCCGTGTGAACCATGTGA	CCAAATGCGGCATCTTCAA	TGATGCTGCTTACATGTCTCGATCCCACT	TET
HPRT	TGACACTGGCAAAACAATGCA	GGTCCTTTTCACCAGCAAGCT	CTTGACCATCTTTGGATTATACTGCCTGACCA	TET
PBGD	CTGGTAACGGCAATGCGGCT	GCAGATGGCTCCGATGGTGA	CGAATCACTCTCATCTTTGGGCT	TET
TBP	CACGAACCACGGCACTGATT	TTTTCTTGCTGCCAGTCTGGAC	TGTGCACAGGAGCCAAGAGTGAAGA	FAM

hypertrophy, diffuse mesangial and focal nodular glomerulosclerosis, arteriolar hyalinosis, focal and segmental glomerulosclerosis, and interstitial fibrosis. The relative mRNA levels for VEGF, TGF-ß and nephrin in microdissected diabetic glomeruli were compared to those in glomeruli from 8 control samples, which were described previously (12)

Immunohistochemistry

To validate difference in mRNA for VEGF and nephrin at the protein level, immunohistochemical (IHC)stainings were performed using specific antibodies. For the VEGF staining, 4 µm paraffin sections of the control and diabetic kidneys were cut. After removing the paraffin, the sections were pre-treated with 0.4% pepsin for 20 min at 37°C. For the nephrin staining, we used 3 µm cryostat sections. The slides were washed in PBS and incubated for 2 h at room temperature with the primary antibody, diluted in 1% bovine serum albumin in PBS (rabbit anti-nephrin 1:1000, a generous gift of Dr. Kawachi (12); rabbit anti-VEGF 1:100, Santa Cruz Biotechnology, CA, USA). After washing with PBS, the slides were incubated for 30 min with horseradish peroxidase–conjugated anti-rabbit Envision (DAKO, Glostrup, Denmark). The slides were washed in PBS, and the staining was developed with diaminobenzidine. The color was enhanced by rinsing the slides in 0.5% $CuSO_4$ solution for 5 min. After counterstaining with haematoxylin, the slides were dehydrated and mounted.

Statistics

To determine the reproducibility of the individual microarray analyses within and between groups (i.e. the control group and the diabetic nephropathy group) we calculated coefficients of correlation. Clustering analysis was performed using Spotfire® 7.1 software. We used the Z-score normalization to normalize our data. The normalized value for gene a is calculated as: (a) = (a- mean value of all samples for gene A)/ STD (*A*), where (a) is the normalized value, a is

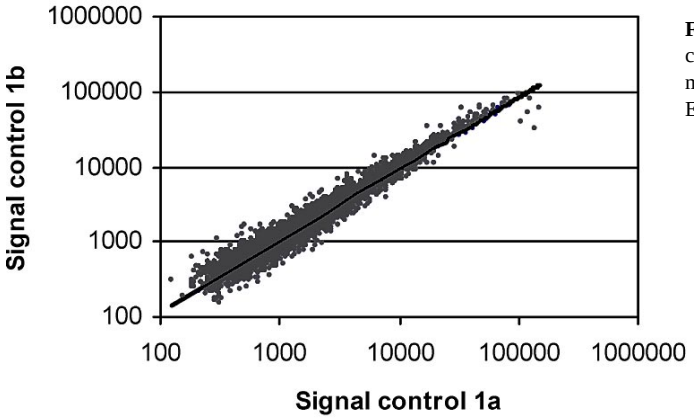

Figure 2. A graph of the correlation between duplicate measurements of a control kidney. Each point represents one gene.

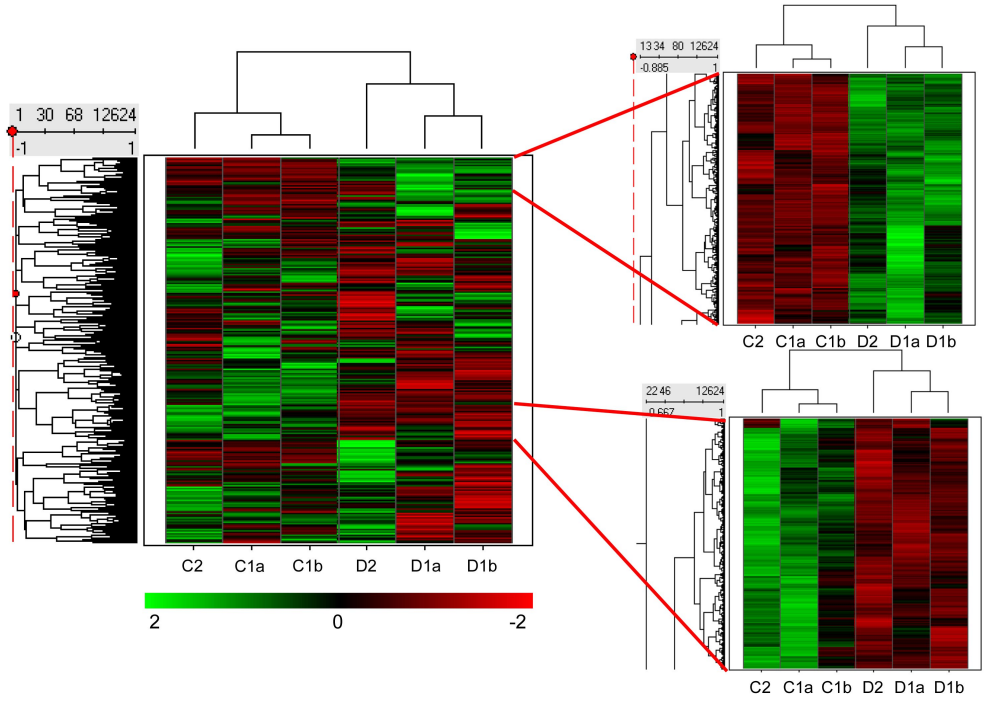

Figure 3. Dendrogram of unsupervised hierarchical clustering on the basis of similarity in gene-expression patterns of the six different arrays. (C1a = control 1, C1b = duplicate of control 1, C2 = control 2, D1a = diabetes 1, D1b = duplicate of diabetes 1, D2 = diabetes 2). The dendrogram showing the degree of relationships of samples. The different colors showed the normalized Z-score for each gene. The normalized Z-score for gene a is calculated as: (a) = (a- mean value of all samples for gene A)/ STD (*A*), where (a) is the normalized value, a is the value of sample a for gene A. Green are upregulated genes and red are downregulated genes.

the value of sample a for gene A. If all values for gene A are identical, then all values for gene A are set to zero. These normalized expression values of the six different arrays were analyzed in an unsupervised fashion using the hierarchical clustering method with complete linkage and correlation. The data was ordered by average value and visualized in a dendrogram.

To identify genes of which expression was altered consistently in the diseased samples, we used either those genes which were present on all six chips, or those which were present in all three control samples and absent in all three diabetic samples, or those which were absent in all three control samples and present in all three diabetic samples. We employed multiple pair-wise comparisons between control and disease groups using the OpenStat statistics package. We selected only those genes for which the mRNA level showed an at least 2-fold difference between controls and diabetic samples (students t-test, $p<0.01$).

Gene clustering on basis of Gene Ontology (GO), to identify gene clusters on the basis of gene function, was performed with the MAPPfinder1.0 program (13). MAPPFinder, which can

be downloaded from http://www.genmapp.org, is a program that works in combination with GenMAPP and Gene Ontology to identify global biological trends in gene expression data. MAPPFinder relates microarray data to each term in the (GO) hierarchy, calculating the percentage of genes changed for each GO biological process, cellular component, and molecular function term. Using this percentage and a z- score based on the mean and standard deviation of the hypergeometric distribution, the user can order by GO function with the highest z score. This z-score is calculated as:

$$Zscore = \frac{\left(r - n\frac{R}{N}\right)}{\sqrt{n\left(\frac{R}{N}\right)\left(1-\frac{R}{N}\right)\left(1-\frac{n-1}{N-1}\right)}}$$

where : N = the total number of genes measured, R = the total number of genes meeting the criterion, n = the total number of genes in this specific GO term, and r = the number of genes meeting the criterion in this specific GO term.

Statistical analysis for the real-time data was performed using the one-way analysis of variance (ANOVA), and values of $p<0.01$ were considered to be significant.

Results

Patient characteristics

Characteristics of the donors are summarized in Table 1. Both kidneys with diabetic nephropathy were obtained from patients with a clinical history of type II diabetes for at least 5 years. Gender, cold-ischemia time, the type of perfusion fluid used, and cause of death were similar for the patients. Serum glucose of the control patients was normal, while the glucose levels in the diabetic patients were elevated (up to 18.1 mmol/L). Consistent with a diagnosis of diabetic nephropathy, the urinary protein level in the diabetic patients was increased. The control kidneys showed a normal morphology without histological abnormalities. Both diabetic kidneys showed glomerular hypertrophy, diffuse mesangial and focal nodular glomerulosclerosis in 20-30% of the glomeruli, arteriolar hyalinosis, and focal and segmental glomerulosclerosis. Interstitial fibrosis was seen in 25-50% of the tubulo-interstitial area (Fig. 1).

Gene expression profiles of control and diabetic glomeruli.

From the approximately 12,000 genes displayed on the microchip, 2042 genes gave a positive signal on all three chips after hybridization with the RNA from the kidneys with diabetic nephropathy. In the glomeruli from control kidneys, 4297 genes gave a positive signal in all three samples after hybridization. The correlation coefficient between duplicate control samples

and duplicate diabetic samples were 0.972 and 0.932 respectively. A graph of the correlation between a duplicate of control 1 is shown in Fig. 2. The correlation between controls 1 and 2 and the two different diabetic samples were also high (0.930 and 0.900 respectively). The mean of the correlations between the different control samples and the different diabetic samples was lower (0.731). Unsupervised hierarchical clustering of the expression data as visualized in a dendrogram (Fig 3), shows the same relations between the samples. This dendrogram is based on the similarity between the different samples. By this method the software recognized the highest similarity between duplicate hybridizations, between all three controls, and between all three diabetic samples.

Using the statistics as mentioned in the materials and method we end up with a list of 96 candidate genes that were increased in DN and 519 that were decreased genes. A list of the top fifty of the upregulated genes in the diabetic glomeruli is presented in Table 3 (ratios varying between 2.3 and 4.9 fold). The fifty most down-regulated genes are presented in Table 4 (ratios varying between 6.6 and 22.8 fold). In these lists the unidentified ESTs are not shown. A list of all significantly up- and down regulated genes can be found on: www-onderzoek.lumc.nl/pathology/kidney/diabeticnephropathy/ .

Analysis of the genes, that were either increased or decreased, with Mappfinder was performed to cluster the genes on basis of their GO function. The results are summarized in Table 5. If we look at the results of the decreased genes there is a high z-score for actin cytoskeleton and actin binding GO function and for nucleobase, nucleoside, nucleotide and nucleic acid metabolism. The increased genes are especially related to homeostasis and phosphatases.

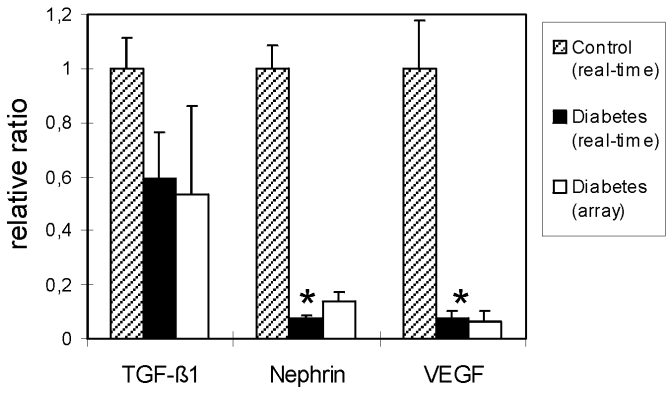

Figure 4. Validation of microarray results for TGFß1, nephrin, and VEGF by real-time PCR. Data have been normalized for a panel of five different housekeeping genes, while the array data are normalized for total chip signals and compared to the control kidneys. (* P<0.001 compared to control (one-way ANOVA)).

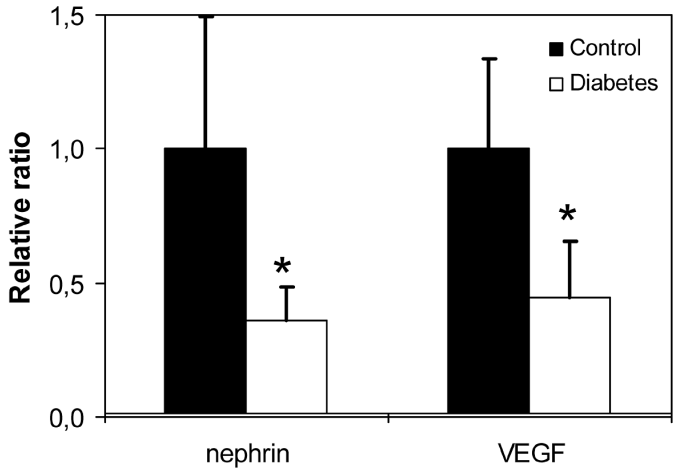

Figure 5. Nephrin and VEGF mRNA levels measured with real-time PCR in an independent group of 5 patients with diabetic nephropathy. Relative levels were compared to a panel of 8 control kidneys (* P<0.05 compared to control (students t-test)).

Confirmation of microarray data by real-time PCR.

To validate the results obtained with microarray, we performed real-time PCR assays for several transcripts. Results of the quantification of mRNA levels for TGF-ß, nephrin, and VEGF are summarized in Fig 4. With microarray and real-time PCR the ratios between TGF-β1 from the controls and diabetic kidneys were found not to be significant (1.87 and 1.82, P=ns). Array analysis showed that nephrin was downregulated (7.3-fold) in DN. Real-time PCR for nephrin also showed a decrease (15.4-fold, P<0.01 compared to the controls) in DN. For VEGF the ratios were 19.5 and 14.2, (P<0.01 compared to the controls) respectively. There was no significant difference between the ratios measured with the microarray and real-time PCR techniques. We also confirmed our data in an independent and larger patient group. The results of these measurements are shown in Fig 5. We found a significant decrease of 2.75 times for nephrin and 2.25 times decrease for VEGF (p<0.05).

Immunohistochemistry

Results for VEGF and nephrin at the RNA level were further investigated at the protein level using IHC. In normal kidneys, VEGF and nephrin showed an intense epithelial staining along the peripheral capillary loops of the glomeruli (Fig 6 A and C). VEGF also showed a weak staining in some tubular epithelial cells. In glomeruli of diabetic kidneys, the staining for both VEGF and nephrin was weaker or absent (Fig 6 B and D).

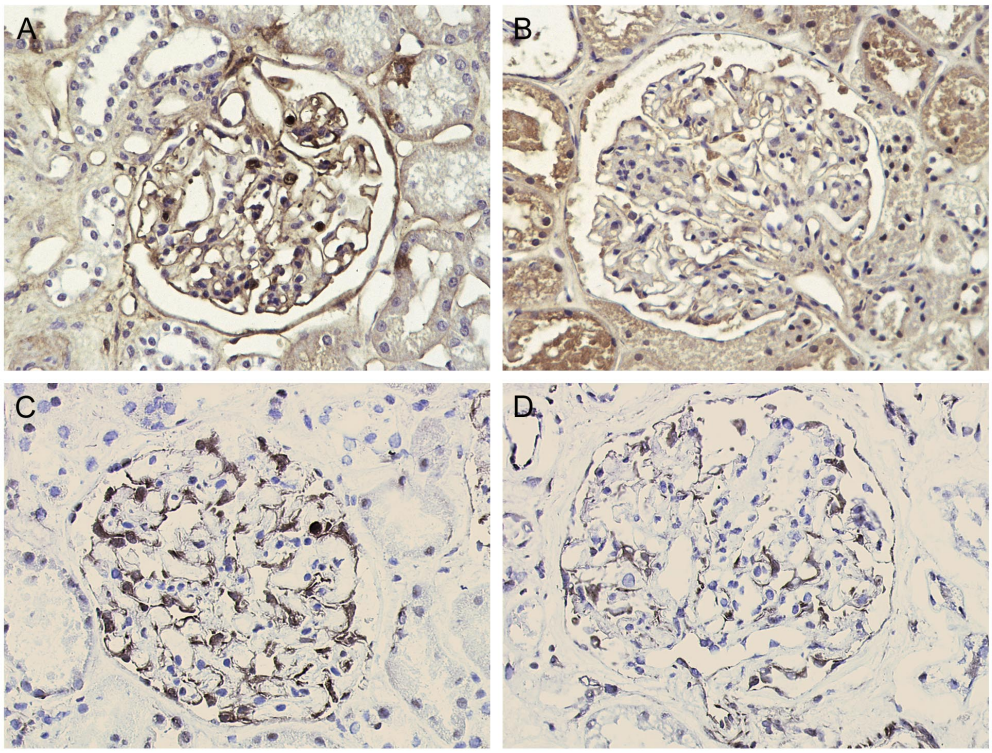

Figure 6. Representative photographs of renal tissue stained for VEGF or nephrin. The upper panel shows VEGF staining on paraffin sections of glomeruli of a control (A) or a diabetic (B) kidney. The control kidney shows abundant VEGF staining in glomerular podocytes. This staining was reduced in the glomerulus of a diabetic kidney. The lower panel shows the nephrin staining on frozen sections of a control (C) or a diabetic (D) kidney. Nephrin was also reduced in the podocytes of the diabetic kidney. Original magnification 200x

Discussion

In this study, we describe gene profiles of control and diabetic glomeruli from human kidneys. RNA was extracted from isolated glomeruli of cadaveric donor kidneys. These kidneys were unsuitable for transplantation due to, non-kidney involved, technical reasons. It is known that these kidneys have been exposed to ischemia, which can alter the gene expression (14). For this reason we compared diabetic kidneys with control kidneys that underwent the same handling prior to the isolation of glomeruli. The isolation was performed on ice and took about 5-10 min for each kidney. From other studies it is known that handling of the glomeruli on ice within 3 hours does not alter the mRNA expression for several pro-fibrotic genes (15). The labeling procedure and hybridization from one of the controls and one of the diabetic glomerular samples were performed in duplicate to calculate the inter-assay variation. The correlation

coefficient was near to 1 indicating that the labeling and hybridization procedure is highly reproducible. The correlation between different control samples and between different diabetic samples was also very high, indicating relatively low heterogeneity within groups. On the other hand the correlation coefficient between control and diabetic samples was lower, reflecting higher heterogeneity between groups. This was also found with the hierarchical clustering analyses (Fig. 3). By unsupervised analysis of the data, the program recognized gene clusters specific for control and diabetic samples based on their correlation. These findings supports the idea that, given the observations that the inter-assay variation and the variation of the gene expression of samples within one group are relatively low, factors such as ischemia, technical procedure, and biological variation probably influence the expression data to only limited extent.

To confirm the data obtained from the microarray, we performed real-time PCR for nephrin, VEGF, and TGF-β1. The relative levels for nephrin and VEGF were significantly decreased in DN compared to controls. No significant differences were observed between the real-time measurements and the microarray results. With both techniques the difference in TGF-β between the controls and diabetic kidneys was found not to be significant. To validate that our findings obtained with cadaveric donor kidneys apply to renal biopsy material, we also measured the mRNA levels of nephrin and VEGF in renal biopsy specimens from 5 patients with diabetic nephropathy and from 8 controls. These patients similarly showed a decrease in message for nephrin and VEGF. To show where the protein was present immunohistochemistry was performed for nephrin and VEGF. We found that VEGF and nephrin in particular were present in the podocytes along the glomerular basement membrane. At the protein level a decrease for these molecules was detected, a finding in line with that at the RNA level.

In the diabetic kidneys more genes were downregulated than there were upregulated compared to controls. This is in accordance with the fact that the number of genes on the chip giving a positive signal after hybridization (present genes) for the diabetic glomeruli was lower than the number of present genes on the chips for the controls (2042 versus 4297). These results are suggestive that downregulation of genes occurs considerably more often in the development of diabetic nephropathy. This idea is supported by the results of Mappfinder. The nucleotide metabolism is in the top 10 of decreased GO functions. There is also a reduction in diabetic nephropathy of the mRNA level of genes that are involved in the formation of the actin skeleton. Downregulation of these pathways in diabetic nephropathy might in part account for the general downregulation seen for many other genes on the chip. Another reason for the difference in the number of present genes between diabetic samples and control samples might be the stringency with which the microarray analyses were performed. We wanted to be sure to include only highly reproducible data in our list of differentially expressed genes. Therefore

Table 3. Top fifty of the most increased genes in all diabetic glomeruli versus controls.

Accession	Ratio	Gene name	Gene function
AI547258	4.9	metallothionein 2A	protects against heavy-metal toxicity
U96078	4.7	hyaluronoglucosaminidase 1	involved in cell proliferation, migration and differentiation
M16941	4.5	major histocompatibility complex, class II, DR	antigen presentation
U02388	4.3	cytochrome P450, subfamily IVF, polypeptide 2	Leukotriene B4 omega-hydroxylase
X85030	3.9	calpain 3	skeletal muscle-specific calcium-dependent cysteine protease
D17793	3.8	aldo-keto reductase family 1	catalyze the conversion of aldehydes and ketones
U19599	3.6	B-cell lymphoma-2-associated X protein	an apoptotic activator
X58288	3.3	protein tyrosine phosphatase, receptor type, M	signaling molecules that regulate a variety of cellular processes including cell growth, differentiation, mitotic cycle, and oncogenic transformation
D83402	3.2	prostacyclin synthase	vasodilator and inhibitor of platelet aggregation
H94881	3.2	FXYD domain-containing ion transport regulator 2	Gamma subunit of the Na+/K+-ATPase
AB020722	3.0	Rho guanine exchange factor 15	form a complex with G proteins and stimulate Rho-dependent signals.
M25915	3.0	clusterin (complement lysis inhibitor)	plays a role in the terminal complement reaction
J05257	3.0	dipeptidase 1	zinc-dependent metalloprotease
X16832	2.9	cathepsin H	lysosomal cysteine (thiol) proteinase
D13640	2.8	protein phosphatase 1F	inactivates the p21-activated kinase (PAK)
D87002	2.8	immunoglobin light chain	inflammation
AB018258	2.8	Adenosine tri phosphate(ATP)ase, Class V, type 10B	ATPase activity
U95299	2.7	Notch homolog 4 (Drosophila)	has multiple epidermal growth factor (EGF)like, notch, and ankyrin repeats
L48215	2.7	hemoglobin, beta	transports oxygen and carbon dioxide
L11702	2.7	glycosylphosphatidylinositol phospholipase D1	hydrolyzes inositol-PO4 linkage in PtdIns-glycan anchored proteins
U09577	2.7	hyaluronoglucosaminidase 2	lysosomal enzyme
Y07846	2.7	growth arrest-specific 2 like 1	an actin-associated protein expressed at high levels in growth-arrested cells
X64559	2.6	tetranectin	functions in mineralization during osteogenesis
L13720	2.6	growth arrest-specific 6	involved in the stimulation of cell proliferation
M73554	2.6	cyclin D1	alters cell cycle progression
AI762547	2.5	protein phosphatase 3	Ca(2+)-dependent modifier of phosphorylation status
M93311	2.5	metallothionein 3	inhibits cortical neuron survival and neurite formation
J03910	2.5	metallothionein 1G	protect against reactive oxygen species and metals
X58022	2.5	corticotropin releasing hormone-binding protein	inhibits stimulation of pituitary adrenocorticotropic hormone release
D90144	2.5	macrophage inflammtory protein 1-alpha	Small inducible cytokine
X58288	2.5	protein tyrosine phosphatase, receptor type, M	signaling molecules that regulate a variety of cellular processes including cell growth, differentiation, mitotic cycle, and oncogenic transformation

Table 3. Top fifty of the most increased genes in all diabetic glomeruli versus controls (continued).

Accession	Ratio	Gene name	Gene function
L33930	2.5	CD24 antigen	glycosyl phosphatidylinositol-linked glycoprotein that differentiates and activates granulocytes and B lymphocytes
AB009698	2.5	solute carrier family 22	Renal p-aminohippurate/alpha-ketoglutarate exchanger
AA100961	2.5	PECAM1	transendothelial migration of leukocytes, angiogenesis, and integrin activation
U67733	2.5	phosphodiesterase 2A	hydrolyzes cyclic adenosin monophosphate and cyclic guanine monophosphate
U45973	2.5	kidney enriched inositol phosphatase	may negatively regulate actin cytoskeleton
X07732	2.5	hepsin	transmembrane serine protease
AI017574	2.4	cysteine-rich protein 1	may function as a zinc carrier protein
U03056	2.4	hyaluronoglucosaminidase 1	involved in cell proliferation, migration and differentiation
M13929	2.4	c-myc	Promotor for c-myc
U21931	2.4	fructose-1,6-biphosphatase	fructose-1,6-biphosphatase
L06139	2.4	tyrosine kinase, endothelial (TEK)	critical for endothelial cell-smooth muscle cell communication
S53911	2.4	CD34 antigen	Cell surface antigen expressed on hematopoietic stem cells, and vascular endothelium
AB002438	2.4	Semaphorin 6B	migration
U41518	2.4	aquaporin 1	water channel protein
U11863	2.4	amiloride binding protein 1	deaminates putrescine and histamine
AJ001015	2.4	receptor (calcitonin) activity modifying protein 2	involved in core glycosylation
AF004230	2.3	leukocyte immunoglobulin-like receptor B1	binds cellular and viral major histocompatibility complex (MHC) class I antigens
U40391	2.3	serotonin N-acetyltransferase	enzyme in melatonin synthesis
X65784	2.3	cell matrix adhesion regulator	promotes adhesion of cells to components of the extracellular matrix

Table 4. Top fifty of the most decreased genes in diabetic glomerular samples versus control glomerular samples.

Accession	Ratio	Gene name	Gene function
L76465	22.8	hydroxyprostaglandin dehydrogenase 15	inactivates many prostaglandins
M11810	20.6	2'-5' oligoadenylate synthetase gene	catalyze the synthesis of 2-prime,5-prime oligomers of adenosine
M63978	19.5	vascular endothelial growth factor	mitogen for vascular endothelial cells
M22489	18.3	bone morphogenetic protein 2	member of the TGF-beta family of growth factors
Y16241	15.5	nebulette	binds to actin, tropomyosin, and alpha-actinin
AF009314	15.1	TUA8 Cri-du-chat region	unknown
AF042377	15.0	mannose 4,6-dehydratase	plays a role in the synthesis of fucosylated oligosaccharides

Table 4. Top fifty of the most decreased genes in diabetic glomerular samples versus control glomerular samples (continued).

Accession	Ratio	Gene name	Gene function
Z48541	14.7	glomerular epithelium protein 1	receptor-type protein tyrosine phosphatase
AI207842	14.3	prostaglandin D2 synthase	catalyzes synthesis of prostaglandin D
J03779	14.0	membrane metallo-endopeptidase	inactivates several peptide hormones including glucagon
L13698	13.6	growth arrest-specific 1	plays a role in growth suppression
L12468	13.5	aminopeptidase A	glycosylated zinc-dependent metalloprotease
X59065	12.7	fibroblast growth factor 1	potent mitogen for a variety of cell types
U49392	12.5	Allograft inflammatory factor 1	cytokine inducible protein associated with vascular injury
Y07593	12.2	coxsackie virus and adenovirus receptor	receptor for coxsackievirus and adenovirus
AB014524	11.9	SLAC2-B	unknown
D78014	11.9	dihydropyrimidinase-like 3	mediate signals involved in axonal outgrowth
AF078096	11.3	forkhead/winged helix-like transcription factor 7	transcription factor
X81053	11.2	collagen, type IV, alpha 4	extracellular matrix protein that forms basement membranes
X04371	10.9	2',5'-oligoadenylate synthetase 1	catalyze the synthesis of 2-prime,5-prime oligomers of adenosine
AB029000	10.5	sulfatase FP	sulfatase
U17034	10.4	phospholipase A2 receptor 1	Secretory phospholipases A2 receptor
L28997	9.7	adenosin-di-phosphate-ribosylation factor-like 1	stimulate phospholipase D
U65887	9.4	cytosin-di-phosphate (CDP)-diacylglycerol synthase	converts phosphatidic acid to CDP-diacylglycerol
S37730	9.3	insulin-like growth factor binding protein-2	binds to and modulates insulin-like growth factor activity
X73608	9.2	sparc/osteonectin(testican)	function may be related to protease inhibition.
U24152	9.1	p21/Cdc42/Rac1-activated kinase 1	regulates cell motility and morphology.
X14034	9.0	phospholipase C, gamma 2	hydrolyzes phosphatidyl inositol
M22489	8.6	bone morphogenetic protein 2	signals through receptor serine/threonine kinases
AF047419	8.4	epicardin, podocyte-expressed 1	transcription factor
M97935	8.4	Signal Transducer and Activator of Transcription 1	transcription factor
L17418	8.3	complement receptor type 1	binds complement
AB014605	8.2	atrophin-1 interacting protein 1	interact with atrophin-1
X74819	8.2	troponin T2	the tropomyosin-binding subunit of troponin
M24594	8.1	interferon-induced protein	unkown
U42360	7.9	Putative prostate cancer tumor suppressor	Putative integral membrane tumor suppressor protein
J02931	7.8	coagulation factor III	initiates the coagulation protease cascade assembly and propagation
M97936	7.7	IFN-stimulated gene factor-3 (ISGF-3)	transcription factor
L25124	7.6	prostaglandin E receptor 4	receptor that signals through a stimulatory G-protein
AF022375	7.5	vascular endothelial growth factor	induces endothelial cell proliferation and vascular permeability
U50534	7.5	breast cancer 2 (BRCA 2)	involved in DNA repair processes

Table 4. Top fifty of the most decreased genes in diabetic glomerular samples versus control glomerular samples (continued).

Accession	Ratio	Gene name	Gene function
AB022918	7.2	alpha2,3-sialyltransferase	plays a role in synthesis of sialyl-paragloboside
AB006746	7.1	phospholipid scramblase 1	plays a role in the EGF-induced metabolic or mitogenic response.
U18934	7.0	protein tyrosine kinase	receptor protein tyrosine kinase
AJ001381	7.0	myosin IB	Member of the myosin family of motor ATPases
D17517	7.0	TYRO3 protein tyrosine kinase	Receptor protein tyrosine kinase
Y08374	7.0	cartilage GP-39	associated with monocyte to macrophage maturation
M62424	6.9	coagulation factor II receptor	involved in platelet activation
J02611	6.7	apolipoprotein D	component of high density lipoprotein
AI401567	6.6	glutamate receptor	ligand-gated ion channel selectively permeable to sodium and calcium

only those genes, which were present in all three diabetic arrays, were included. There is more heterogeneity in gene expression patterns among diabetic samples than among control samples. This would mean that, due to this difference in heterogeneity, the chance that a certain gene is positive on all three chips in the diabetic group is lower than the same gene being present in all three chips of the normal samples.

One of the major clinical problems in patients with diabetes is the presence of vascular abnormalities, such as increased endothelial permeability to macromolecules and endothelial proliferation (16). Considerable research has focused on the pathogenesis of endothelial dysfunction, but the exact mechanisms have remained unclear. VEGF is one of the most important factors in endothelial repair and angiogenesis. It has recently been shown that subtotally nephrectomized rats show a reduction of VEGF mRNA in the kidney (17). Treatment of these rats with angiotensin converting enzyme inhibitors leads to normalization of both glomerular VEGF mRNA levels and capillary endothelial cell density. In animal models for diabetic nephropathy, an increase of VEGF was found in diseased renal tissue (18). In contrast, in human renal biopsies with diabetic nephropathy a decrease of VEGF at both the protein and the mRNA level was shown (19). The notion that VEGF mRNA was found to be decreased in human DN is supported by our observations (20). Another gene for which expression was significantly decreased in the diabetic glomeruli is fibroblast growth factor 1 (FGF1). This protein functions as a modifier of endothelial cell migration and proliferation, and an angiogenic factor, and it can protect the kidney against ischemia-reperfusion injury (21). The expression of PECAM-1, a molecule that is involved in angiogenesis and leukocyte trafficking, was increased in the diabetic kidneys.

Accumulation of extracellular matrix (ECM) proteins has been found in animal models and in biopsies from patients

Table 5. Top 10 of the Mappfinder results based on gene ontology (GO) function ranked on basis of highest z-Score.

Mappfinder results based on decreased genes		
GO ID	GO Name	z-Score
7242	intracellular signaling cascade	2.14
5515	protein binding	2.11
15629	actin cytoskeleton	2.07
4	biological_process unknown	1.97
6886	intracellular protein transport	1.95
5488	binding	1.89
8285	negative regulation of cell proliferation	1.83
3779	actin binding	1.83
3677	DNA binding	1.81
6139	nucleobase, nucleoside, nucleotide and nucleic acid metabolism	1.78
Mappfinder results based on increased genes		
GO ID	GO Name	z-Score
19725	homeostasis	4.81
30005	di-, tri-valent inorganic cation homeostasis	4.30
16302	phosphatase	4.25
16791	phosphoric monoester hydrolase	3.84
30006	heavy metal ion homeostasis	3.72
5505	heavy metal binding	3.19
16788	hydrolase, acting on ester bonds	3.13
4437	inositol/phosphatidylinositol phosphatase	3.03
7218	neuropeptide signaling pathway	3.03
19730	antimicrobial humoral response	3.03

with diabetic nephropathy (22). Expansion of the ECM can be the result of a disturbed balance between ECM synthesis and ECM degradation, or a combination of these mechanisms. Of note, we found an increase of message for metargidin, a disintegrin metalloproteinase (23), and a decrease of message for collagen α4(IV), a major structural component of the GBM. In a previous study, an increase for overall collagen type IV protein was observed in glomeruli from patients with diabetic nephropathy (3). In animal cell cultures under high glucose levels an increase in collagen type IV mRNA was mainly found for the alpha 1, alpha 3, and alpha 5 chains (24). In this study we did not find a change in the mRNA level for TGF-β. In the literature the role of TGF-β. has been described in several animal models (summarized in (25)) and a small increase of the mRNA level in human glomeruli have been reported (26,27). A reason of the opposing result for TGF-β between previous studies and our study might be that this molecule was studied in different stages of the disease. Alternatively, the mRNA levels for TGF-β we described in our study might not reflect the level or activity of the corresponding protein. An increase of active TGF-β can also be explained by increased translation, or increased activation of latent TGF-β. A decrease of the natural inhibitors can also increase the bioactivity of TGF-β.

Recently it has also been shown that high-glucose can induce fibronectin and collagen type III expression in renal fibroblasts independent of TGF-β1(28). The growth factor BMP-2, the growth factor inhibitor syndecan-2, and the growth factor receptor insulin-like growth factor binding protein-2 (IGFBP-2) were all decreased in DN. These components are known to play a role in ECM remodeling (29-31).

The diabetic kidneys analyzed in this study morphologically showed glomerular hypertrophy and proliferation, a common event seen in diabetic nephropathy (32). With respect to proliferating cells in diabetic glomeruli, expression profiling of these glomeruli as reported here shows many genes that play an important role in cell cycle regulation. In kidneys with DN, we saw an increase of hyaluronoglucosaminidase 1 and a decrease in BMP-2 and growth arrest-specific 1 protein, all suggestive for increased proliferation. It has recently shown that treatment of streptozotocin induced diabetic rats with BMP-7 preserves the GFR, reduces the proteinuria and prevents glomerulosclerosis (33). For breast cancer 2 (BRCA-2), nedcin, and the cytokines FGF-1 and VEGF, a role in cell cycle control has been described (34-36).

The pathogenesis of albuminuria, one of the earliest clinical signs of diabetic nephropathy, has not been fully clarified. It is generally assumed that the filtration apparatus of the glomerular capillary wall is of central importance in this process. It has been shown that the slit diaphragm located between the foot processes of the podocytes plays a crucial role in the filtration of macromolecules (37). The expression of nephrin, a transmembrane protein that localizes in the slit pore of the glomerular epithelial cells, was found to be decreased in diabetic glomeruli in our study. This observation is in agreement with the reduction of glomerular nephrin gene expression and with the increase in albuminuria at a later stage of the disease both in human diabetic nephropathy (38,39) and in diabetic and hypertensive rats (40). The transcription of podocalyxin, a protein expressed in the slit pore, is regulated by the transcription factor Wilms tumor 1 (WT1)(not present in the top 50, but 6.9-fold decreased) (41). Downregulation of this transcription factor may lead to a lack of podocalyxin. These findings support the hypothesis that slit pore-associated proteins play a role in the development of proteinuria.

In conclusion, we found that in diabetic nephropathy more genes were downregulated than there were upregulated, compared to controls, which might be explained for a large part by a decreased nucleotide metabolism. We also found a disturbed cytoskeleton formation in diabetic nephropathy. Many other tissue repair related genes as BMP-2, FGF-1, insulin-like growth factor binding protein-2 and CTGF were downregulated in diabetic nephropathy, all suggestive for a reduced tissue repair capacity. On top of that, message for VEGF was decreased in DN compared to controls. This finding for VEGF was validated at the protein level, and additionally, tissue VEGF levels were found to be decreased in an independent group of diabetic patients. These findings suggest that the progression of diabetic nephropathy might at least in

part be a result of a diminished repair mechanism in the endothelium of the capillaries.

The results described in this study underscore the potential of gene chip technology as a methodology for unraveling the complexities of the renal response to diabetes mellitus. This powerful technique allows simultaneously analysis of the expression profile of thousands of genes. We discussed several genes differentially expressed between array data sets, which are functionally related to vascular damage, mesangial matrix expansion, proliferation, and proteinuria, events seen in diabetic nephropathy. Further elucidation of the functional involvement of these genes by studies in larger patients groups and time course experiments will lead to an even better understanding of the processes leading to diabetic nephrosclerosis.

Acknowledgements

We thank Dr. Kawachi (Niigata, Japan) for providing us with the anti-nephrin antibody and Wendy Bouwman and Klaas Koop for the immunohistological staining of VEGF and nephrin.

References

1. John L, Kirubakaran MG, Shastry JC: Diabetic nephropathy: a clinical study of 498 patients. *J Diabet Complications* 1:87-90, 1987
2. Mogensen CE, Chachati A, Christensen CK, Close CF, Deckert T, Hommel E, Kastrup J, Lefebvre P, Mathiesen ER, Feldt-Rasmussen B: Microalbuminuria: an early marker of renal involvement in diabetes. *Uremia Invest* 9:85-95, 1985
3. Vleming LJ, Baelde JJ, Westendorp RG, Daha MR, van Es LA, Bruijn JA: The glomerular deposition of PAS positive material correlates with renal function in human kidney diseases. *Clin Nephrol* 47:158-167, 1997
4. Ziyadeh FN: The extracellular matrix in diabetic nephropathy. *Am J Kidney Dis* 22:736-744, 1993
5. Yamamoto T, Nakamura T, Noble NA, Ruoslahti E, Border WA: Expression of transforming growth factor β is elevated in human and experimental diabetic nephropathy. *Proc Natl Acad Sci USA* 90:1814-1818, 1993
6. Gambaro G, Baggio B: Growth factors and the kidney in diabetes mellitus. *Crit Rev Clin Lab Sci* 35:117-151, 1998
7. Wada J, Zhang H, Tsuchiyama Y, Hiragushi K, Hida K, Shikata K, Kanwar YS, Makino H: Gene expression profile in streptozotocin-induced diabetic mice kidneys undergoing glomerulosclerosis. *Kidney Int* 59:1363-1373, 2001
8. Spiro RG: Studies on the renal glomerular basement membrane. Preparation and chemical composition. *J Biol Chem* 242:1915-1922, 1967
9. Eikmans M, Sijpkens YW, Baelde HJ, De Heer E, Paul LC, Bruijn JA: High transforming growth factor-beta and extracellular matrix mRNA response in renal allografts during early acute rejection is associated with absence of chronic rejection. *Transplantation* 73:573-579, 2002
10. Vandesompele J, De Preter K, Pattyn F, Poppe B, Van Roy N, De Paepe A, Speleman F: Accurate normalization of real-time quantitative RT-PCR data by geometric averaging of multiple internal control genes. *Genome Biol* 3:34, 2002
11. Specht K, Richter T, Muller U, Walch A, Werner M, Hofler H: Quantitative gene expression analysis in microdissected archival formalin-fixed and paraffin-embedded tumor tissue. *Am J Pathol* 158:419-429, 2001
12. Koop K, Eikmans M, Baelde HJ, Kawachi H, De Heer E, Paul LC, Bruijn JA: Expression of podocyte-associated molecules in acquired human kidney diseases. *J Am Soc Nephrol* 14:2063-2071, 2003
13. Doniger SW, Salomonis N, Dahlquist KD, Vranizan K, Lawlor SC, Conklin BR: MAPPFinder: using Gene Ontology and GenMAPP to create a global gene-expression profile from microarray data. *Genome Biol* 4:R7, 2003
14. Azuma H, Nadeau K, Takada M, Mackenzie HS, Tilney NL: Cellular and molecular predictors of chronic renal dysfunction after initial ischemia/reperfusion injury of a single kidney. *Transplantation* 64:190-197, 1997
15. Eikmans M, Baelde HJ, De Heer E, Bruijn JA: Processing renal biopsies for diagnostic mRNA quantification: improvement of RNA extraction and storage conditions. *J Am Soc Nephrol* 11:868-873, 2000
16. Stehouwer CD, Lambert J, Donker AJ, van Hinsbergh VW: Endothelial dysfunction and pathogenesis of diabetic angiopathy. *Cardiovasc Res* 34:55-68, 1997
17. Kelly DJ, Hepper C, Wu LL, Cox AJ, Gilbert RE: Vascular endothelial growth factor expression and glomerular endothelial cell loss in the remnant kidney model. *Nephrol Dial Transplant* 18:1286-1292, 2003
18. de Vriese AS, Tilton RG, Elger M, Stephan CC, Kriz W, Lameire NH: Antibodies against vascular endothelial growth factor improve early renal dysfunction in experimental diabetes. *J Am Soc Nephrol* 12:993-1000, 2001
19. Bailey E, Bottomley MJ, Westwell S, Pringle JH, Furness PN, Feehally J, Brenchley PE, Harper SJ: Vascular endothelial growth factor mRNA expression in minimal change, membranous, and diabetic nephropathy demonstrated by non-isotopic in situ hybridisation. *J Clin Pathol* 52:735-738, 1999
20. Shulman K, Rosen S, Tognazzi K, Manseau EJ, Brown LF: Expression of vascular permeability factor (VPF/VEGF) is altered in many glomerular diseases. *J Am Soc Nephrol* 7:661-666, 1996
21. Cuevas P, Martinez-Coso V, Fu X, Orte L, Reimers D, Gimenez-Gallego G, Forssmann WG, Saenz DT,

I: Fibroblast growth factor protects the kidney against ischemia-reperfusion injury. *Eur J Med Res* 4:403-410, 1999
22. Striker GE, Eastman RD, Striker LJ: Diabetic nephropathy: molecular analysis of extracellular matrix and clinical studies update. *Nephrol Dial Transplant* 11 Suppl 5:58-61.:58-61, 1996
23. Bohm BB, Aigner T, Blobel CP, Kalden JR, Burkhardt H: Highly enhanced expression of the disintegrin metalloproteinase MDC15 (metargidin) in rheumatoid synovial tissue. *Arthritis Rheum* 44:2046-2054, 2001
24. Sharma K, Jin Y, Guo J, Ziyadeh FN: Neutralization of TGF-beta by anti-TGF-beta antibody attenuates kidney hypertrophy and the enhanced extracellular matrix gene expression in STZ-induced diabetic mice. *Diabetes* 45:522-530, 1996
25. Chen S, Hong SW, Iglesias-de la Cruz MC, Isono M, Casaretto A, Ziyadeh FN: The key role of the transforming growth factor-beta system in the pathogenesis of diabetic nephropathy. *Ren Fail* 23:471-481, 2001
26. Iwano M, Kubo A, Nishino T, Sato H, Nishioka H, Akai Y, Kurioka H, Fujii Y, Kanauchi M, Shiiki H, Dohi K: Quantification of glomerular TGF-beta 1 mRNA in patients with diabetes mellitus. *Kidney Int* 49:1120-1126, 1996
27. Yamamoto T, Noble NA, Cohen AH, Nast CC, Hishida A, Gold LI, Border WA: Expression of transforming growth factor-beta isoforms in human glomerular diseases. *Kidney Int* 49:461-469, 1996
28. Lam S, Verhagen NA, Strutz F, Van Der Pijl JW, Daha MR, Van Kooten C: Glucose-induced fibronectin and collagen type III expression in renal fibroblasts can occur independent of TGF-beta1. *Kidney Int* 63:878-888, 2003
29. Clayton A, Thomas J, Thomas GJ, Davies M, Steadman R: Cell surface heparan sulfate proteoglycans control the response of renal interstitial fibroblasts to fibroblast growth factor-2. *Kidney Int* 59:2084-2094, 2001
30. Price GJ, Berka JL, Werther GA, Bach LA: Cell-specific regulation of mRNAs for IGF-I and IGF-binding proteins-4 and -5 in streptozotocin-diabetic rat kidney. *J Mol Endocrinol* 18:5-14, 1997
31. McMahon R, Murphy M, Clarkson M, Taal M, Mackenzie HS, Godson C, Martin F, Brady HR: IHG-2, a mesangial cell gene induced by high glucose, is human gremlin. Regulation by extracellular glucose concentration, cyclic mechanical strain, and transforming growth factor-beta1. *J Biol Chem* 275:9901-9904, 2000
32. Wolf G: Cell cycle regulation in diabetic nephropathy. *Kidney Int Suppl* 77:S59-66.:S59-S66, 2000
33. Wang S, Chen Q, Simon TC, Strebeck F, Chaudhary L, Morrissey J, Liapis H, Klahr S, Hruska KA: Bone morphogenic protein-7 (BMP-7), a novel therapy for diabetic nephropathy. *Kidney Int* 63:2037-2049, 2003
34. Nakada Y, Taniura H, Uetsuki T, Inazawa J, Yoshikawa K: The human chromosomal gene for necdin, a neuronal growth suppressor, in the Prader-Willi syndrome deletion region. *Gene* 213:65-72, 1998
35. Diamandis EP: Clinical applications of tumor suppressor genes and oncogenes in cancer. *Clin Chim Acta* 257:157-180, 1997
36. Ichimura T, Maier JA, Maciag T, Zhang G, Stevens JL: FGF-1 in normal and regenerating kidney: expression in mononuclear, interstitial, and regenerating epithelial cells. *Am J Physiol* 269:F653-F662, 1995
37. Kestila M, Lenkkeri U, Mannikko M, Lamerdin J, McCready P, Putaala H, Ruotsalainen V, Morita T, Nissinen M, Herva R, Kashtan CE, Peltonen L, Holmberg C, Olsen A, Tryggvason K: Positionally cloned gene for a novel glomerular protein—nephrin—is mutated in congenital nephrotic syndrome. *Mol Cell* 1:575-582, 1998
38. Langham RG, Kelly DJ, Cox AJ, Thomson NM, Holthofer H, Zaoui P, Pinel N, Cordonnier DJ, Gilbert RE: Proteinuria and the expression of the podocyte slit diaphragm protein, nephrin, in diabetic nephropathy: effects of angiotensin converting enzyme inhibition. *Diabetologia* 45:1572-1576, 2002
39. Doublier S, Salvidio G, Lupia E, Ruotsalainen V, Verzola D, Deferrari G, Camussi G: Nephrin Expression Is Reduced in Human Diabetic Nephropathy: Evidence for a Distinct Role for Glycated Albumin and Angiotensin II. *Diabetes 2003 Apr;52 (4):1023 -1030* 52:1023-1030, 2003
40. Forbes JM, Bonnet F, Russo LM, Burns WC, Cao Z, Candido R, Kawachi H, Allen TJ, Cooper ME, Jerums G, Osicka TM: Modulation of nephrin in the diabetic kidney: association with systemic hypertension and increasing albuminuria. *J Hypertens* 20:985-992, 2002
41. Palmer RE, Kotsianti A, Cadman B, Boyd T, Gerald W, Haber DA: WT1 regulates the expression of the major glomerular podocyte membrane protein Podocalyxin. *Curr Biol* 11:1805-1809, 2001

(Colour picture from page 125)

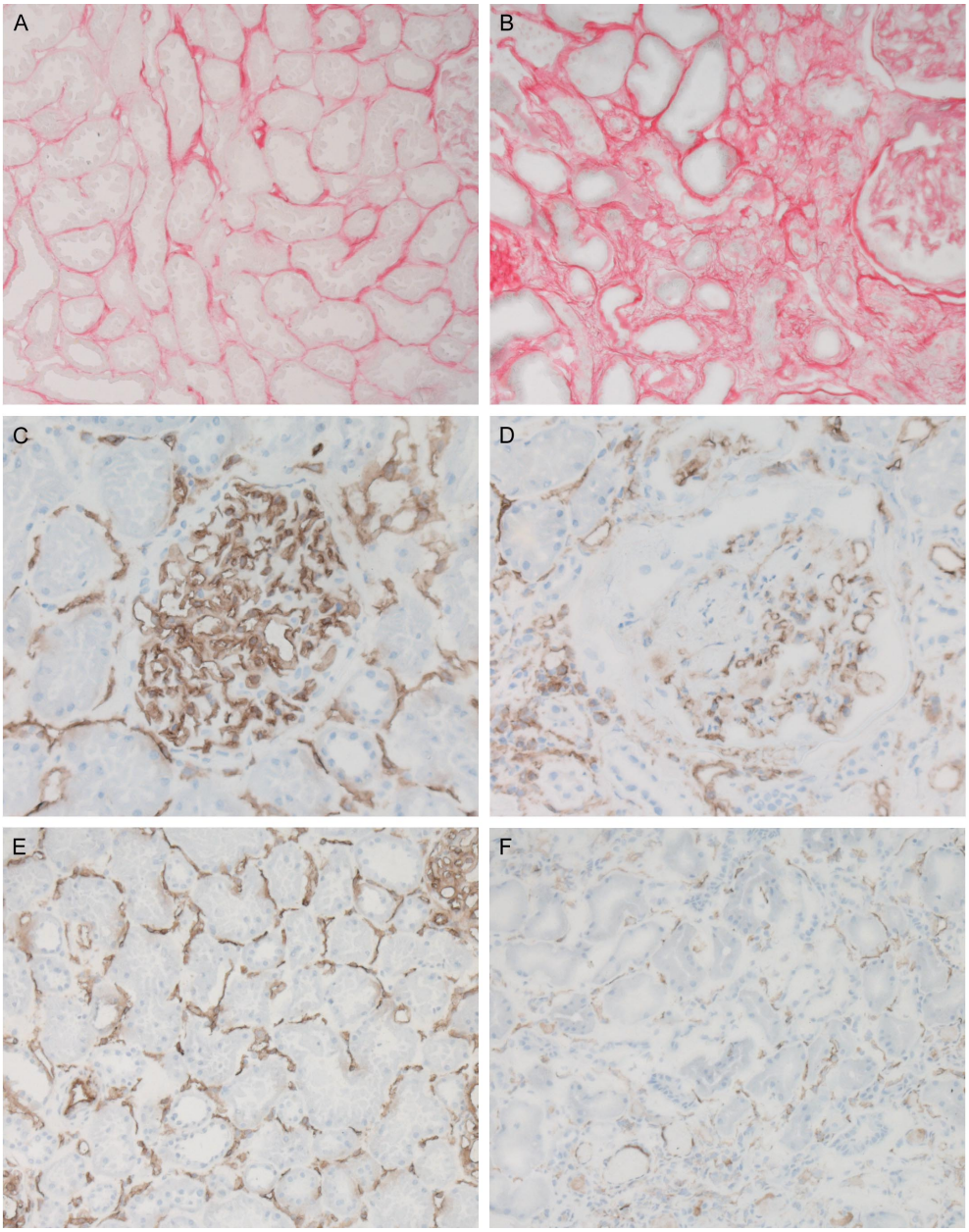

Figure 4. Sirius Red and CD31 staining in the biopsies**.** A and B are representative illustrations of the Sirius Red staining in a control patient and in a patient with DN, respectively. C-F are representative pictures of CD31 staining: glomerulus of a control patient (C), glomerulus of a patient with DN (D), the tubulo-interstitial part of a control patient (E) and the tubulo-interstitial part of a diabetic patient (F).

Chapter 7

Renal cortical and glomerular message for angiogenic factors is decreased in human diabetic nephropathy

H.J. Baelde[1], M.Eikmans[1], D.W.P. Lappin[2], P.P. Doran[2], D. Hohenadel[3], P.Th. Brinkkoetter[3], R. Waldherr[4], T.J. Rabelink[5], E. de Heer[1], J.A. Bruijn[1]

[1]Department of Pathology, Leiden University Medical Center, Leiden, The Netherlands.
[2]Department of Medicine and Therapeutics, Mater Misericordiae Hospital, University College Dublin and Dublin Molecular Medicine Centre, Dublin, Ireland.
[3]Department of Nephrology/Endocrinology/Rheumatology, University Hospital of Mannheim, University of Heidelberg.
[4]Institute for Clinical Pathology, Heidelberg
[5]Department of Nephrology, Leiden University Medical Center, Leiden, The Netherlands.

Submitted for publication

Abstract

Vascular complications in diabetic patients are being increasingly appreciated as a significant clinical challenge. Experiments in animal models indicate that perturbed angiogenesis and corresponding alterations of expression of angiogenic growth factors play a role in the development of diabetic nephropathy (DN). We investigated expression levels of angiogenic factors in human DN in relation to fibrosis and the number of endothelial cells.

Cortical and glomerular mRNA levels for vascular endothelial growth factor (VEGF), connective tissue growth factor (CTGF), transforming growth factor-beta (TGF-β), fibroblast growth factor 2 (FGF2) and syndecan were measured using real-time PCR in biopsy material from 29 patients with DN and in 24 control samples. Laser capture microdissection was applied to obtain glomerular RNA. Interstitial fibrosis was quantified with Sirius Red staining and the number of endothelial cells by CD31 staining.

Both cortical and glomerular VEGF and CTGF mRNA levels were decreased in DN compared to control samples ($P<0.01$). Expression of TGF-β, FGF2 and syndecan was not significantly different between diabetic patients and controls. Glomerular mRNA levels for VEGF showed an inverse correlation with the extent of interstitial fibrosis and a positive association with CTGF expression and the number of endothelial cells.

The results are suggestive for a disturbed angiogenesis in patients with DN. We hypothesize that decreased secretion of VEGF and CTGF due to damage of glomerular epithelial cells in DN leads to a disturbed maintenance of glomerular endothelial cells and a loss of glomerular and interstitial capillaries.

Introduction

Diabetic nephropathy (DN) is a major complication of both type 1 and type 2 diabetes. It is the most common single cause of end-stage renal disease (1,2). One of the earliest clinical signs of diabetic nephropathy is microalbuminuria, which may progress to proteinuria (3) and hyperfiltration followed by a decrease in the glomerular filtration rate (GFR). Morphologically, DN is characterized by glomerular hypertrophy, progressive expansion of the mesangial matrix, and thickening of the glomerular and tubular basement membranes (4,5). In later stages of the disease, glomerulosclerosis and interstitial fibrosis, resulting from an imbalance between synthesis and degradation of extracellular matrix (ECM) components (6), are prominent.

Although many factors including high glucose, insulin, advanced glycation end products (AGE) and high blood pressure have been found to play a role in the initiation and progression of DN, the precise molecular mechanism is still unclear. Several cytokines and growth factors have been proposed to mediate the development of DN. Transforming growth factor-beta (TGF-β) is the most widely investigated molecule in relation to diabetic glomerulosclerosis and interstitial fibrosis, most notably in animal models (7). Vascular endothelial cell dysfunction is a common finding in patients with type 2 diabetes mellitus. Endothelial cell loss may be involved in the development of renal disease and the progression to sclerosis. In diabetic retinopathy, neovascularization can result in loss of vision. Increased VEGF protein has been demonstrated in nonvascular cells in the retina of patients with diabetes even in the absence of retinopathy (8). A role for VEGF in DN has also been described. In STZ-induced diabetic rats, it has been demonstrated that treatment with monoclonal anti-VEGF antibodies decreased hyperfiltration, albuminuria, and glomerular hypertrophy (9). Others studies have reported that VEGF is reduced in rat glomeruli one week after diabetes induction with streptozotocin (10). In human DN it has been suggested that VEGF is important in maintaining glomerular endothelial cell function, and that a decrease in local VEGF levels accounts for abnormal remodelling of the glomerular capillaries (11,12). Despite recent progress in elucidating the role of perturbed vascular biology in progressive renal disease, the role of VEGF in the pathogenesis of DN is still unclear (13).

Several other growth factors have been identified, which play a role in angiogenesis. For example, CTGF has been shown to play an important role in invasive new vessel formation, in addition to its profibrotic activity downstream of TGF-β. A similar involvement has been described for FGF2 (14). Syndecan can amplify the availability of FGF2 via specific binding to FGF2 (15).

In this study we investigated the gene expression levels of different angiogenic factors in renal biopsies from patients with DN. These factors have been identified in a previous study of gene expression profiling of human kidneys with DN (11). Correlations of expression levels

with clinical parameters and morphological changes were tested to obtain further insights in the role of these mediators in the development of DN.

Materials and methods

Array studies on diabetic kidneys

Hybridizations were performed on the Human Genome U95Av2 Array (Affymetrix® Santa Clara, CA, USA). This array contains ~12,000 sequences characterized previously in terms of function or disease association. Ten µg of total RNA from three control kidneys and three kidneys from patients with diabetic nephropathy (11) was converted to complementary (c)DNA, double stranded (ds)DNA, and transcribed *in vitro* according to the instructions of the manufacturer. After hybridization, the microchips were scanned and analyzed with Affymetrix® Microarray Suite 5.0 software. To normalize the data from different microarray experiments, the expression levels of all genes on the chip were scaled to a standard value and the mean of the scaling factors was calculated. This value served as the normalization factor for all genes represented on the different microarray chips. To obtain normalized expression values, the expression level for each gene was multiplied by the normalization factor. Statistics of this method can be found in the Microarray Suite User's Guide, Version 5.0, which is available at http://www.affymetrix.com/support/technical/manuals.affx.

To identify genes of which expression was altered consistently in the disease samples, we used either those genes which were present on all six chips, or those which were present in all three control samples and absent in all three diabetic samples, or vice versa. We employed multiple pair-wise comparisons between control and disease groups using the OpenStat statistics package (students t-test, $p<0.01$).

Renal biopsies

Frozen biopsies from patients with DN (n=29) were selected from the pathology archive of the Leiden University Medical Center and the Institute for Clinical Pathology, Heidelberg. All patients were diagnosed with type 2 diabetes. Diabetic nephropathy was histologically confirmed by Periodic acid-Schiff (PAS) stained paraffin sections. Criteria for diabetic nephropathy included glomerular hypertrophy, diffuse mesangial and focal nodular glomerulosclerosis, arteriolar hyalinosis, focal and segmental glomerulosclerosis, the presence of hyaline drops between Bowman's capsule and epithelial cells, and interstitial fibrosis. Serum creatinine levels and albuminuria of the patients are summarized in Figure 1. As a control group (n=22), native kidneys with normal function and histology were obtained at autopsy (n=3), from cadaver donor kidneys unsuitable for transplantation for technical reasons (n = 7), and

from the non-affected part of tumour nephrectomy samples (n = 12). There were no significant differences within the different control groups between all parameters measured. Patient studies were approved by the institutional ethical committee.

Microdissection and RNA isolation from glomeruli

The PALM Laser-MicroBeam System (P.A.L.M., Wolfratshausen, Germany) was used for microdissection of glomeruli from renal biopsies according to the method of Specht et al (16). In brief, three frozen sections of 4 µm were put on a polyethylene foil coated slide. After selecting the glomeruli (20 ± 5 glomeruli from each biopsy), they were dissected with a laser beam and catapulted into a reaction tube containing RLT buffer (RNeasy kit, QIAGEN GmbH, Germany). RNA was isolated from these glomeruli by adding of 200µl Trizol®. After adding 40 µl chloroform and mixing for 1 min, the suspension was centrifuged at 15,000g for 10 min. RNA was precipitated with isopropanol in the presence of 5 µg glycogen.

RNA isolation from renal cortex

Cryostat sections were cut from each biopsy. The presence of cortex was determined on the basis of light-microscopic localization of glomeruli in the sections. Ten slides of 10 µm thickness were cut and collected in a reaction tube. RNA was isolated using RNeasy Mini columns (QIAGEN GmbH, Germany), according to the instructions of the manufacturer. After elution, the RNA was precipitated with 3 M NaAc and ethanol in the presence of 5 µg glycogen.

cDNA synthesis

RNA from glomerular and whole kidney was converted into cDNA using avian myeloblastosis virus reverse transcriptase (Roche Applied Science) in combination with oligo-dT and random hexamer (0.5 µg/reaction) priming. RNA without

Table 1 . Primer and Taqman® probes sequences.

Gene	Forward primer	Reverse primer	Taqman® probe
VEGF	AAACCCTGAGGGAGGCTCC	TACTTGCAGATGTGACAAGCCG	CCTCCTGCCCGGCTCACCGC
CTGF	GGAAGAGAACATTAAGAAGGGCAA	CTCGGTATGTCTTCATGCTGGTG	CGTACTCCCAAAATCTCCAAGCCTATCA
TGF-β1	CCCAGCATCTGCAAAGCTC	GTCAATGTACAGCTGCCGCA	ACACCAACTATTGCTTCAGCTCCACGGA
Fibronectin	GGAGAATTCAAGTGTGACCCTCA	TGCCACTGTTCTCCTACGTGG	AGGCAACGTGTTACGATGATGGGAAGACAT
FGF-2	CGACGGCCGAGTTGACGG	CAGGTAACGGTTAGCACACACTCC	AAGAGCGACCCTCACATCAAGCTACAACTTCA
Syndecan	GAGCTGCGTGTCCTTCCAAG	CCCAGAGACCAACGTTCAAGC	TGCCCCCTGAAGATCAAGATGGCTC
GAPDH	TTCCAGGAGCGAGATCCCT	CACCCATGACGAACATGGG	CCCAGCCTTCTCCATGGTGGTGAA
HPRT	TGACACTGGCAAAACAATGCA	GGTCCTTTTCACCAGCAAGCT	CTTGACCATCTTTGGATTATACTGCCTGACCA
TBP	CACGAACCACGGCACTGATT	TTTTCTTGCTGCCAGTCTGGAC	TGTGCACAGGAGCCAAGAGTGAAGA

reverse transcriptase was used as a negative control for the PCR.

Quantitative real-time polymerase chain reaction

Quantitative real-time polymerase chain reaction (Q-PCR) (17) was used in combination with Taqman® probes to quantify the gene transcription levels for VEGF, TGF-β, CTGF, FGF2, and syndecan. Primer and probe sequences can be found in Table 1. In brief, the cDNA samples were diluted 25 times. Five µl was used for quantitation of each transcript. Each PCR consisted of the following components: 300 pmol primers, 100 pmol probe 0.25 mM dNTPs, 6 mM $MgCl_2$, 0.5 U of Hot Gold Star polymerase, 1 x real-time PCR buffer (Eurogentec). Further details concerning the real-time PCR protocol have been described elsewhere (18). The transcription levels of the genes of interest were determined and corrected to a panel of three housekeeping genes, i.e., glyceraldehyde-phosphate-dehydrogenase (GAPDH), hypoxanthine phosphoribosyl transferase (HPRT), and TATA box binding protein (TBP), as described by Vandesomple et al (19). These housekeeping genes were selected from a panel of 5 different housekeeping genes (20) on basis of the highest correlations between each other ($r \geq 0.85$). To calculate the relative mRNA levels we measured the threshold cycle (Ct) values of a standard curve with a known amount of total RNA. For each housekeeping gene the relative amount of the samples were calculated by linear regression analysis from their standard curve. The relative values of each of the 3 different housekeeping genes of the controls were adjusted to one by dividing the samples by the mean of all samples. After this correction the mean of the 3 different housekeeping genes was calculated. The relative expression levels of the genes of interest

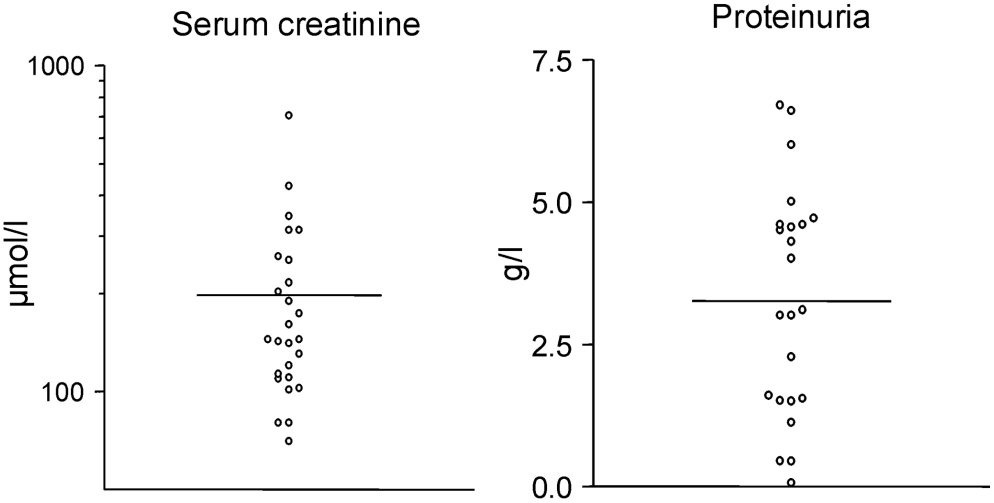

Figure 1. Clinical characteristics of the diabetic patients. Serum creatinine levels (µmol/l) (A) and urine protein excretion (g/l) (B).

were calculated by dividing the value of the gene by the mean of the different housekeeping genes. The relative values were set to one for the controls.

(Immuno)histochemistry

To quantify the number of endothelial cells, frozen section were stained for CD31. In brief, the slides were washed in PBS and incubated for 2 h at room temperature with the primary antibody (Rabbit anti CD31, DAKO, Glostrup, Denmark), diluted in 1% bovine serum albumin in PBS. After washing with PBS, the slides were incubated for 30 min with horseradish peroxidase–conjugated anti-rabbit Envision (DAKO, Glostrup, Denmark). The slides were again washed with PBS, and the staining was developed with diaminobenzidine. The color was enhanced by rinsing the slides in 0.5% $CuSO_4$ solution for 5 min. After counterstaining with haematoxylin, the slides were dehydrated and mounted. Sirius Red staining was used to quantify the amount of interstitial fibrosis. All sections were stained in one session simultaneously.

Digital image analysis

Digital image analysis was performed using a Zeiss microscope equipped with a full-color 3CCD camera (Sony DXC 950p) and KS-400 image analysis software version 3.0 (Zeiss-Kontron, Eching, Germany). The percentage of the area stained for CD31 was calculated and used as a measure for the number of endothelial cells. To count the number of glomerular endothelial cells, images of all of the glomeruli (3-15) present in the slides were taken. For the interstitial endothelial cells 10 random images were taken. To quantify the amount of interstitial fibrosis the percentage of the area in the sections stained by Sirius Red was measured in 10 adjacent microscopic fields of the renal cortex.

Statistics

Statistical analysis for comparison of mRNA expression, Sirius Red stained area and CD31 stained area, between groups was performed using independent Student's T-test. Pearson correlations were calculated using the SPSS version 10 software. Values of $p<0.05$ were considered to be significant.

Results

Microarray experiments

In earlier gene expression profiling experiments on isolated glomeruli from patients with DN, a significant decrease of mRNA levels for VEGF (19.5 times) and CTGF (6.5 times) was found (11). To further expand the scope of these investigations, we have performed oligonucleotide

microarray profiling of RNA isolated from the total cortical part of kidneys from the same patients as those described in the previous study. A total of 6 chips were hybridized with RNA from 3 controls and 3 patients with diabetic nephropathy. Results of these experiments can be found in detail at : http://www-onderzoek.lumc.nl/pathology/kidney/diabeticnephropathy/ and http://www.ncbi.nlm.nih.gov/geo/gds/gds browse.cgi?gds=961. Whole cortex mRNA levels of VEGF (2.2 times), CTGF (1.7 times), and syndecan (2.2 times) were decreased, while expression of fibronectin (FN) (1.7 times) was increased in patients with DN compared to controls. There were no significant differences between DN and control tissue with respect to TGF-β mRNA levels.

Clinical parameters

Protein excretion and serum creatinine levels at the time of biopsy for the 29 patients with DN are summarized in Figure 1. Serum creatinine levels ranged from 70 to 700 μmol/l (Fig 1A) and protein excretion ranged from 0.061 to 6.7 gram/l (Fig 1B). There was no difference in age (60.6 ± 10.9 years versus 59.9 ± 10.0 years) and gender between control and diabetic patients.

Glomerular and whole cortical mRNA levels.

Having identified transcripts as being differentially regulated in DN using oligonucleotide microarrays, we validated their mRNA levels in a large, independent group of 29 patients and 22 controls. VEGF mRNA levels in microdissected glomeruli as measured by Q-PCR were 2.6 times decreased ($P<0.01$) in patients with DN compared to control kidneys (Fig 2A). In whole cortex RNA, VEGF mRNA levels in patients with DN were decreased 2.5 fold compared to controls ($P<0.01$) (Fig 3A). A similar pattern of downregulation was observed for CTGF. Glomerular and whole cortex mRNA levels for CTGF were 1.6 times decreased ($P<0.05$) in patients with DN (Fig 2B) (Fig 3B). There were no significant differences in TGF-β mRNA levels between controls and patients with DN in both glomerular and whole kidney RNA (Fig 2C and 3C). There was a slight increase in TGF-β mRNA levels (1.3 fold) in whole kidney RNA from patients with DN compared to controls. This difference was not significant ($P= 0.103$).The levels for FN mRNA in patients with DN were 2.8 times increased in glomerular samples ($P<0.05$) (Fig 2D) and 1.9 times increased in whole cortex ($P<0.05$) (Fig 3D), compared to controls. FGF2 and syndecan whole cortex mRNA levels were not significantly different between diabetic patients and controls (Fig 3E and 3F).

(Immuno)histochemistry

Interstitial fibrosis was quantified by morphometric analysis on frozen sections stained with Sirius Red. There was a significant increase in the extent of Sirius Red staining in patients with

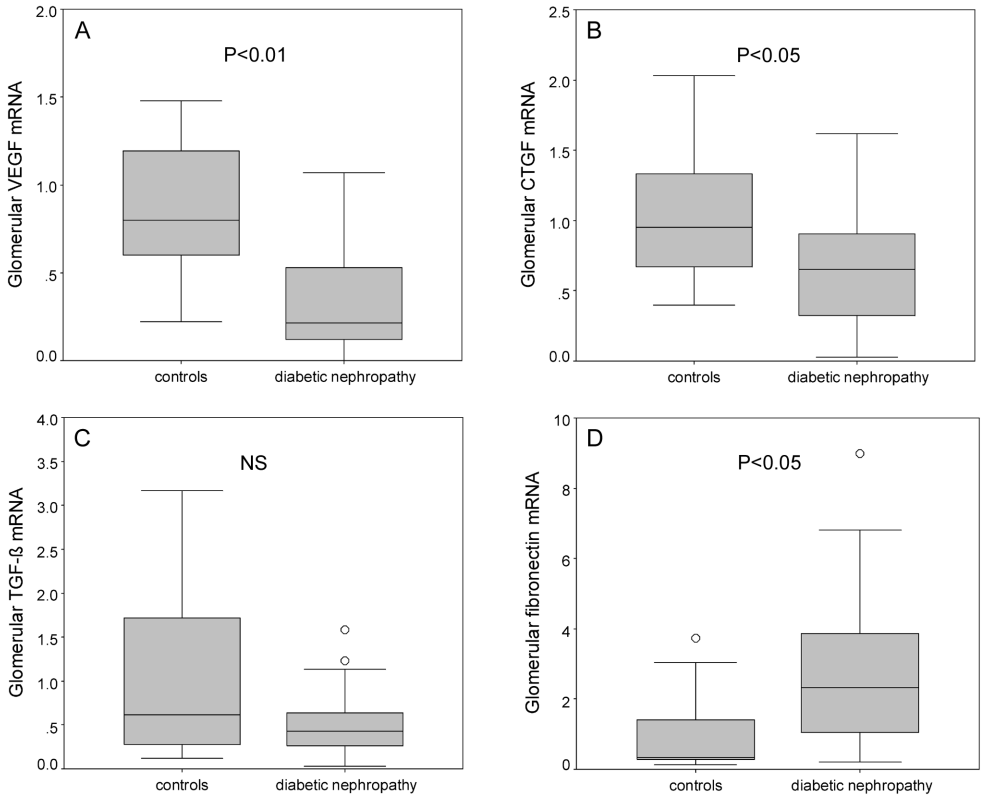

Figure 2. Box and whisker plots of glomerular mRNA levels. The boxes contain 50% of the values. The upper and lower border indicate the 25th and the 75th percentile. The upper and lower whisker indicate the highest and lowest value. The black line in the box indicates the median and open circles indicate outliers. Relative glomerular mRNA levels for VEGF (P<0.01) (A), CTGF (P<0.05) (B), TGF-β (not significant) (C), and fibronectin (P<0.05) (D).

DN compared to controls (33.3% versus 18.7%) (Fig 5 A). The numbers of CD31 positive cells are quantified by measuring the CD31 positive area. Both in the glomerular (Fig 5B) and tubulo-interstitial (Fig 5C) area of patients with DN there was a significant decrease in the extent of CD31 staining compared to controls (7.0% versus 22.6% for the glomeruli and 5.8% versus 9.9% in the tubulo-interstitial part), suggesting a reduction in the number of capillaries/ endothelial cells in DN. Representative pictures of these stainings can be found in Fig 4.

Correlations

To identify statistically significant relationships between variables, Pearson correlations were calculated between clinical, histological, and mRNA levels. Results of these correlations are summarized in Table 2. There was a positive correlation between glomerular VEGF and CTGF

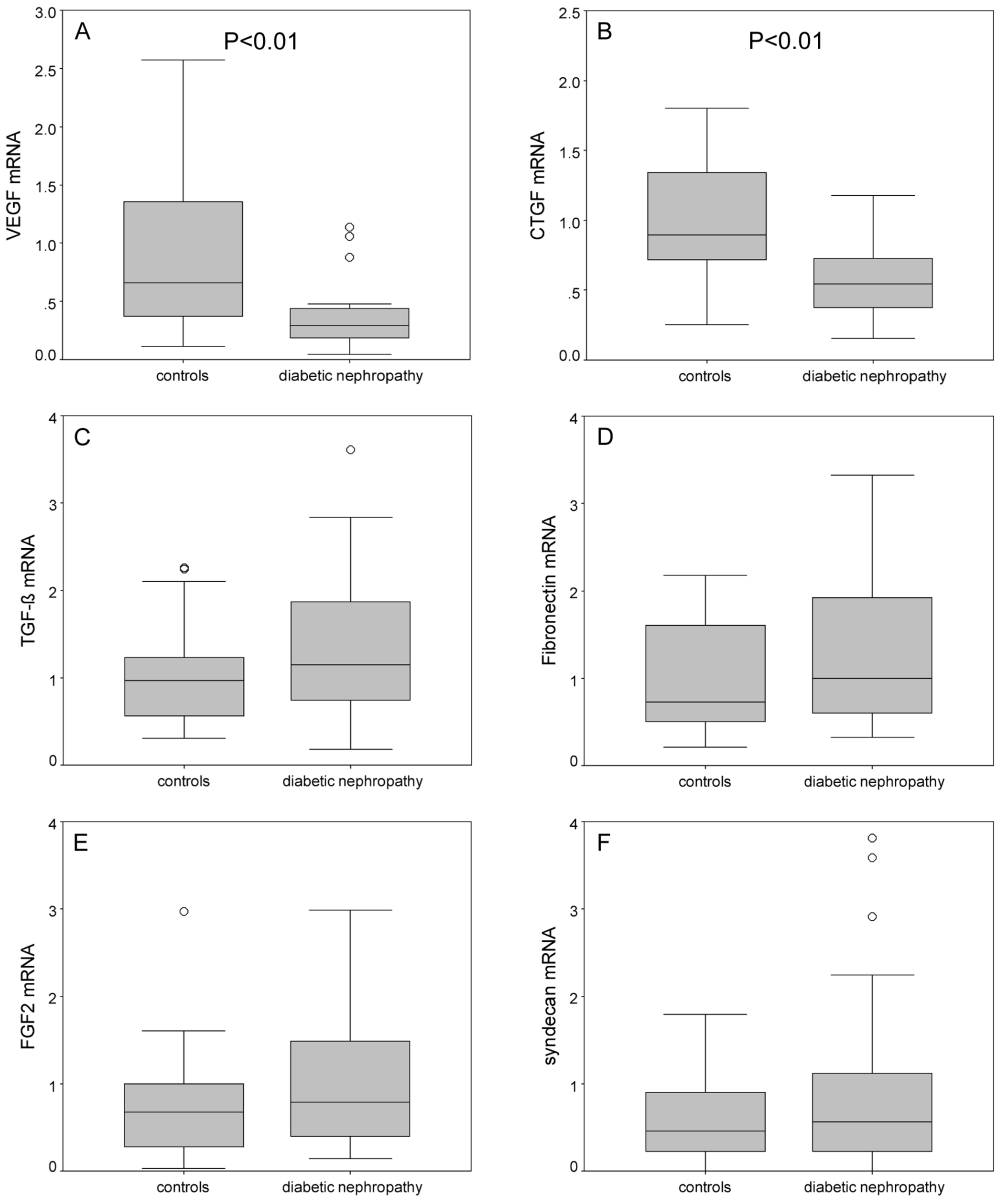

Figure 3. Box and whisker plots of whole cortex mRNA levels. Relative tubulo-interstitial mRNA levels for VEGF (P<0.01) (A), CTGF (P<0.01) (B), TGF-β (not significant) (C), fibronectin (P<0.05)(D), FGF2 (not significant)(E), and syndecan 1 (not significant) (F).

mRNA levels within the diabetic patients (R=0.61, P<0.01). A negative correlation was found for glomerular VEGF mRNA levels and Sirius Red positive area (R=-0.62, P<0.01). In other words,

Table 2. Pearson correlations.

					Interstitial mRNA level						Interstitial		Glomerular	Glomerular mRNA level			
			Serum creat.	Prot.	FGF2	VEGF	TGF-β	CTGF	FN	Syndecan	Sirius Red	CD31	CD31	VEGF	TGF-β	CTGF	FN
	Serum creat.	correlation (R)	1.000														
		P-value	.														
	Prot.	correlation (R)	0.462	1.000													
		P-value	0.030	.													
Interstitial	FGF2	correlation (R)	0.001	0.133	1.000												
mRNA		P-value	0.997	0.566	.												
level	VEGF	correlation (R)	-0.223	-0.259	0.017	1.000											
		P-value	0.274	0.245	0.926	.											
	TGF-β	correlation (R)	-0.062	0.313	0.568	-0.022	1.000										
		P-value	0.763	0.157	0.001*	0.904	.										
	CTGF	correlation (R)	0.007	0.443	0.400	0.095	0.518	1.000									
		P-value	0.974	0.044	0.020	0.598	0.002*	.									
	FN	correlation (R)	0.016	0.483	0.302	-0.033	0.447	0.342	1.000								
		P-value	0.936	0.023	0.099	0.857	0.010*	0.060	.								
	syndecan	correlation (R)	-0.137	-0.428	-0.221	0.089	-0.206	-0.127	-0.365	1.000							
		P-value	0.503	0.047	0.216	0.617	0.249	0.481	0.040	.							
Interstitial	Sirius Red	correlation (R)	0.191	0.287	0.208	-0.233	-0.001	0.022	-0.138	-0.381	1.000						
		P-value	0.383	0.234	0.319	0.251	0.995	0.916	0.510	0.055	.						
	CD31	correlation (R)	0.472	0.334	-0.334	0.201	-0.278	-0.223	0.247	0.172	-0.123	1.000					
		P-value	0.019	0.150	0.089	0.304	0.160	0.263	0.215	0.382	0.548	.					
Glomerular	CD31	correlation (R)	0.265	0.149	-0.309	0.531	-0.233	-0.044	0.149	0.296	-0.455	0.675	1.000				
		P-value	0.222	0.541	0.125	0.004*	0.252	0.831	0.467	0.133	0.019	0.000*	.				
Glomerular	VEGF	correlation (R)	-0.066	0.011	-0.462	0.328	-0.261	-0.135	-0.132	0.020	-0.618	-0.021	0.327	1.000			
mRNA		P-value	0.765	0.963	0.020	0.102	0.208	0.521	0.530	0.924	0.001*	0.923	0.119	.			
level	TGF-β	correlation (R)	-0.137	-0.173	0.084	-0.121	0.382	0.264	0.025	0.513	-0.105	-0.261	-0.291	-0.204	1.000		
		P-value	0.525	0.466	0.683	0.548	0.054	0.193	0.902	0.006*	0.616	0.207	0.158	0.317	.		
	CTGF	correlation (R)	-0.220	0.089	-0.147	0.196	0.045	0.263	-0.108	0.035	-0.255	-0.256	-0.134	0.611	0.158	1.000	
		P-value	0.301	0.709	0.474	0.328	0.829	0.194	0.599	0.864	0.219	0.217	0.522	0.001*	0.432	.	
	FN	correlation (R)	-0.229	0.189	0.046	-0.105	0.394	0.320	0.308	-0.072	-0.143	-0.128	-0.171	-0.037	0.385	0.291	1.000
		P-value	0.293	0.439	0.826	0.610	0.052	0.119	0.134	0.726	0.506	0.550	0.424	0.862	0.052	0.149	.

* P< 0.01

there was a relationship between the amount of interstitial fibrosis and the reduction of glomerular VEGF mRNA. Glomerular mRNA levels for VEGF also correlated with glomerular nephrin mRNA levels ($R=0.57$, $P<0.01$, data not shown). Whole cortex mRNA measurements showed correlations between TGF-β and CTGF ($R=0.52$, $P<0.01$), between TGF-β and FN ($R=0.45$, $P=0.01$), between TGF-β and FGF-2 ($R=0.57$, $P<0.01$), and between VEGF and glomerular CD31. When evaluating all samples together (controls and DN), a significant correlation was found between VEGF and the CD31 positive area both for the glomerular ($R=0.50$, $P<0.01$) and the tubulo-interstitial compartments ($R=0.42$, $P<0.01$) (data not shown).

Discussion

In the present study mRNA levels of genes involved in angiogenesis were studied in the renal cortex and in microdissected glomeruli in renal biopsies from patients with DN and healthy controls. We found downregulation of VEGF and CTGF. These levels were related to serum levels of creatinine, the degree of albuminuria, the degree of interstitial fibrosis, and the number of endothelial cells.

The genes measured in this study were identified using microarray analysis on glomerular and tubulo-interstitial mRNA from diabetes patients with DN and healthy controls. Many genes were differentially expressed (see: http://www-onderzoek.lumc.nl/pathology/kidney/diabeticnephropathy/). These lists of differentially expressed transcripts showed several genes that may play a role in endothelial cell maintenance and angiogenesis. To explore the implications of these gene expression alterations, a number of these genes were further investigated in a larger group of patients with different stages of disease, so that the roles of these growth factors in each phase of the disease could be further investigated.

VEGF is one of the most important angiogenic growth factors regulating vasculogenesis and permeability of endothelial cells. Our results show decreased VEGF mRNA levels in patients with DN. Quantification of VEGF mRNA levels in biopsies from patients with DN was shown for the first time by Bailey et al (21). Using *in situ* hybridization, they found a decrease in VEGF mRNA in glomeruli from patients with DN. These results were subsequently confirmed by others in both the interstitial (22) and the glomerular compartments (12). In addition, a correlation was found between glomerular VEGF levels and proteinuria. Results from different animal studies on the action of VEGF are contradictory. In streptozotocin (STZ)-induced diabetic rats, treatment with anti-VEGF antibodies decreased hyperfiltration, albuminuria, and glomerular hypertrophy (23). Tumstatin peptide, an inhibitor of angiogenesis, suppressed glomerular matrix expansion, the development of albuminuria, and renal mRNA expression of VEGF in STZ-induced diabetic mice (24). Other studies report that glomerular expression of VEGF is

(Figure has been printed in full-colour on page 112)

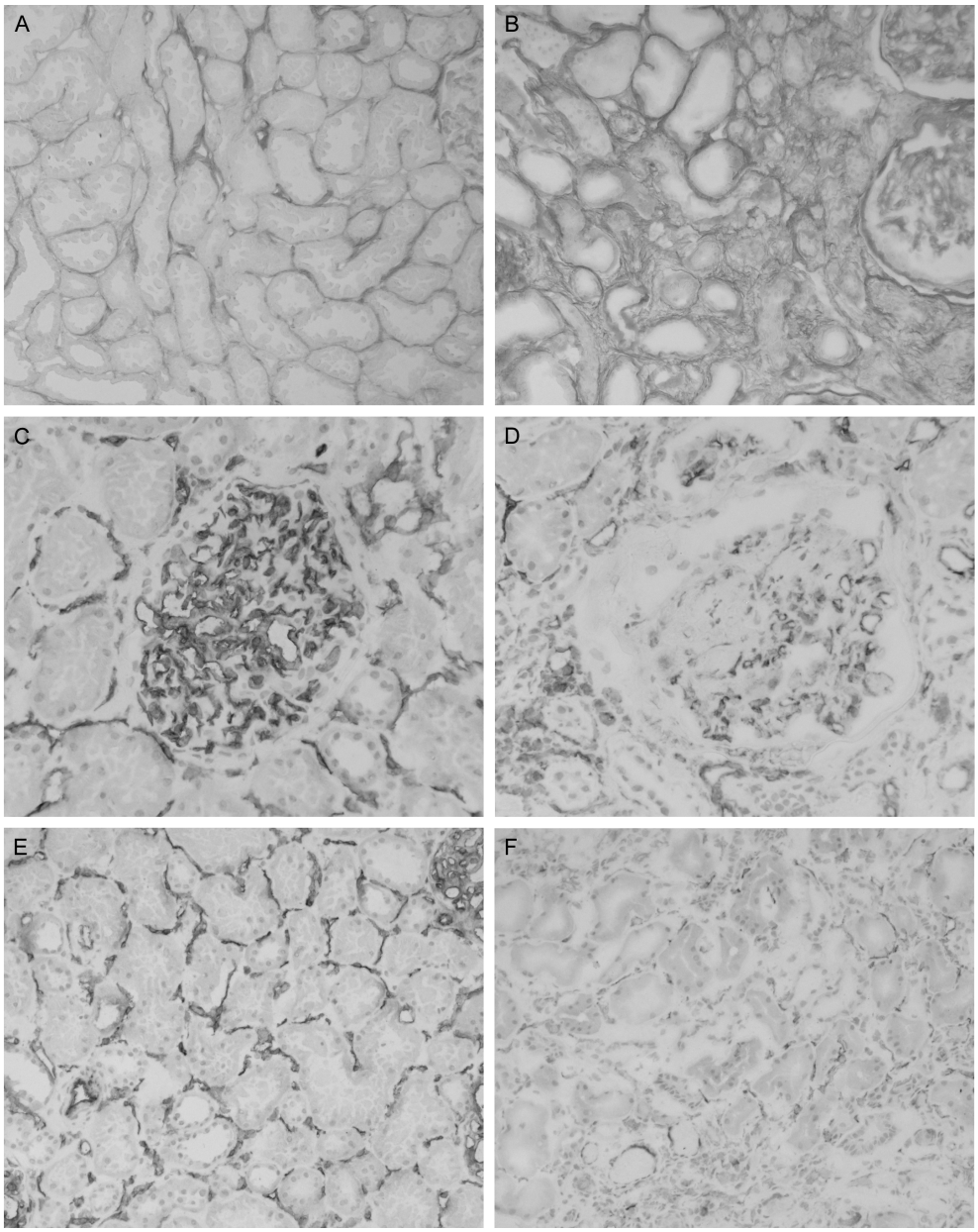

Figure 4. Sirius Red and CD31 staining in the biopsies**.** A and B are representative illustrations of the Sirius Red staining in a control patient and in a patient with DN, respectively. C-F are representative pictures of CD31 staining: glomerulus of a control patient (C), glomerulus of a patient with DN (D), the tubulo-interstitial part of a control patient (E) and the tubulo-interstitial part of a diabetic patient (F).

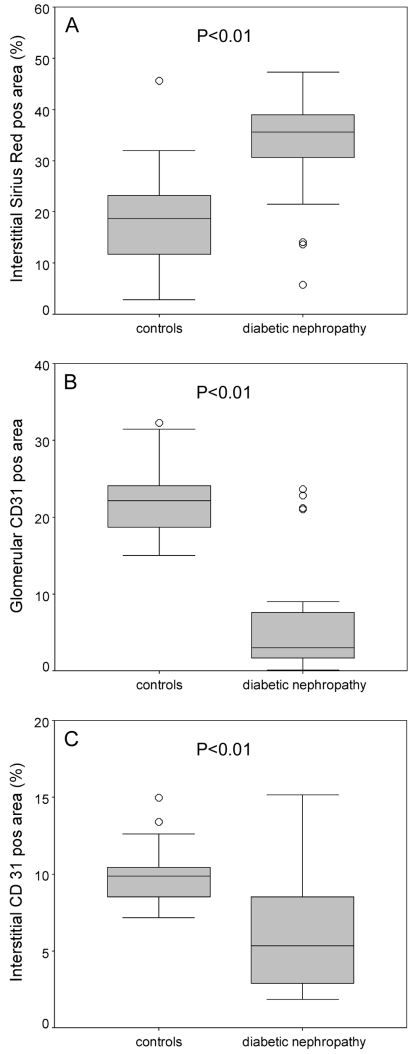

Figure 5. Box and whisker plots of Sirius Red and CD31 staining in the biopsies. (A) The extent of interstitial fibrosis measured as the percentage of the interstitial Sirius Red positive area in the renal cortex. Diabetic patients showed significantly more fibrosis than controls (P<0.01). (B) Percentage of glomerular CD31 staining. (C) Percentage of tubulo-interstitial CD31 staining. The percentage of CD31 positive area in both the glomerular and tubulo-interstitial compartments in patients with DN were significantly decreased compared to controls (P< 0.01).

reduced one week after STZ-induction. This reduction could be restored by treatment of the rats with insulin (10). Decreased VEGF expression was recently documented in the remnant kidney model, and treatment of these animals with VEGF reduces renal fibrosis (25). Studies in mice show that glomerular-selective depletion or overexpression of VEGF-A leads to glomerular abnormalities (26).

In our study CTGF mRNA expression levels were downregulated in both the glomerular and tubulo-interstitial regions. Our findings are in contrast with those from other studies. With suppression subtractive hybridization, the expression of CTGF was found to be increased in mesangial cells under high glucose conditions (27). Ito et al showed an increase in CTGF expression in human biopsies with different progressive renal diseases including DN (28). An increase of CTGF mRNA has also been found in glomeruli from patients with type 1 diabetes (29). However, these data represented the number of mRNA molecules per glomerulus while our data represents relative steady state mRNA levels corrected for three different housekeeping genes. In our studies we did not find increased expression of TGF-β in DN, although in the tubulo-interstitial mRNA samples there was a slight but non-significant increase in TGF-β mRNA levels. This small increase is in line with studies on human glomeruli in which a small increase in TGF-β expression has also been found (30,31), while a key role for TGF-β has been described in animal models of DN (7).

Fibronectin, one of the major extracellular matrix proteins present in glomerulosclerotic and interstitial fibrotic lesions, showed an increase in patients with DN. Although there was no significant increase for TGF-β, a correlation was found between interstitial

TGF-β and FN mRNA within the diabetic patient group. Similarly, interstitial CTGF and TGF-β mRNA showed a significant correlation with each other. This observation corresponds with previous studies that indicate that CTGF might act as a downstream mediator of TGF-β bioactivity (32). The observation that expression of FN is upregulated in DN, while the expression of TGF-β and that of CTGF are not may be explained by studies demonstrating that high glucose can induce FN independent of TGF-β1(33) and CTGF (34).

mRNA levels measured in our study correspond in broad lines with those described in the literature, especially with what has been reported in humans. The discrepancies between the expression levels reported in animal models and those in our study can be explained by several factors. Firstly, it should be noted that animal models do not completely mimic the physiological state of patients with diabetes, and it is likely that mechanisms for initiation and progression of DN in animals differ from those seen in humans (35). Another reason for the differences between our findings and those reported in the literature may be that the stage of the diseases studied is different. Animal models are often studied in an early phase of the disease while most of our patients were already in a moderate to severe stage of the disease. In patient studies, it is often difficult to receive biopsy material at an early stage of disease, as patients do not normally present to a nephrologist until the disease has become manifest.

To obtain more insight into the role of the studied molecules during the progression of DN, we quantified the amount of interstitial fibrosis in the biopsies with Sirius Red. Because we know that histological grading of tubulo-interstitial fibrosis is closely correlated with the loss of renal function (36), quantitative measurements of the Sirius Red staining were used as a morphological marker for renal function. We found a significant increase in the amount of Sirius Red staining in patients with DN compared to controls. The observation that VEGF mRNA levels negatively correlated with the amount of Sirius Red staining support the concept that loss of VEGF is related to progression of the disease. This was already suggested by Bortoloso et al (12) who found a negative correlation between VEGF and urinary protein excretion. There was a positive correlation between glomerular mRNA levels of CTGF and VEGF. This suggests that CTGF, normally present in the podocyte, in combination with other angiogenic factors, may contribute to the normal maintenance of glomerular endothelial cells.

We have also examined whether there is a correlation between the reduced mRNA levels of angiogenic factors and the number of endothelial cells. The extent of CD31 staining, a marker for endothelial cells, was quantified. Both the glomeruli and whole cortex showed a significant decrease in the CD31 positive area in DN indicating a reduction in the number of endothelial cells. This reduction correlated with the reduced VEGF mRNA levels, indicating an association between the number of endothelial cells and the angiogenic growth factor VEGF.

The question remains as to the precise mechanism accounting for the down-regulation of

VEGF and CTGF mRNA in DN. One explanation may be that specific down regulation occurs in a diabetic milieu. This is unlikely since cell culture experiments have shown that glucose, insulin, and advanced glycated end products (AGEs) increase levels of VEGF and CTGF (37-40) . It is more likely that the decrease in expression of angiogenic factors, normally produced by podocytes, results from podocyte loss. The number of podocytes decreases over the course of DN (41,42). Decreased expression in patients with DN of several podocyte specific genes such as nephrin, Wilms tumour 1 (WT1), and GLEPP1, in our glomerular gene profile supports this hypothesis.

From the results of this study we speculate that loss of angiogenic factors contributes to the progression of DN. Podocyte injury in response to diabetes leads to loss of the slit diaphragms and proteinuria. The resulting podocyte loss then leads to a reduction in expression of angiogenic factors, which are necessary for the normal maintenance of the endothelial cells. The reduced endothelial cell maintenance in combination with endothelial cell dysfunction leads to a loss of endothelial cells followed by a loss of glomerular capillaries. This hypothesis is corroborated by the finding that patients with POEMS (Crow-Fukase) syndrome, who have elevated plasma VEGF levels, in combination with Type 2 diabetes do not develop DN (43). The role of VEGF in the maintenance of endothelial cells is also supported by the finding that soluble Flt1 (fms-like tyrosine kinase 1), a splice variant of the major VEGF receptor Flt1, can induce proteinuria in preeclampsia (44). Soluble Flt1 acts as a strong antagonist of VEGF. Increased levels of circulating sFlt1 are associated with decreased circulating levels of VEGF, and administration of soluble Flt1 to pregnant rats results in proteinuria and glomerular endotheliosis (44). Loss of endothelial cells can lead to thrombotic microangiopathy followed by loss of capillaries. Development of the latter has been shown by fragmented red blood cells, and PAI-1, a marker for progression of thrombosis to sclerosis, in glomeruli from diabetic patients with severe nodular lesions (45).

For the observed tubulo-interstitial down regulation of VEGF, we found supporting evidence in the hypothesis of Kang et al (13) that reduction of peritubular capillaries results in impaired delivery of oxygen and nutrients to the tubules and interstitial cells leading to ischemia, cytokine-induced proliferation of fibroblasts, and ECM synthesis. Loss of peritubular capillaries in interstitial fibrosis has been observed in human renal diseases (46) and in several models of interstitial fibrosis.

In conclusion, this study demonstrates a reduction in mRNA levels of angiogenic factors in glomerular and whole kidney mRNA samples from renal biopsies of patients suffering from type 2 diabetes induced DN. Reduction of these factors correlated with the extent of interstitial fibrosis. We also found a reduction of glomerular and interstitial endothelial cells measured with CD31 staining in DN. These results may suggest an important role for angiogenic factors

in the maintenance of endothelial cells. Reduced expression of angiogenic factors may be involved in the progression of DN.

References

1. Andersen AR, Christiansen JS, Andersen JK, Kreiner S, Deckert T: Diabetic nephropathy in Type 1 (insulin-dependent) diabetes: an epidemiological study. *Diabetologia* 25:496-501, 1983
2. US Renal Data System. *USRDS 2001 Annual Data Report*. National Institutes of Health, National Institute of Diabetes and Digestive and Kidney Diseases, Bethesda, MD. 2001.
3. Mogensen CE, Chachati A, Christensen CK, Close CF, Deckert T, Hommel E, Kastrup J, Lefebvre P, Mathiesen ER, Feldt-Rasmussen B: Microalbuminuria: an early marker of renal involvement in diabetes. *Uremia Invest* 9:85-95, 1985
4. Vleming LJ, Baelde JJ, Westendorp RG, Daha MR, van Es LA, Bruijn JA: The glomerular deposition of PAS positive material correlates with renal function in human kidney diseases. *Clin Nephrol* 47:158-167, 1997
5. Ziyadeh FN: The extracellular matrix in diabetic nephropathy. *Am J Kidney Dis* 22:736-744, 1993
6. Adler S: Structure-function relationships associated with extracellular matrix alterations in diabetic glomerulopathy. *J Am Soc Nephrol* 5:1165-1172, 1994
7. Chen S, Hong SW, Iglesias-De La Cruz MC, Isono M, Casaretto A, Ziyadeh FN: The key role of the transforming growth factor-beta system in the pathogenesis of diabetic nephropathy. *Ren Fail* 23:471-481, 2001
8. Amin RH, Frank RN, Kennedy A, Eliott D, Puklin JE, Abrams GW: Vascular endothelial growth factor is present in glial cells of the retina and optic nerve of human subjects with nonproliferative diabetic retinopathy. *Invest Ophthalmol Vis Sci* 38:36-47, 1997
9. Vriese ASD, Tilton RG, Elger MARL, Stephan CC, Kriz WILH, Lameire NH: Antibodies against Vascular Endothelial Growth Factor Improve Early Renal Dysfunction in Experimental Diabetes. *J Am Soc Nephrol* 12:993-1000, 2001
10. Singh AK, Gudehithlu KP, Pegoraro AA, Singh GK, Basheerudin K, Robey RB, Arruda JA, Dunea G: Vascular factors altered in glucose-treated mesangial cells and diabetic glomeruli. Changes in vascular factors impair endothelial cell growth and matrix. *Lab Invest* 84:597-606, 2004
11. Baelde HJ, Eikmans M, Doran PP, Lappin DWP, De Heer E, Bruijn JA: Gene expression profiling in glomeruli from human kidneys with diabetic nephropathy. *Am J Kidney Dis* 43:636-650, 2004
12. Bortoloso E, Del Prete D, Dalla VM, Gambaro G, Saller A, Antonucci F, Baggio B, Anglani F, Fioretto P: Quantitave and qualitative changes in vascular endothelial growth factor gene expression in glomeruli of patients with type 2 diabetes. *Eur J Endocrinol* 150:799-807, 2004
13. Kang DH, Johnson RJ: Vascular endothelial growth factor: a new player in the pathogenesis of renal fibrosis. *Curr Opin Nephrol Hypertens* 12:43-49, 2003
14. Chang LK, Garcia-Cardena G, Farnebo F, Fannon M, Chen EJ, Butterfield C, Moses MA, Mulligan RC, Folkman J, Kaipainen A: Dose-dependent response of FGF-2 for lymphangiogenesis. *Proc Natl Acad Sci U S A* 101:11658-11663, 2004
15. Salmivirta M, Heino J, Jalkanen M: Basic fibroblast growth factor-syndecan complex at cell surface or immobilized to matrix promotes cell growth. *J Biol Chem* 267:17606-17610, 1992
16. Specht K, Richter T, Muller U, Walch A, Werner M, Hofler H: Quantitative gene expression analysis in microdissected archival formalin-fixed and paraffin-embedded tumor tissue. *Am J Pathol* 158:419-429, 2001
17. Heid CA, Stevens J, Livak KJ, Williams PM: Real time quantitative PCR. *Genome Res* 6:986-994, 1996
18. Eikmans M, Baelde HJ, De Heer E, Bruijn JA: Effect of age and biopsy site on extracellular matrix mRNA and protein levels in human kidney biopsies. *Kidney Int* 60:974-981, 2001
19. Vandesompele J, De Preter K, Pattyn F, Poppe B, Van Roy N, De Paepe A, Speleman F: Accurate normalization of real-time quantitative RT-PCR data by geometric averaging of multiple internal control genes. *Genome Biol* 3:34, 2002
20. Koop K, Eikmans M, Baelde HJ, Kawachi H, De Heer E, Paul LC, Bruijn JA: Expression of podocyte-associated molecules in acquired human kidney diseases. *J Am Soc Nephrol* 14:2063-2071, 2003
21. Bailey E, Bottomley MJ, Westwell S, Pringle JH, Furness PN, Feehally J, Brenchley PE, Harper SJ: Vascular endothelial growth factor mRNA expression in minimal change, membranous, and diabetic nephropathy demonstrated by non-isotopic in situ hybridisation. *J Clin Pathol* 52:735-738, 1999
22. Bortoloso E, Del Prete D, Gambaro G, Dalla VM, Sailer A, Baggio B, Antonucci F, Fioretto P, Anglani F: Vascular endothelial growth factor (VEGF) and VEGF receptors in diabetic nephropathy: expression

studies in biopsies of type 2 diabetic patients. *Ren Fail* 23:483-493, 2001
23. de Vriese AS, Tilton RG, Elger M, Stephan CC, Kriz W, Lameire NH: Antibodies against vascular endothelial growth factor improve early renal dysfunction in experimental diabetes. *J Am Soc Nephrol* 12:993-1000, 2001
24. Yamamoto Y, Maeshima Y, Kitayama H, Kitamura S, Takazawa Y, Sugiyama H, Yamasaki Y, Makino H: Tumstatin peptide, an inhibitor of angiogenesis, prevents glomerular hypertrophy in the early stage of diabetic nephropathy. *Diabetes* 53:1831-1840, 2004
25. Kang DH, Hughes J, Mazzali M, Schreiner GF, Johnson RJ: Impaired angiogenesis in the remnant kidney model: II. Vascular endothelial growth factor administration reduces renal fibrosis and stabilizes renal function. *J Am Soc Nephrol* 12:1448-1457, 2001
26. Eremina V, Sood M, Haigh J, Nagy A, Lajoie G, Ferrara N, Gerber HP, Kikkawa Y, Miner JH, Quaggin SE: Glomerular-specific alterations of VEGF-A expression lead to distinct congenital and acquired renal diseases. *J Clin Invest* 111:707-716, 2003
27. Murphy M, Godson C, Cannon S, Kato S, Mackenzie HS, Martin F, Brady HR: Suppression subtractive hybridization identifies high glucose levels as a stimulus for expression of connective tissue growth factor and other genes in human mesangial cells. *J Biol Chem* 274:5830-5834, 1999
28. Ito Y, Aten J, Bende RJ, Oemar BS, Rabelink TJ, Weening JJ, Goldschmeding R: Expression of connective tissue growth factor in human renal fibrosis. *Kidney Int* 53:853-861, 1998
29. Adler SG, Kang SW, Feld S, Cha DR, Barba L, Striker L, Striker G, Riser BL, Lapage J, Nast CC: Glomerular mRNAs in human type 1 diabetes: biochemical evidence for microalbuminuria as a manifestation of diabetic nephropathy. *Kidney Int* 60:2330-2336, 2001
30. Iwano M, Kubo A, Nishino T, Sato H, Nishioka H, Akai Y, Kurioka H, Fujii Y, Kanauchi M, Shiiki H, Dohi K: Quantification of glomerular TGF-beta 1 mRNA in patients with diabetes mellitus. *Kidney Int* 49:1120-1126, 1996
31. Yamamoto T, Noble NA, Cohen AH, Nast CC, Hishida A, Gold LI, Border WA: Expression of transforming growth factor-beta isoforms in human glomerular diseases. *Kidney Int* 49:461-469, 1996
32. Leask A, Holmes A, Black CM, Abraham DJ: Connective tissue growth factor gene regulation. Requirements for its induction by transforming growth factor-beta 2 in fibroblasts. *J Biol Chem* 278:13008-13015, 2003
33. Lam S, Verhagen NA, Strutz F, Van Der Pijl JW, Daha MR, Van Kooten C: Glucose-induced fibronectin and collagen type III expression in renal fibroblasts can occur independent of TGF-beta1. *Kidney Int* 63:878-888, 2003
34. Wahab NA, Yevdokimova N, Weston BS, Roberts T, Li XJ, Brinkman H, Mason RM: Role of connective tissue growth factor in the pathogenesis of diabetic nephropathy. *Biochem J* 359:77-87, 2001
35. Roep BO, Atkinson M, von Herrath M: Satisfaction (not) guaranteed: re-evaluating the use of animal models of type 1 diabetes. *Nat Rev Immunol* 4:989-997, 2004
36. Nath KA: Tubulointerstitial changes as a major determinant in the progression of renal damage. *Am J Kidney Dis* 20:1-17, 1992
37. Lam S, van der Geest RN, Verhagen NA, van Nieuwenhoven FA, Blom IE, Aten J, Goldschmeding R, Daha MR, Van Kooten C: Connective tissue growth factor and igf-I are produced by human renal fibroblasts and cooperate in the induction of collagen production by high glucose. *Diabetes* 52:2975-2983, 2003
38. Iglesias-de la Cruz MC, Ziyadeh FN, Isono M, Kouahou M, Han DC, Kalluri R, Mundel P, Chen S: Effects of high glucose and TGF-beta1 on the expression of collagen IV and vascular endothelial growth factor in mouse podocytes. *Kidney Int* 62:901-913, 2002
39. Paradis V, Perlemuter G, Bonvoust F, Dargere D, Parfait B, Vidaud M, Conti M, Huet S, Ba N, Buffet C, Bedossa P: High glucose and hyperinsulinemia stimulate connective tissue growth factor expression: a potential mechanism involved in progression to fibrosis in nonalcoholic steatohepatitis. *Hepatology* 34:738-744, 2001
40. Wahab NA, Yevdokimova N, Weston BS, Roberts T, Li XJ, Brinkman H, Mason RM: Role of connective tissue growth factor in the pathogenesis of diabetic nephropathy. *Biochem J* 359:77-87, 2001
41. Pagtalunan ME, Miller PL, Jumping-Eagle S, Nelson RG, Myers BD, Rennke HG, Coplon NS, Sun L, Meyer TW: Podocyte loss and progressive glomerular injury in type II diabetes. *J Clin Invest* 99:342-348, 1997
42. Dalla VM, Masiero A, Roiter AM, Saller A, Crepaldi G, Fioretto P: Is podocyte injury relevant in diabetic nephropathy? Studies in patients with type 2 diabetes. *Diabetes* 52:1031-1035, 2003

43. Baba T, Osterby R, Neugebauer-Baba S, Nozawa Y, Watanabe T, Sakurai K, Katoh T, Watanabe T: No nephropathy in Type 2 diabetic patient with POEMS syndrome with an elevated plasma VEGF. *Diabet Med* 21:292-294, 2004
44. Maynard SE, Min JY, Merchan J, Lim KH, Li J, Mondal S, Libermann TA, Morgan JP, Sellke FW, Stillman IE, Epstein FH, Sukhatme VP, Karumanchi SA: Excess placental soluble fms-like tyrosine kinase 1 (sFlt1) may contribute to endothelial dysfunction, hypertension, and proteinuria in preeclampsia. *J Clin Invest* 111:649-658, 2003
45. Paueksakon P, Revelo MP, Ma LJ, Marcantoni C, Fogo AB: Microangiopathic injury and augmented PAI-1 in human diabetic nephropathy. *Kidney Int* 61:2142-2148, 2002
46. Bohle A, Mackensen-Haen S, Wehrmann M: Significance of postglomerular capillaries in the pathogenesis of chronic renal failure. *Kidney Blood Press Res* 19:191-195, 1996

Chapter 8

Summary and General Discussion

Summary and general discussion

Molecular biology offers new opportunities for experimental and clinical medicine. Promising clinical applications for patient care include identification of mRNA expression patterns (gene profiling) in diseased organs in correlation with diagnosis, prognosis, and responsiveness to different treatments. The development of novel technologies, such as microarray analysis and real-time PCR, allows study of gene expression networks, even in small renal biopsies. These technologies, in combination with the development of laser capture microdissection, enables specific gene expression analysis in a specific nephron segment.

Chapter 2 describes a method to isolate RNA from purified glomeruli. Because the size of mouse glomeruli is similar to that of mouse tubules, mouse glomeruli cannot be isolated using relatively simple sieving techniques. The development of a purification method for mouse glomeruli is mandatory for extraction of mouse glomerular RNA (1-3). One of the major problems with RNA isolation is that mRNAs are very sensitive to degradation by endonucleases and exonucleases. In normal living eukaryotic cells, several pathways have been identified that play a role in mRNA degradation. One of these involves the exosome, a multi-protein complex that degrades transcripts in the 3' to 5' direction and that contains nucleases related to the enzymes of the bacterial degradosome (4). Another mechanism is de-adenylation–dependent decapping. This decapping is triggered by removal of the poly(A) tail by exonucleases, followed by cleavage of the 5' cap by decapping enzymes. After decapping, which normally prevents the mRNA from being translated, the mRNA undergoes rapid exonuclease digestion starting at the 5' end. Normally, mRNA degradation is strictly regulated by this multi-protein complex. However, after cell death, endonucleases such as RNase E and RNase III, which make internal cuts in RNA molecules, and RNase II, which is an exonuclease that removes nucleotides in the 3' to 5' direction are released from their regulatory complexes and rapidly degrade mRNA. In this study, we tested the feasibility of using a novel glomerular isolation method in combination with RNA extraction. To optimize this procedure, the necessity of using RNase inhibitors was investigated in combination with different RNA isolation methods. We found that including RNase inhibitors was not necessary for obtaining intact mRNA, despite the fact that the whole procedure takes 2 to 3 hours. We conclude that the cells survive the isolation method and thus, the RNA is protected against degradation. Indeed, in another study we demonstrated that it is possible to culture viable mesangial cells from isolated mouse glomeruli (5). From the RNA extraction methods we have tested, the yield of the lithium chloride (LiCl)/phenol/chloroform method was about two to three times higher than the cesium chloride (CsCl) method (6). Based on the levels of intact 28S and the 18S ribosomal RNA bands after gel electrophoresis and signal intensity after hybridization with a collagen α1(IV) cDNA probe, the LiCl/phenol/chloroform

method gives the best RNA quality and quantity. For several years, kits based on phenol/chloroform extraction without the use of LiCl have been available (e.g., Trizol®, Invitrogen). More recently, silica-gel spin columns were developed [e.g., RNeasy Mini columns (QIAGEN GmbH, Germany)], which can be used in combination with the stringency of guanidine-isothiocyanate lysis. We successfully used these kits with glomerular samples.

Chapter 3 describes the distribution of alternatively spliced fibronectin isoforms in human renal disease with developing glomerulosclerosis. From animal studies it is known that fibronectin is one of the major components of sclerotic lesions in the kidney (7). Furthermore, it was found that the extent of glomerular fibronectin deposition correlated with the severity of glomerular structural abnormalities in human renal diseases (8). The EDA exon in the fibronectin molecule was found more often in skin wound healing compared to normal skin (9). In Chapter 3 we describe our immunohistochemical investigations into the distribution of the various fibronectin isoforms in glomerulosclerotic lesions and in regions of tubulointerstitial fibrosis in several progressive human renal diseases. In areas of glomerulosclerosis and interstitial fibrosis, we found increased deposition of total fibronectin. EDA- and EDB-positive fibronectin isoforms were found in significantly increased amounts in glomerulosclerotic lesions compared to normal glomeruli. In areas with interstitial fibrosis, an increase in the amount of EDA-positive fibronectin was found, but no EDB-positive fibronectin was deposited in the fibrotic interstitium. These results show that in renal disease, oncofetal fibronectin (FDC6) and EDA- and EDB-containing fibronectin isoforms are upregulated at specific locations within the renal tissue, suggesting a specific pathogenic role for these fibronectin isoforms during disease development. There were no statistically significant differences in the expression of the various fibronectin isoforms among any of the patient groups. This finding suggests that excessive fibronectin accumulation is a final common phenomenon in the development of glomerulosclerosis and interstitial fibrosis.

Chapter 4 describes a study of alternatively spliced isoforms of fibronectin at the mRNA level in different animal models for immune-mediated glomerulosclerosis, and in human biopsies from patients developing glomerulosclerosis. Using cultured mesangial cells, we studied the effect of TGF-β and IL-4 on the splicing of fibronectin in the EDA and EDB regions. Using primers flanking the EDA or EDB regions, we performed RT-PCR on glomerular mRNA isolated from different animal models at several time points after induction of the disease, and on mRNA from renal biopsies from patients suffering from different glomerulopathies. Normal mice and rats did not express the oncofetal domains EDA and EDB. Induction of α-GBM nephritis, chronic serum sickness, or anti-Thy-1 nephritis resulted in inclusion of both the EDA and EDB domains in the fibronectin mRNA. However, induction of GvHD in mice had no effect on the splicing pattern of fibronectin mRNA. Culturing of glomerular mesangial cells in the presence of TGF-β led to inclusion of the EDA region, while IL-4–overexpressing mesangial cells showed

a significant decrease in EDA^+ fibronectin mRNA levels. This decrease may have resulted from reduced TGF-β levels in the IL-4–overexpressing cells. A relation between the presence of TGF-β mRNA and EDA^+ mRNA was also found in the animal models for glomerulonephritis and in patients developing glomerulosclerosis. This finding suggests that TGF-β plays a role in the induction of EDA^+ fibronectin in the kidney and thus in the development of glomerulosclerosis. On the other hand, GVH-diseased animals develop glomerulosclerosis containing large amounts of fibronectin without demonstrable increase of TGF-β or EDA inclusion. In an earlier study we have shown that in these mice, the accumulation of fibronectin is a result of specific trapping of plasma fibronectin from the circulation (7). In addition, mice with constitutive transgenic expression of IL-4 show progressive glomerulosclerosis with mesangial accumulation of collagen types I, IV, and V in the absence of TGF-β1 upregulation. Although TGF-β and alternative splicing of fibronectin play a role in the progression to glomerulosclerosis, neither alternative fibronectin splicing nor high transcription levels of TFG-β appears to be a general prerequisite for the development of glomerulosclerosis.

In **Chapter 5**, trapping of plasma fibronectin from the circulation during development was investigated. Earlier studies have shown that plasma fibronectin can accumulate from the circulation in sclerotic lesions. To obtain more insight into the molecular binding sites that play a role in the accumulation of fibronectin in pre-sclerotic lesions, fibronectin was cut into different fragments. The different fragments were separated on a heparin affinity column, resulting in two batches of fragments with either low or high affinity for heparin. The fragments were labeled with fluorescein isothiocyanate (FITC) and injected into chronic GVH mice developing glomerulosclerosis. These fragments were also pre-incubated with heparin or N-desulfated non-anticoagulant heparin to investigate the role of the heparin binding site in the accumulation of fibronectin in sclerotic lesions. Whole, labelled plasma fibronectin (pFN) molecules were injected intravenously into mice 10 to 12 weeks after induction of GVH disease in mice and accumulated in the glomerulosclerotic lesions. The pattern of trapped fibronectin was comparable to that seen in PAS-positive glomerulosclerotic lesions. *Ex vivo* pre-incubation of pFN-FITC with heparin resulted in a reduced accumulation of pFN-FITC upon injection. Injection of pFN pre-incubated with non-anticoagulant, N-desulfated heparin also prevented the accumulation of pFN-FITC in the glomerular lesions. There was no difference between the accumulation of pFN-FITC pre-treated with heparin or non-anticoagulant heparin. Intravenous injection of the digested FITC-conjugated pFN fragments with low affinity for heparin resulted in accumulation in sclerotic glomeruli. This accumulation did not occur when the low-affinity fraction was injected in control mice. The FITC-conjugated pFN fragments with high affinity for heparin did not accumulate in glomeruli of GvHD mice. From these results, we conclude that the protective effect of heparin treatment may be the result of steric interference with the

specific binding sites, and not specifically because of blockade of the heparin binding site itself. Fibronectin can directly bind to ECM via its collagen binding sites. Secondly, fibronectin contains integrin binding sites for $\alpha 5\beta 1$ integrin that were increased in areas surrounding the glomerulosclerotic lesions. A third mechanism that may be involved in the accumulation of pFN in the glomerulus is activation of the coagulation system. However, based on the observation that both heparin or non-anticoagulant heparin can inhibit fibronectin accumulation, it is unlikely that this mechanism plays a role in the accumulation of fibronectin.

Chapter 6 shows the results of gene expression profiling of glomeruli from human kidneys with DN. DN is a major cause of morbidity in patients with type II diabetes (10). Although several factors, including high glucose, insulin, AGEs, and high blood pressure, may be involved in the progression of DN, the precise mechanism is still unclear. Therefore, we investigated the gene expression profile of glomerular RNA isolated from morphologically and functionally normal kidneys and from kidneys of patients with DN. About 100 genes were upregulated in the diabetic glomeruli, and about 500 genes were downregulated. One of the downregulated genes was VEGF, which is one of the most important factors in endothelial repair and angiogenesis. Considerable research has focused on the pathogenesis of endothelial dysfunction in patients with diabetes, but the exact role for VEGF during the development of DN has remained unclear until now.

In **Chapter 7**, we investigated expression of angiogenic factors identified by microarray analysis of kidneys from patients with DN or with normal kidneys. Endothelial cell loss and the role of VEGF in that loss determine development of renal disease and the progression to sclerosis. In human DN it has been suggested that VEGF is important in maintaining the glomerular endothelial cells and that a decrease in local VEGF levels accounts for abnormal remodeling of the glomerular capillaries (11,12). On microarray analysis, factors including CTGF, FGF2, and syndecan, which can induce new vessel formation (13,14), showed a decrease in patients with DN. We investigated the gene expression level of different angiogenic factors in renal biopsies from a larger patient group with DN. We found that VEGF and CTGF mRNA levels in both microdissected glomeruli and whole cortex were decreased in patients with DN compared to control kidneys. A negative correlation was found between glomerular VEGF mRNA and the extent of interstitial fibrosis. In other words, there is a relationship between progression of the disease and the reduction of glomerular VEGF mRNA. We also found a decreased number of endothelial cells both in glomerular and the tubulointerstitial tissue of patients with DN. From the results of this study, we speculate that loss of angiogenic factors contributes to the progression of DN. Podocyte injury resulting from the action of diabetic factors leads to loss of slit diaphragms and proteinuria. The resulting podocyte loss then leads to a reduction in expression of angiogenic factors, which are necessary for the normal

maintenance of the endothelial cells. The reduced endothelial cell maintenance in combination with endothelial cell dysfunction leads to a loss of endothelial cells followed by a loss of glomerular capillaries (Fig. 1).

On the other hand, it has been shown that urinary VEGF levels in patients with DN are increased. Although measurements of urine VEGF levels seem to be controversial in the literature, it has recently been demonstrated in a large patient group that urinary VEGF levels were increased and that this strongly correlated with 24-hour albumin excretion levels (15). In the same patients, plasma VEGF levels remained unchanged compared to a control group. The increase of urinary VEGF levels can be a result of VEGF synthesis in the kidney. The glomerular podocyte is the major site for renal VEGF synthesis, suggesting that the increased urinary VEGF excretion may be of glomerular origin. VEGF protein has also been found in proximal tubules of patients with late DN (16), suggesting that VEGF originating from renal tubules can also contribute to high levels of urinary VEGF. Based on our results and results from the literature, which show that both glomerular and tubularinterstitial VEGF mRNA levels decrease in DN (12,17), it is unlikely that the increased urinary VEGF levels result from increased VEGF production in the kidney. Because plasma VEGF levels remain unchanged in patients with DN, the explanations for higher urinary VEGF levels in patients with DN would be increased leakage of VEGF through the glomerular filtration barrier or a diminished absorption by proximal tubular

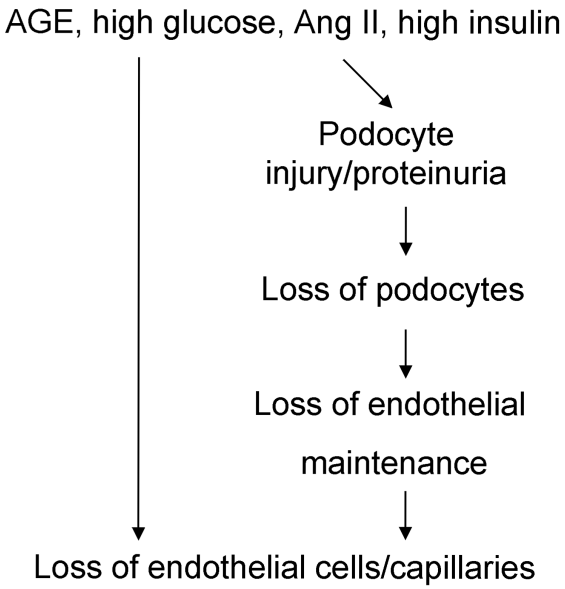

Figure 1. Partly speculative schematic illustration of endothelial cell/glomerular capillary loss in patients with diabetic nephropathy.

epithelial cells. This increased leakage of VEGF through the filtration barrier may also explain the correlation found between urinary VEGF levels and urinary albumin excretion in patients with DN. The activity of VEGF is highly regulated by sFlt-1, a naturally occurring soluble form of VEGF receptor. More studies are necessary to define the exact role of VEGF, together with sFlt-1 and other angiogenic factors, in the development and progression of DN

Further perspectives of gene expression profiling in renal diseases

With microarray technology, thousands of genes can be measured within one experiment, resulting in an expression profile of a biological sample. This information can be used for functional categorization of renal disease and may help in improving treatment of patients. Bioinformatics can also be used as a tool, leading to a better understanding of the molecular mechanisms that play a role in the progression of disease. With the interconnection of databases (e.g., NCBI, EMBL) containing information about gene sequences, chromosome locations, SNPs, gene ontology, and gene expression levels in different tissues and diseases, important information comes together and can be studied more easily. Also, programs such as Pathfinder® and the KEGG database are helpful tools to use in recognizing pathways involved in biological processes. A statistical global test for groups of differentially expressed genes within pathways is now available for the analysis of results obtained by microarrays (18).

In addition, the development of laser microdissection techniques (19) has enabled the separation of nephron segments in frozen or fixed sections. This development, in combination with new amplification protocols with a more than 1,000-fold linear amplification efficiency (20), gives us the opportunity for generation of nephron segment-specific gene profiles in frozen or paraffin-embedded patient material. Microfluidic biochips and nanotechnology-based biochips will gain importance as tools to study molecular mechanisms at the single-cell level (21).

The mRNA itself is not functionally active and must be translated into biologically active proteins. As with any multi-step biological process, eukaryotic translation can be regulated at various levels. The predominant step in the control of translation is ribosome binding. A large number of regulatory sequences have been identified in the 5' and especially in the 3' untranslated regions of mRNA. In addition, several factors, eukaryotic translation initiation factor 2 and 4E are the most important, play a crucial role in the regulation of translation initiation. Activation of these molecules is regulated by kinases (22), which are activated by environmental stress (23). These data imply that the number of transcripts for any mRNA molecule is not necessarily associated with the amount of the corresponding protein being translated. On the other hand, it is unlikely that cells expend a lot of energy on mRNA transcription without specific reasons. Although there are discrepancies between levels of

mRNA and the amount of protein, these differences can usually be explained by the occurrence of posttranslational processes, such as storage of proteins until they are necessary (for example coagulation factor VIII), or rapid protein degradation by proteolytic enzymes. Another explanation is slow protein turnover in normal maintenance of tissue, as occurs with ECM molecules. Although one can measure increased mRNA levels for these matrix molecules, it is possible to find no increase at the protein level because of a disturbed balance between production and degradation.

Within the framework of studying molecular biological processes, the logical step after genome-wide mRNA expression profiling is genome-wide protein expression profiling, also called proteomics. The goal of proteomics is a comprehensive, quantitative description of protein expression (24). The field of proteomics is growing rapidly. The rapid progress of proteomics over the past few years is a result of: (1) the completion of the human genome projects; (2) the improvement of gel-based protein separation techniques; and (3) the development of mass spectrometry (MS). One of the first applications of proteomics in renal disease was performed by Witzmann et al., who used the two-dimensional gel electrophoresis technique and MS analysis to study heat-shock and glucose-regulated proteins in the rat kidney (25). More recently, proteins derived from whole-kidney lysate of diabetic OVE26 transgenic mice were separated by two-dimensional PAGE and identified by matrix-assisted laser desorption/ionization time-of-flight (MALDI-TOF)-MS. Several proteins were differentially expressed in diabetic kidneys (26). Among these altered proteins, expression of monocyte/neutrophil elastase inhibitor was increased, whereas elastase IIIB was decreased in diabetic kidneys.

When the expression of a gene is changed during disease, studies in animal models are necessary to confirm the functional role of that gene. Germ-line transgenic mouse models were developed to knock out or introduce a specific gene in the mouse genome (27). The disadvantage of this approach is that knockout of a gene often leads to (embryonic) lethality. To overcome these problems, an alternative approach is the use of conditional knockout strategies in combination with organ or cell specific transgene expression. Cell-type specific gene knockouts can be made with the use of Cre/lox system (28). This Cre recombinase system can be used in combination with an inducible cell specific promoter. Administration of a drug targeting the cre-construct in these mice induces excision of an integrated gene flanked by loxP sites in the selected tissues or cells (29).

Other methods for specific gene silencing are transfection of cells or tissues with RNA or DNA constructs that can turn off a gene. Several methods for transfecting cells are available. Commercial kits are available to transfect DNA constructs into cells *in vitro*. For *in vivo* applications, different methods have been described. Glomerular cells have been transfected

with the use of viruses such as hemagglutinating virus of Japan in combination with liposome transfection (30). Also, mesangial cells have been used to carry the gene construct into the renal glomerulus. The cDNA construct was introduced into cultured rat mesangial cells, and stably transfected vector cells were established (31). These cells were then delivered into the glomeruli of rats via the circulation. More recently, electroporation has been applied to introduce DNA into several organs. DNA/RNA constructs were injected into the left renal artery followed by electroporation of the injected kidney between a pair of tweezers-type electrodes (32). The advantage of electroporation compared to conventional methods is that this procedure is free from the oncogenicity, immunogenicity, and cytotoxicity of viral vectors or transfected cells. In addition, co-transfection with a mixture of different constructs may be achieved easily by electroporation (32).

Several methods can be used to turn off a specific gene. One of the oldest methods is the use of antisense RNA molecules to modulate the expression of selected genes. The principle is based on specific annealing of mRNA with complementary antisense RNA molecules resulting in double-stranded RNA that is no longer available for translation (33). The disadvantage of this technique is the short half-life time and the low efficiency of these antisense molecules (34). To overcome this problem, the use of double-stranded (ds) interfering RNA was developed. Compared to single-stranded RNA, dsRNA is relatively stable and does not require chemical modifications to achieve a satisfactory half-life. Long, double-stranded RNA molecules are processed by the endonuclease dicer into 21- to 23-nt small interfering RNAs (siRNAs), which specifically suppress gene expression in mammalian cell lines, including human embryonic kidney cells (35). Formation of dsRNAs results in loss of the corresponding mRNA. Binding to promoter and intronic sequences, results in largely ineffective transcription, and dsRNA can induce genomic methylation of sequences homologous to the silencing trigger, resulting in loss of transcription (36). It was found that the siRNA technique is at least 10 times more potent than conventional antisense RNAs in silencing a gene (37). Next to inactivation of mRNAs, exon skipping with the use of stabilized antisense oligonucleotides (AONs) can also be used to knock-down a gene function. Modulation of splicing by AONs that restored normal splicing by skipping exons with several different mutations in the ß-globin gene has been described by Dominski et al. (38). In addition to AON-mediated modulation of splicing, loss of gene function by skipping those exons that are necessary for a normal function of the gene has been proposed as a useful method of gene silencing.

Despite the ability to assess expression of thousands of genes simultaneously, which can give us insight into molecular biological processes at the single-cell level, and in spite of the current knowledge of many different pathways involved in disease, the precise mechanisms of the progression to glomerulosclerosis have not yet been fully clarified. We have to realize that

of the ~30,000 known genes in the human genome, 30–40% can be alternatively spliced at at least two different sites (39), which may theoretically result in about 100,000 different gene products that can also influence each other in a dose-dependent manner. This probability suggests that there is an enormous number of combinations that can influence the physiological state of a cell. More research is necessary, especially in the field of bioinformatics, that can recognize disease-specific gene expression patterns and improve our understanding of at least a part of the mechanisms behind the progression to glomerulosclerosis and interstitial fibrosis.

References

1. Gauthier VJ, Mannik M: A method for isolation of mouse glomeruli for quantitation of immune deposits. *Kidney Int* 33:897-899, 1988
2. Assmann KJM, Van Son JPHF, Koene RAP: Improved method for the isolation of mouse glomeruli. *J Am Soc Nephrol* 2:944-946, 1991
3. Baelde HJ, Bergijk EC, Bruijn JA: Isolation and characterization of mouse glomerular basement membrane. *J Clin Lab Immunol* 33:17-20, 1990
4. Hilleren P, McCarthy T, Rosbash M, Parker R, Jensen TH: Quality control of mRNA 3[prime]-end processing is linked to the nuclear exosome. *Nature* 413:538-542, 2001
5. Baelde HJ, Eikmans M, Van Vliet AI, Bergijk EC, De Heer E, Bruijn JA: Alternatively spliced isoforms of fibronectin in immune-mediated glomerulosclerosis: the role of TGF beta and IL-4. *J Pathol* 204:248-257, 2004
6. Auffray C, Rougeon F: Purification mouse Ig heavy chain mRNAs from total myeloma tumor RNA. *Eur J Biochem* 107:303-314, 1980
7. Bergijk EC, Baelde HJ, De Heer E, Killen PD, Bruijn JA: Specific accumulation of exogenous fibronectin in experimental glomerulosclerosis. *J Pathol* 176:191-199, 1995
8. Vleming LJ, Baelde JJ, Westendorp RG, Daha MR, van Es LA, Bruijn JA: The glomerular deposition of PAS positive material correlates with renal function in human kidney diseases. *Clin Nephrol* 47:158-167, 1997
9. Muro AF, Chauhan AK, Gajovic S, Iaconcig A, Porro F, Stanta G, Baralle FE: Regulated splicing of the fibronectin EDA exon is essential for proper skin wound healing and normal lifespan. *J Cell Biol* 162:149-160, 2003
10. John L, Kirubakaran MG, Shastry JC: Diabetic nephropathy: a clinical study of 498 patients. *J Diabet Complications* 1:87-90, 1987
11. Baelde HJ, Eikmans M, Doran PP, Lappin DWP, De Heer E, Bruijn JA: Gene expression profiling in glomeruli from human kidneys with diabetic nephropathy. *Am J Kidney Dis* 43:636-650, 2004
12. Bortoloso E, Del Prete D, Dalla VM, Gambaro G, Saller A, Antonucci F, Baggio B, Anglani F, Fioretto P: Quantitave and qualitative changes in vascular endothelial growth factor gene expression in glomeruli of patients with type 2 diabetes. *Eur J Endocrinol* 150:799-807, 2004
13. Kondo S, Kubota S, Shimo T, Nishida T, Yosimichi G, Eguchi T, Sugahara T, Takigawa M: Connective tissue growth factor increased by hypoxia may initiate angiogenesis in collaboration with matrix metalloproteinases. *Carcinogenesis* 23:769-776, 2002
14. Chang LK, Garcia-Cardena G, Farnebo F, Fannon M, Chen EJ, Butterfield C, Moses MA, Mulligan RC, Folkman J, Kaipainen A: Dose-dependent response of FGF-2 for lymphangiogenesis. *Proc Natl Acad Sci U S A* 101:11658-11663, 2004
15. Kim NH, Oh JH, Seo JA, Lee KW, Kim SG, Choi KM, Baik SH, Choi DS, Kang YS, Han SY, Han KH, Ji YH, Cha DR: Vascular endothelial growth factor (VEGF) and soluble VEGF receptor FLT-1 in diabetic nephropathy. *Kidney Int* 67:167-177, 2005
16. Cha DR, Kim NH, Yoon JW, Jo SK, Cho WY, Kim HK, Won NH: Role of vascular endothelial growth factor in diabetic nephropathy. *Kidney Int Suppl* 77:S104-S112, 2000
17. Bortoloso E, Del Prete D, Gambaro G, Dalla VM, Sailer A, Baggio B, Antonucci F, Fioretto P, Anglani F: Vascular endothelial growth factor (VEGF) and VEGF receptors in diabetic nephropathy: expression studies in biopsies of type 2 diabetic patients. *Ren Fail* 23:483-493, 2001
18. Goeman JJ, van de Geer SA, de Kort F, van Houwelingen HC: A global test for groups of genes: testing association with a clinical outcome. *Bioinformatics* 20:93-99, 2004
19. Specht K, Richter T, Muller U, Walch A, Hofler MW: Quantitative gene expression analysis in microdissected archival tissue by real-time RT-PCR. *J Mol Med* 78:B27, 2000
20. Upson JJ, Stoyanova R, Cooper HS, Patriotis C, Ross EA, Boman B, Clapper ML, Knudson AG, Bellacosa A: Optimized procedures for microarray analysis of histological specimens processed by laser capture microdissection. *J Cell Physiol* 201:366-373, 2004
21. Jain KK: Applications of biochips: from diagnostics to personalized medicine. *Curr Opin Drug Discov Devel* 7:285-289, 2004

22. Lu L, Han AP, Chen JJ: Translation Initiation Control by Heme-Regulated Eukaryotic Initiation Factor 2alpha Kinase in Erythroid Cells under Cytoplasmic Stresses. *Mol Cell Biol* 21:7971-7980, 2001
23. Clemens MJ: Initiation factor eIF2 alpha phosphorylation in stress responses and apoptosis. *Prog Mol Subcell Biol* 27:57-89, 2001
24. PersidisAris: Proteomics. *Nat Biotech* 16:393-394, 1998
25. Witzmann F, Clack J, Fultz C, Jarnot B: Two-dimensional electrophoretic mapping of hepatic and renal stress proteins. *Electrophoresis* 16:451-459, 1995
26. Thongboonkerd V, Barati MT, McLeish KR, Benarafa C, Remold-O'Donnell E, Zheng S, Rovin BH, Pierce WM, Epstein PN, Klein JB: Alterations in the renal elastin-elastase system in type 1 diabetic nephropathy identified by proteomic analysis. *J Am Soc Nephrol* 15:650-662, 2004
27. Jaenisch R: Germ line integration and Mendelian transmission of the exogenous Moloney leukemia virus. *Proc Natl Acad Sci U S A* 73:1260-1264, 1976
28. Sauer B, Henderson N: Cre-stimulated recombination at loxP-containing DNA sequences placed into the mammalian genome. *Nucleic Acids Res* 17:147-161, 1989
29. Metzger D, Chambon P: Site- and Time-Specific Gene Targeting in the Mouse. *Methods* 24:71-80, 2001
30. Arai M, Wada A, Isaka Y, Akagi Y, Sugiura T, Miyazaki M, Moriyama T, Kaneda Y, Naruse K, Naruse M: In Vivo Transfection of Genes for Renin and Angiotensinogen into the Glomerular Cells Induced Phenotypic Change of the Mesangial Cells and Glomerular Sclerosis. *Biochemical and Biophysical Research Communications* 206:525-532, 1995
31. Akagi Y, Isaka Y, Arai M, Kaneko T, Takenaka M, Moriyama T, Kaneda Y, Ando A, Orita Y, Kamada T, Ueda N, Imai E: Inhibition of TGF-beta 1 expression by antisense oligonucleotides suppressed extracellular matrix accumulation in experimental glomerulonephritis. *Kidney Int* 50:148-155, 1996
32. Tsujie M, Isaka Y, Nakamura H, Imai E, Hori M: Electroporation-Mediated Gene Transfer that Targets Glomeruli. *J Am Soc Nephrol* 12:949-954, 2001
33. Gutierrez AA, Lemoine NR, Sikora K: Gene therapy for cancer. *Lancet* 339:715-721, 1992
34. Braasch DA, Jensen S, Liu Y, Kaur K, Arar K, White MA, Corey DR: RNA interference in mammalian cells by chemically-modified RNA. *Biochemistry* 42:7967-7975, 2003
35. Elbashir SM, Harborth J, Lendeckel W, Yalcin A, Weber K, Tuschl T: Duplexes of 21-nucleotide RNAs mediate RNA interference in cultured mammalian cells. *Nature* 411:494-498, 2001
36. Hannon GJ: RNA interference. *Nature* 418:244-251, 2002
37. Fire A, Xu S, Montgomery MK, Kostas SA, Driver SE, Mello CC: Potent and specific genetic interference by double-stranded RNA in Caenorhabditis elegans. *Nature* 391:806-811, 1998
38. Dominski Z, Kole R: Restoration of Correct Splicing in Thalassemic Pre-mRNA by Antisense Oligonucleotides. *Proc Natl Acad Sci U S A* 90:8673-8677, 1993
39. Huang HD, Horng JT, Lin FM, Chang YC, Huang CC: SpliceInfo: an information repository for mRNA alternative splicing in human genome. *Nucleic Acids Res* 33:D80-D85, 2005

Nederlandse Samenvatting

Nederlandse samenvatting

De nieren hebben een belangrijke functie in het menselijk lichaam: ze zijn onder andere verantwoordelijk voor het zuiveren van bloed en het produceren van urine. Wanneer de nier chronisch beschadigd wordt door bijvoorbeeld glomerulonefritis, hoge bloeddruk (hypertensie), afwijkingen van de stofwisseling (diabetes) of opname van giftige stoffen (bijv. sommige geneesmiddelen) kan dit leiden tot verbindweefseling in de nier. Deze schade kan klinisch leiden tot een langzame achteruitgang van de nierfunctie en histologisch tot een toename van extracellulaire matrix (ECM) componenten. Uiteindelijk zal dit leiden tot de ontwikkeling van glomerulosclerose en interstitiële fibrose, een proces dat ook wel fibrogenese wordt genoemd. Dit leidt tot een totaal verlies van de nierfunctie. De toename van ECM componenten kan een gevolg zijn van een verhoogde aanmaak in de nier, stapeling van ECM moleculen vanuit de circulatie, een verstoorde afbraak die normaal plaats vindt in het kader van het onderhoud van de ECM, of een combinatie van deze factoren.

Voor de aanmaak van ECM eiwitten maakt de cel gebruik van het transcriptie/translatie systeem. In iedere celkern bevindt zich het genomische DNA dat de code bevat voor het maken van een eiwit. Van een stukje van dit dubbelstrengs DNA wordt een enkelstrengs kopie gemaakt (mRNA) die zich vanuit de celkern naar het cytoplasma verplaatst. Dit proces wordt transcriptie genoemd. Op basis van de code van dit mRNA molecuul wordt door middel van translatie een eiwit gevormd. Het meten van specifieke mRNA moleculen (RNA expressie) in de cel kan dus belangrijke informatie geven over een cel. Dit, samen met het aantonen van de gevormde eiwitten, kan inzicht geven in hoe het proces van fibrogenese verloopt.

In **hoofdstuk 2** zijn studies beschreven over het isoleren van mRNA uit muizen glomeruli, de filtratie eenheden in de nier. Muizen worden vaak als proefdiermodel gebruikt om de ontwikkeling van glomerulosclerose te bestuderen. Voor het isoleren van de muizen glomeruli werd gebruik gemaakt van magnetische retractie. Muizennieren werden hiervoor opgespoten met ijzeroxide deeltjes die specifiek vastlopen in de vaatkluwen van de glomerulus. Vervolgens werd de nier door een zeef geperst waardoor de glomeruli vrij in oplossing kwamen. Door vervolgens deze suspensie tegen een magneet te houden kunnen glomeruli geïsoleerd worden. De vraag bij deze methode was of de mRNA moleculen, die erg gevoelig zijn voor afbraak, deze procedure zouden doorstaan en welke RNA-isolatie methode het meest geschikt was om uit de gezuiverde glomeruli mRNA te isoleren. Uit de experimenten blijkt dat glomeruli isolatie met magnetische retractie in combinatie met de ‘LiCl’ RNA isolatie methode de beste resultaten gaf. Northernblot hybridisatie experimenten met een probe tegen hoog moleculair mRNA (dat het meest gevoelig is voor afbraak) gaf een positief signaal. Hieruit konden we concluderen dat de LiCl methode het meest geschikt is om mRNA expressie experimenten mee uit te voeren.

De studies in **hoofdstuk 3** beschrijven de distributie van fibronectine isovormen in nierbiopten van patiënten die glomerulosclerose ontwikkelen. Tijdens de transcriptie van DNA, die leidt tot productie van het mRNA, dat codeert voor fibronectine kunnen er bepaalde stukken van de code verwijderd of juist toegevoegd worden (alternatieve splicing). Hierdoor worden eiwit moleculen gevormd waaraan bepaalde domeinen zijn toegevoegd of waaruit die zijn verwijderd. Van het fibronectine molecuul zijn een aantal domeinen bekend die alternatief gespliced kunnen worden: de EDA, de EDB en de V-regio. Inclusie van deze domeinen vindt vooral plaats tijdens de embryogenese waar deze domeinen een belangrijke rol spelen in de proliferatie en differentiatie van cellen. In normale nieren wordt vooral fibronectine gevonden waarin de EDA en EDB domeinen ontbreken. In patiënten die glomerulosclerose ontwikkelen vonden we naast een toename van fibronectine, dat dit fibronectine positief was voor EDA en EDB. Dit zou erop kunnen duiden dat inclusie van deze domeinen een belangrijke rol speelt in de ontwikkeling van glomerulosclerose.

In **hoofdstuk 4** is vervolgens onderzocht of de aanwezigheid van EDA en EDB domeinen van fibronectine tijdens de ontwikkeling van glomerulosclerose konden worden aangetoond op mRNA niveau en welke factoren een rol spelen bij het verschijnen van deze domeinen. In verschillende proefdiermodellen voor glomerulosclerose vonden we alternatieve splicing van EDA en EDB. In muizen met lupus nefritis was dit echter niet aanwezig. Omdat uit eerder onderzoek bekend is dat TGF-β een belangrijke groeifactor is die leidt tot inclusie van het EDA domein, werd de relatie van de aanwezigheid van TGF-β en EDA positief fibronectine bekeken. Hieruit bleek, dat in de diermodellen waarin een toename van TGF-β te zien is ook een inclusie van EDA plaats vindt. In muizen met lupus nefritis, waarin we geen EDA fibronectine kunnen aantonen, vindt ook geen toename van TGF-β plaats. Omdat in deze ziekte het cytokine IL-4 een belangrijke rol speelt, hebben we in gekweekte glomerulaire mesangiale cellen het effect van TGF-β en IL-4 op het splicingspatroon van fibronectine onderzocht. Mesangiale cellen die gekweekt werden met TGF-β lieten inderdaad een toename zien van EDA inclusie, terwijl aanwezigheid van IL-4 juist tot een afname van EDA inclusie leidde. Deze resultaten konden we bevestigen in humane nierbiopten van patiënten met glomerulosclerose. In nierbiopten van patiënten met lupus nefritis was geen toename van TGF-β en EDA fibronectine te zien in vergelijking met gezonde nieren. Uit deze studies concluderen we dat TGF-β een belangrijke rol speelt bij de inclusie van EDA fibronectine, maar dat patiënten ook glomerulosclerose kunnen ontwikkelen zonder een toename van TGF-β en EDA fibronectine.

In **hoofdstuk 5** onderzochten wij de accumulatie van fibronectine vanuit de circulatie in glomerulosclerotische laesies. Uit eerdere studies is gebleken dat er in sclerotische glomeruli van muizen met lupus nefritis grote hoeveelheden van het ECM molecuul fibronectine te vinden zijn, terwijl er op mRNA niveau nauwelijks een toename van fibronectine waarneembaar

is. Als in deze muizen gelabeld fibronectine werd ingespoten, was dit na 24 uur terug te vinden in de laesies. Wij hebben onderzocht via welke bindingsplaatsen het fibronectine vanuit de circulatie gebonden wordt. Hiervoor is het fibronectine molecuul gezuiverd en in kleinere fragmenten geknipt. Ook is onderzocht of de binding van fibronectine in de laesies met heparine voorkomen kon worden. Omdat heparine als een anti-coagulant werkt, en dus via inhibitie van stolling de fibronectine accumulatie zou kunnen remmen, hebben we gekeken of N-desulfated heparine, dat geen anti-coagulante werking meer heeft, de accumulatie van fibronectine kan voorkomen. Uit de accumulatie experimenten met fibronectine is gebleken dat zowel heparine als N-desulfated heparine de accumulatie van fibronectine kon voorkomen. Echter, uit de accumulatie experimenten met de fibronectine fragmenten bleken juist de fragmenten die een lage affiniteit hebben voor heparine te accumuleren in sclerotische laesies. De accumulatie van fibronectine verloopt dus niet via de heparine-bindingsplaats. Omdat heparine de binding wel kan voorkomen, is het waarschijnlijk een bindingsplaats direct naast de heparine-bindingsplaats, die door sterische hindering door heparine wordt afgeschermd.

De studies in **hoofdstuk 6** beschrijven de resultaten van een microarray analyse in glomeruli van patiënten met diabetische nefropathie (DN). DN is een complicatie die optreedt bij ongeveer 30-40% van de patiënten met diabetes en leidt tot verlies van de nierfunctie en de ontwikkeling van glomerulosclerose en interstitiële fibrose. Met behulp van DNA chips is het mRNA expressie patroon van ongeveer 12000 genen bepaald in glomeruli van patiënten met en zonder DN. Door nu te kijken naar de verschillen in expressie tussen controle nieren en nieren met DN kan men inzicht krijgen in de moleculaire processen die een rol spelen in de ontwikkeling van DN. Wij vonden dat een groot aantal genen verschillend tot expressie kwamen. Het betrof o.a. genen die coderen voor eiwitten die zich bevinden in de filtratie complexen tussen de cellen. Opvallend in nieren met DN was de afgenomen expressie van een aantal genen die betrokken zijn bij het in stand houden van de bloedvaten, zogenaamde angiogenetische factoren.

De expressie van de angiogenetische factoren VEGF en CTGF is vervolgens verder onderzocht in een groot aantal nierbiopten van patiënten met verschillende stadia van DN. De resultaten hiervan zijn terug te vinden in **hoofdstuk 7.** Het doel van dit onderzoek was het bevestigen van de microarray resultaten in een groter patiënten cohort en het beantwoorden van de vraag of er een relatie is tussen de expressieniveaus van de angiogenetische factoren en het beloop van de ziekte. Lasercapture microdissectie werd toegepast om glomeruli uit deze biopten te isoleren. VEGF en CTGF niveaus waren significant verlaagd in patiënten met DN. Ook was er een negatieve correlatie tussen VEGF mRNA niveau en het percentage Sirius Red positieve oppervlakte, een maat voor interstitiële fibrose. Het lijkt er dus op dat progressie van de nierziekte gekoppeld is aan afname van VEGF. VEGF wordt in de glomerulus voornamelijk gemaakt door de podocyten. Een verlaging van VEGF zou het gevolg kunnen zijn van podocyt

verlies, iets wat al eerder beschreven is in patiënten met DN. Omdat VEGF een belangrijke factor is voor het in stand houden van endotheelcellen in de glomerulaire capillairen, zou men kunnen speculeren dat het verlies van podocyten in de glomerulus via een afname van de VEGF expressie leidt tot verlies van endotheel. Verlies van endotheel kan leiden tot microangiopathie waardoor uiteindelijk de glomerulaire capillairen verloren gaan. Indien dit mechanisme inderdaad blijkt te bestaan zou het een opening kunnen bieden voor therapeutische interventie zoals het toedien van VEGF of anticoagulantia. Er is echter meer onderzoek nodig om deze hypothese te bewijzen.

Curriculum Vitae

De auteur van dit proefschrift werd geboren op 7 juni 1966 te Bodegraven. In juni 1984 behaalde hij het diploma voor Hoger Algemeen Voortgezet Onderwijs aan het “Driestar College” te Gouda. Daarna werd begonnen met de studie hoger laboratorium onderwijs (HLO) aan de toenmalige Hogeschool Rijnland. Gekozen werd voor de medische afstudeerrichting met als specialisatie histo/cytopathologie. Daarnaast werd als extra vak Hematologie gevolgd. De algemene cytologiestage werd uitgevoerd op de afdeling Pathologie van Rijksuniversiteit Leiden. De histologie stage en de wetenschappelijke afstudeeropdracht werden uitgevoerd op het Rijks Instituut voor Milieuhygiëne (RIVM) te Bilthoven. Tijdens deze stage werd onderzoek gedaan naar de rol van BCG (bacille Calmette-Guérin) als adjuvant therapie bij de behandeling van blaastumoren. Na zijn afstuderen in juni 1988 kwam hij in dienst als research analist bij de afdeling Pathologie van de medische faculteit van de Rijksuniversiteit Leiden. In 1999 begon de auteur in deeltijd aan een promotie onderzoek bij de afdeling Pathologie. Het promotie onderzoek, waarvan de resultaten beschreven zijn in dit proefschrift, werd uitgevoerd onder leiding van Prof. Dr. J.A. Bruijn, Dr. E. de Heer en Dr. M. Eikmans. Thans zet de auteur dit onderzoek voort waarbij de focus ligt op de progressie van diabetische nefropathie. Daarnaast is de auteur in deeltijd betrokken bij het onderzoek naar het ontstaan van bot- en wekedelen tumoren onder leiding van Prof. Dr. P.C.W. Hogendoorn.

List of publications

1. **Baelde HJ**, Bergijk EC, Bruijn JA: Isolation and characterization of mouse glomerular basement membrane. *J Clin Lab Immunol* 33:17-20, 1990

2. Bruijn JA, van Leer EH, **Baelde HJ**, Corver WE, Hogendoorn PC, Fleuren GJ: Characterization and in vivo transfer of nephritogenic autoantibodies directed against dipeptidyl peptidase IV and laminin in experimental lupus nephritis. *Lab Invest* 63:350-359, 1990

3. Bergijk EC, Munaut C, **Baelde JJ**, Prins F, Foidart JM, Hoedemaeker PJ, Bruijn JA: A histologic study of the extracellular matrix during the development of glomerulosclerosis in murine chronic graft-versus-host disease. *Am J Pathol* 140:1147-1156, 1992

4. Munaut C, Bergijk EC, **Baelde JJ**, Noel A, Foidart JM, Bruijn JA: A molecular biologic study of extracellular matrix components during the development of glomerulosclerosis in murine chronic graft-versus-host disease. *Lab Invest* 67:580-587, 1992

5. Treurniet RA, Bergijk EC, **Baelde JJ**, de Heer E, Hoedemaeker PJ, Bruijn JA: Gender-related influences on the development of chronic graft-versus-host disease-induced experimental lupus nephritis. *Clin Exp Immunol* 91:442-448, 1993

6. **Baelde JJ**, Bergijk EC, Hoedemaeker PJ, de Heer E, Bruijn JA: Optimal method for RNA extraction from mouse glomeruli. *Nephrol Dial Transplant* 9:304-308, 1994

7. Bergijk EC, **Baelde HJ**, de Heer E, Bruijn JA: Prevention of glomerulosclerosis by early cyclosporine treatment of experimental lupus nephritis. *Kidney Int* 46:1663-1673, 1994

8. Bergijk EC, **Baelde HJ**, de Heer E, Killen PD, Bruijn JA: Specific accumulation of exogenous fibronectin in experimental glomerulosclerosis. *J Pathol* 176:191-199, 1995

9. Vleming LJ, **Baelde JJ**, Westendorp RG, Daha MR, van Es LA, Bruijn JA: Progression of chronic renal disease in humans is associated with the deposition of basement membrane components and decorin in the interstitial extracellular matrix. *Clin Nephrol* 44:211-219, 1995

10. Bergijk EC, **Baelde HJ**, de Heer E, Killen PD, Bruijn JA: Role of the extracellular matrix in the development of glomerulosclerosis in experimental chronic serum sickness. *Exp Nephrol* 3:338-347, 1995

11. Bergijk EC, **Baelde HJ**, Kootstra CJ, de Heer E, Killen PD, Bruijn JA: Cloning of the mouse fibronectin V-region and variation of its splicing pattern in experimental immune complex glomerulonephritis. *J Pathol* 178:462-468, 1996

12. Peters DJ, Spruit L, Klingel R, Prins F, **Baelde HJ**, Giordano PC, Bernini LF, de Heer E, Breuning MH, Bruijn JA: Adult, fetal, and polycystic kidney expression of polycystin, the polycystic kidney disease-1 gene product. *Lab Invest* 75:221-230, 1996

13. Kootstra JC, Veninga A, **Baelde JJ**, van Eendenburg J, de Heer E, Bruijn JA: Characterization of reactivity of monoclonal autoantibodies with renal antigens in experimental lupus nephritis. *J Clin Lab Immunol* 48:201-218, 1996

14. Vleming LJ, **Baelde JJ**, Westendorp RG, Daha MR, van Es LA, Bruijn JA: The glomerular deposition of PAS positive material correlates with renal function in human kidney diseases. *Clin Nephrol* 47:158-167, 1997

15. Van Griensven M, Bergijk EC, **Baelde JJ**, de Heer E, Bruijn JA: Differential effects of sex hormones on autoantibody production and proteinuria in chronic graft-versus-host disease-induced experimental lupus nephritis. *Clin Exp Immunol* 107:254-260, 1997

16. Kootstra CJ, Sutmuller M, **Baelde HJ**, de Heer E, Bruijn JA: Association between leukocyte infiltration and development of glomerulosclerosis in experimental lupus nephritis. *J Pathol* 184:219-225, 1998

17. Bergijk EC, van Alderwegen IE, **Baelde HJ**, de Heer E, Funabiki K, Miyai H, Killen PD, Kalluri RK, Bruijn JA: Differential expression of collagen IV isoforms in experimental glomerulosclerosis. *J Pathol* 184:307-315, 1998

18. Sutmuller M, **Baelde HJ**, Tysma OM, de Heer E, Bruijn JA: Experimental glomerulonephritis is attenuated by CD8+ T cell chimerism and prevented by Mls-1-incompatible thymocytes. *Clin Immunol Immunopathol* 88:114-122, 1998

19. Sutmuller M, **Baelde HJ**, Ouellette S, de Heer E, Bruijn JA: T-cell receptor Vbeta gene expression in experimental lupus nephritis. *Immunology* 95:18-25, 1998

20. Sutmuller M, **Baelde JJ**, Madaio MP, Bruijn JA, de Heer E: Idiotype usage by polyclonally activated B cells in experimental autoimmunity and infection. *Clin Exp Immunol* 115:275-280, 1999

21. Kruidering M, van de WB, Zhan Y, **Baelde JJ**, Heer E, Mulder GJ, Stevens JL, Nagelkerke JF: Cisplatin effects on F-actin and matrix proteins precede renal tubular cell detachment and apoptosis in vitro. *Cell Death Differ* 5:601-614, 1998

22. Natte R, de Boer WI, Maat-Schieman ML, **Baelde HJ**, Vinters HV, Roos RA, van Duinen SG: Amyloid beta precursor protein-mRNA is expressed throughout cerebral vessel walls. *Brain Res* 828:179-183, 1999

23. Ussing AP, **Baelde HJ**, Olesen LS, Naeser P, Prause JU, Bruijn JA: Haematopathology of 'Sjogren-mice': histopathological changes in spleens after semiallogeneic cell transfer.

Scand J Immunol 49:641-648, 1999

24. van Vliet AI, van Alderwegen IE, **Baelde HJ**, de Heer E, Killen PD, Kalluri RK, Bruijn JA, Bergijk EC: Differential expression of collagen type IV alpha-chains in the tubulointerstitial compartment in experimental chronic serum sickness nephritis. *J Pathol* 189:279-287, 1999

25. Eikmans M, **Baelde HJ**, de Heer E, Bruijn JA: Processing renal biopsies for diagnostic mRNA quantification: improvement of RNA extraction and storage conditions. *J Am Soc Nephrol* 11:868-873, 2000

26. Van Vliet A, **Baelde HJ**, Vleming LJ, de Heer E, Bruijn JA: Distribution of fibronectin isoforms in human renal disease. *J Pathol* 193:256-262, 2001

27. Langezaal SM, Graadt van Roggen JF, Cleton-Jansen AM, **Baelde JJ**, Hogendoorn PC: Malignant melanoma is genetically distinct from clear cell sarcoma of tendons and aponeurosis (malignant melanoma of soft parts). *Br J Cancer* 84:535-538, 2001

28. Eikmans M, **Baelde HJ**, de Heer E, Bruijn JA: Effect of age and biopsy site on extracellular matrix mRNA and protein levels in human kidney biopsies. *Kidney Int* 60:974-981, 2001

29. **Baelde HJ**, Cleton-Jansen AM, van Beerendonk H, Namba M, Bovee JV, Hogendoorn PC: High quality RNA isolation from tumours with low cellularity and high extracellular matrix component for cDNA microarrays: application to chondrosarcoma. *J Clin Pathol* 54:778-782, 2001

30. Hazelbag S, Fleuren GJ, **Baelde JJ**, Schuuring E, Kenter GG, Gorter A: Cytokine profile of cervical cancer cells. *Gynecol Oncol* 83:235-243, 2001

31. van Vliet AI, van Alderwegen IE, **Baelde HJ**, de Heer E, Bruijn JA: Fibronectin accumulation in glomerulosclerotic lesions: self-assembly sites and the heparin II binding domain. *Kidney Int* 61:481-489, 2002

32. Eikmans M, Sijpkens YW, **Baelde HJ**, de Heer E, Paul LC, Bruijn JA: High transforming growth factor-beta and extracellular matrix mRNA response in renal allografts during early acute rejection is associated with absence of chronic rejection. *Transplantation* 73:573-579, 2002

33. Eikmans M, **Baelde HJ**, de Heer E, Bruijn JA: RNA expression profiling as prognostic tool in renal patients: toward nephrogenomics. *Kidney Int* 62:1125-1135, 2002

34. Xu W, **Baelde HJ**, Lagaaij EL, de Heer E, Paul LC, Bruijn JA: Endothelial cell chimerism after renal transplantation in a rat model. *Transplantation* 74:1316-1320, 2002

35. Eikmans M, **Baelde HJ**, Hagen EC, Paul LC, Eilers PH, de Heer E, Bruijn JA: Renal mRNA levels as prognostic tools in kidney diseases. *J Am Soc Nephrol* 14:899-907, 2003

36. Eikmans M, **Baelde JJ**, de Heer E, Bruijn JA: ECM homeostasis in renal diseases: a genomic approach. *J Pathol* 200:526-536, 2003

37. Koop K, Eikmans M, **Baelde HJ**, Kawachi H, de Heer E, Paul LC, Bruijn JA: Expression of podocyte-associated molecules in acquired human kidney diseases. *J Am Soc Nephrol* 14:2063-2071, 2003

38. Kapojos JJ, Poelstra K, Borghuis T, Van Den BA, **Baelde HJ**, Klok PA, Bakker WW: Induction of glomerular alkaline phosphatase after challenge with lipopolysaccharide. *Int J Exp Pathol* 84:135-144, 2003

39. Leussink BT, **Baelde HJ**, Broekhuizen-van den Berg TM, de Heer E, van der Voet GB, Slikkerveer A, Bruijn JA, de Wolff FA: Renal epithelial gene expression profile and bismuth-induced resistance against cisplatin nephrotoxicity. *Hum Exp Toxicol* 22:535-540, 2003

40. Roos-van Groningen MC, Eikmans M, **Baelde HJ**, de Heer E, Bruijn JA: Improvement of extraction and processing of RNA from renal biopsies. *Kidney Int* 65:97-105, 2004

41. **Baelde HJ**, Eikmans M, Doran PP, Lappin DW, de Heer E, Bruijn JA: Gene expression profiling in glomeruli from human kidneys with diabetic nephropathy. *Am J Kidney Dis* 43:636-650, 2004

42. **Baelde HJ**, Eikmans M, van Vliet AI, Bergijk EC, de Heer E, Bruijn JA: Alternatively spliced isoforms of fibronectin in immune-mediated glomerulosclerosis: the role of TGFbeta and IL-4. *J Pathol* 204:248-257, 2004

43. Hutloff A, Buchner K, Reiter K, **Baelde HJ**, Odendahl M, Jacobi A, Dorner T, Kroczek RA: Involvement of inducible costimulator in the exaggerated memory B cell and plasma cell generation in systemic lupus erythematosus. *Arthritis Rheum* 50:3211-3220, 2004

44. Eikmans M, Ijpelaar DH, **Baelde HJ**, de Heer E, Bruijn JA: The use of extracellular matrix probes and extracellular matrix-related probes for assessing diagnosis and prognosis in renal diseases. *Curr Opin Nephrol Hypertens* 13:641-647, 2004

45. Koop K, Bakker RC, Eikmans M, **Baelde HJ**, de Heer E, Paul LC, Bruijn JA: Differentiation between chronic rejection and chronic cyclosporine toxicity by analysis of renal cortical mRNA. *Kidney Int* 66:2038-2046, 2004

46. Lantinga-van Leeuwen IS, Dauwerse JG, **Baelde HJ**, Leonhard WN, van de WA, Ward CJ, Verbeek S, Deruiter MC, Breuning MH, de Heer E, Peters DJ: Lowering of Pkd1 expression is sufficient to cause polycystic kidney disease. *Hum Mol Genet* 13:3069-3077, 2004

47. Lantinga-van Leeuwen IS, Leonhard WN, Dauwerse H, **Baelde HJ**, van Oost BA, Breuning MH, Peters DJ: Common regulatory elements in the polycystic kidney disease 1 and 2 promoter regions. *Eur J Hum Genet* 13:649-659, 2005

48. Koopmans M, Hovinga IC, **Baelde HJ**, Fernandes RJ, de Heer E, Bruijn JA, Bajema IM: Chimerism in kidneys, livers and hearts of normal women: implications for transplantation studies. *Am J Transplant* 5:1495-1502, 2005

49. van Poelgeest EP, **Baelde HJ**, Lagaaij EL, Sijpkens YWJ, de Heer E, Bruijn JA, Bajema IM: Endothelial cell chimerism occurs more often and earlier in female than in male recipients of kidney transplants. *Kidney International* 68:847-853, 2005

50. Janssen B, Hohenadel D, Brinkkoetter P, Peters V, Rind N, Fischer C, Rychlik I, Cerna M, Romzova M, de Heer E, **Baelde HJ**, Bakker SJL, Zirie M, Rondeau E, Mathieson P, Saleem MA, Meyer J, Koppel H, Sauerhoefer S, Bartram CR, Nawroth P, Hammes HP, Yard BA, Zschocke J, van der Woude FJ: Carnosine as a Protective Factor in Diabetic Nephropathy: Association With a Leucine Repeat of the Carnosinase Gene CNDP1. *Diabetes* 54:2320-2327, 2005

51. Eikmans M, **Baelde HJ**, de Heer E, Bruijn JA: Messenger RNA assessment in clinical nephrology: perspectives and progress of methodology. *Nephrol Dial Transplant*, in press

52. Eikmans M, Roos-van Groningen MC, Sijpkens YWJ, Ehrchen J, Roth J, **Baelde HJ**, Bajema IM, de Fijter JW, de Heer E, Bruijn JA: Expression of surfactant protein-C, S100A8, S100A9, and B cell markers in renal allografts: investigation of the prognostic value. *J Am Soc Nephrol*, in press

Naschrift

In dit naschrift wil ik graag van de gelegenheid gebruik maken om iedereen te bedanken die op enigerlei wijze heeft bijgedragen aan de totstandkoming van dit proefschrift. Dan denk ik aan de mensen van de ‘nierengroep’ in het bijzonder, en alle (ex)collega’s van de pathologie in het algemeen. Bedankt voor jullie inbreng, op wat voor manier dan ook. Het is voor mij onmogelijk om iedereen bij naam te noemen omdat ik in de afgelopen jaren veel mensen heb zien komen en gaan die op een positieve manier hebben bijgedragen aan mijn onderzoek.

Daarnaast wil ik ook het thuisfront bedanken. Lieve Janine, zonder jou hulp was het zeker niet gelukt. Jij hebt mij veel taken uit handen genomen zodat ik me op mijn onderzoek kon concentreren. Wilbert, Rianne en Coert, bedankt voor het begrip dat jullie hadden voor het feit dat papa afgelopen jaar regelmatig ‘s avonds pas heel laat thuis was of thuis geen zin meer had om iets met jullie te gaan doen. Altijd als ik aan jullie denk besef ik dat jullie veel belangrijker voor me zijn, hoe mooi en uitdagend het onderzoek ook is.